

PHYSICAL MODEL STUDIES ON BREAKWATERS WITH GEOTEXTILE SAND CONTAINER ARMOUR UNITS

Thesis

Submitted in partial fulfilment of the requirements for the degree of

DOCTOR OF PHILOSOPHY

by

TOM ELIAS

(Reg. No: 177094AM010)



DEPARTMENT OF WATER RESOURCES AND OCEAN ENGINEERING

NATIONAL INSTITUTE OF TECHNOLOGY KARNATAKA,

SURATHKAL, MANGALURU - 575 025

February, 2023

DECLARATION

by the Ph.D. Research Scholar

I hereby *declare* that the Research Thesis entitled “**Physical model studies on breakwaters with geotextile sand container armour units**” which is being submitted to the National Institute of Technology Karnataka, Surathkal in partial fulfilment of the requirements for the award of the Degree of Doctor of Philosophy in **Department of Water Resources and Ocean Engineering** is a *bonafide report of the research work carried out by me*. The material contained in this Research Thesis has not been submitted to any University or Institution for the award of any degree.



177094AM010, TOM ELIAS

Department of Water Resources and Ocean Engineering

Place: NITK-Surathkal

Date: 03-03-2022

CERTIFICATE

This is to *certify* that the Research Thesis entitled “**Physical model studies on breakwaters with geotextile sand container armour units**” submitted by **Tom Elias** (Register Number: 177094AM010) as the record of the research work carried out by him, is *accepted as the Research Thesis submission* in partial fulfilment of the requirements for the award of degree of Doctor of Philosophy.



Prof. Kiran G. Shirlal

Research Guide



Prof. B. M. Dodamani

Chairman-DRPC

Chairman (DRPC)
Dept. of Water Resources & Ocean Engineering

ACKNOWLEDGEMENTS

With a deep sense of gratitude, I express heartfelt thanks to my research supervisor, Prof. Kiran G. Shirlal, Department of Water Resources and Ocean Engineering, NITK, Surathkal, who has been a constant mentor and pillar of support throughout my research journey. I acknowledge his input and efforts in forming the research topic, guiding physical experimentations and unconditional support in attaining research progress. I deeply value the time spent on discussions, corrections and invaluable refinement of research work that yielded quality research publications, which is a matter of great pride and confidence to me. I am deeply indebted to him for shaping a better person in me.

I express my gratitude to Research Progress Assessment Committee (RPAC) members, Prof. M. C. Narasimhan, Department of Civil Engineering, NITK, Surathkal and Dr. T. Nasar, Department of Water Resources and Ocean Engineering, NITK, Surathkal, for their wholehearted efforts in the betterment of this research work. I thank Prof. B. M. Dodamani, Head of the Department and Prof. Amai Mahesha and Prof. Amba Shetty, former Head of the Department, for granting permission to utilise the laboratory and departmental facilities in carrying out the current work. I extend my gratitude to all the faculty members of the department for their encouragement and support.

I would like to express my gratitude to Prof. Prasad Krishna, Director, Prof. Udaykumar R. Yaragatti and Prof. Karanam Uma Maheshwar Rao, former Directors, NITK Surathkal, for permitting me to use the institutional infrastructure facilities.

Thanks to Prof. Aloysius Henry Sequeira, Prof. Arkal Vittal Hegde, Prof. Subba Roa for guiding me as great teachers during PhD course work. The love and support of Prof. G. S. Dwarakish are fondly remembered.

I would like to extend my sincere gratitude to the authors of all the academic works cited in this thesis. I also appreciate the time and effort made by each reviewer for their valuable comments on how to improve the present research work.

Thanks to Khator Technical Textiles for supporting this research by providing geotextile material free of cost.

Thanks to my co-research scholars Dr. Dinu Maria Jose Ashwitha Krishnaraj, Alka Abraham, Parthasarthy K. S. S., Amala Mary Vincent, Athul Krishna K. R., Mansoor C. B., Ajnas M., Shara Mathew, Dr. Nithya Govind, Chaithanya Krishnan, Basil Baby, Rony J. S., Kunhimamu Paravath, Dr. Beena Mary John, Dr. Vishnu M., Anjali Vijay, Dr. Parveen Suvarna, Arunakumar H. S, for all the discussions, support, and encouragement. I gratefully acknowledge the support and all help rendered by postgraduate students: Kajal E. V., Patchava Mahendra Naidu, Ramayanam Balaji, Jishnual K, Badavat Gopichand, Tiruveedula Geetha. I am incredibly grateful for the assistance forwarded by Athira, Aswathy, Francis, Hari, Divya, Ammu, Ajay, Therese, Sadhik, Hajira, Revathy, Niveditha and An in the preparation of geotextile sand containers. I also convey my regards to Dr. Sreelakshmi S., Paul T. Athikkalam, Sylvin Saju, Michel Joseph, Mridhula G. M, Neeraj Prakash, Dr. Jiya Albert, Dhanya S. and Dr. Athira Krishnan for their moral support and encouragement.

I sincerely acknowledge the help and support rendered by the department staff Mr. Seetharam, Mr. Anil Kumar, Mr. Balakrishna, Mr. Ananda Devadiga, Mr. Viswanath Poojary, Mrs. Prathima, Miss Sweekritha, Mrs. Ashwija and all the staff of the Department.

Of course, thanks to my inherited Toshiba laptop for being a constant companion throughout the PhD journey without fail. Grammarly and Mendeley deserve a standing ovation for making life easy.

Finally, I wish to express gratitude, love and affection to my beloved family members, Father late. Mr. P. S. Eliyachan, Mother, Mrs. Salykutty Thomas, my Grandmother, late Mrs. Mariyamma Thomas, Brother, Aswin Skaria Aliyachen, Sister, Bibil Baby and my dearest Nephew, Simon Aliyachen and all my friends and relatives for their encouragement, moral support and all their big and small sacrifices during the course of this research. I also bow down to the Almighty in making this thesis a reality.

ABSTRACT

Breakwaters are essential constructions providing tranquillity to ports and harbour structures when natural protection is lacking. Traditionally, these massive structures are constructed using natural rocks weighing tonnes. In the present scenario, obtaining huge natural rocks is cumbersome and non-eco-friendly. Harnessing the advantages of geotextile sand containers (GSCs), numerous submerged breakwaters and shoreline protection structures have been constructed worldwide. But an emerged breakwater structure with geotextile armour units, capable of replacing the conventional structures, is rarely discussed. A 1:30 scaled, monochromatic wave flume physical experimentation is carried out as a preliminary investigation to test the feasibility of using GSCs as breakwater armour units. The structural design of the GSC breakwater evolved based on a comprehensive literature survey. Single-layer GSC breakwater structures armoured with sand-filled units differing in size and fill percentage (named Bag 1, Bag 2, Bag 3 and Bag 4) are investigated in the initial stage. Studies on hydraulic performance (wave runup, rundown and reflection) and stability of GSC breakwater are carried out to analyse the efficiency of the structure against the wave conditions of the Mangaluru coast. The study revealed that the reflection coefficient (K_r) for GSC structures could range from 0.26 to 0.69. Additionally, reducing GSC fill percentage from 100 to 80 is found to be more effective (up to 64%) in reducing reflection, runup and rundown rates than altering GSC size. As far as stability is concerned, the best-performing single-layer configuration comprising Bag 3 could withstand wave heights up to 2.7 m in the prototype. The effect of armour unit size and sand fill ratio on the stability of the structure is analysed, and it is concluded that changing the sand fill ratio from 80% to 100% shot up the structural stability to a maximum of 14%. Increasing bag size also resulted in increased stability by up to 8%. Stability curves for all tested configurations are projected as the significant research outcome and can serve as a practical guideline for coastal engineers in designing GSC breakwaters.

It's efficacy to be used as the armour units of breakwaters motivated to advance further in GSC research by adding a second GSC layer to the breakwater model. These double-layered breakwater models with different placement modes are tested for its hydraulic

performance and stability. Double layer placement showed 45 to 52% less K_r than single-layer placement and 38 to 42% lesser than the conventional breakwater, owing to its higher porosity. It is observed that the stability of the structure increased by up to 17% when supplemented with double layers. Structure tends to be stable with increasing armour unit size and fill percentage. Larger bags stacked in double layers is found to be the most stable configuration. 80% filled, slope parallel placement exhibited the least stability. Double layer placement with Bag 3 is found to be stable up to a wave height of 0.132 m on the model scale, which is 3.96 m in the prototype. Stability nomograms for all the tested double-layer GSC breakwater cases are obtained from physical experimentation.

In the last stage, a pilot study is conducted by filling cement and sand to GSC units of the best-performing models from the above experiments. When GSC breakwaters are filled with sand and cement, up to 43% increased stability is observed with a considerable decrease in wave runup, rundown and reflection. As a result, cement-sand-filled GSC units can be suggested as a possible alternative to sand-alone-filled units where vandalism has to be countered.

Keywords: Geotextiles; Coastal Protection; Breakwaters; Wave Flume; Stability; Hydraulic Performance.

CONTENTS

ABSTRACT	i
CONTENTS	iii
LIST OF FIGURES	vi
LIST OF TABLES	ix
NOMENCLATURE	x
CHAPTER 1	
INTRODUCTION	1
1.1 ORGANISATION OF THE THESIS	5
CHAPTER 2	
THEORETICAL BACKGROUND	7
2.1 GEOSYNTHETICS- AN OVERVIEW	7
2.1.1 Sand fill ratio	9
2.2 STABILITY AND DAMAGE ANALYSIS OF GSCS	10
2.2.1 Structural damages of GSCs	10
2.2.2 Anthropogenic Damages	11
2.3 HYDRODYNAMIC STUDIES ON GSC STRUCTURES	13
2.3.1 Wave transmission	13
2.3.2 Wave Reflection	14
2.3.3 Wave Runup	16
2.3.4 Wave rundown	19
2.4 GEOSYNTHETIC STRUCTURES FILLED WITH SAND AND CEMENT	22
2.5 GEOTEXTILE SAND CONTAINMENT SYSTEM	23
2.6 COASTAL PROTECTION WORKS - INDIAN TIMELINE	23
2.6.1 Geotextiles tubes, Shankarpur, West Bengal	24
2.6.2 Nearshore reef at INS Hamla, Mumbai:	25
2.6.3 Nearshore reef, Candolim Goa	25
2.6.4 Nearshore reef, Dahanu, Maharashtra	26
2.6.5 Seawall, Uppada, Andhra Pradesh	26
2.6.6 Nearshore Berms, Ullal, Karnataka:	27
2.6.7 Geotube and gabion seawall, Pentha, Odisha	28
2.6.8 Island Reclamation, Cheruvattor, Kerala	29
2.7 SUMMARY OF LITERATURE REVIEW	30
2.8 OBJECTIVES	30

CHAPTER 3	
METHODOLOGY	31
3.1 LITERATURE SURVEY AND COLLECTION OF INFORMATION:	31
3.2 STRUCTURAL DESIGN	31
3.2.1 Material selection	31
3.2.2 Armour unit placement	32
3.2.3 Structure slope	32
3.2.4 Crest width	33
3.2.5 Armour unit layers	33
3.2.6 Armour unit weight and size	33
3.3 PHYSICAL MODELLING:	35
3.3.1 Wave flume	35
3.3.2 Instrumentation	36
3.3.3 GSC Breakwater Model Construction	36
3.3.4 Test Procedure	40
3.3.5 Experimental data to be recorded:	42
3.3.6 Analysis of results:	42
3.3.7 Assumptions in physical modelling	42
CHAPTER 4	
RESULTS AND DISCUSSION	45
4.1 STUDIES ON GSC SINGLE-LAYER BREAKWATERS (SAND ALONE)	45
4.1.1 Wave runup studies	46
4.1.2 Wave rundown studies	50
4.1.3 Wave reflection studies	54
4.1.4 Stability and Damage analysis	60
4.2 STUDIES ON GSC DOUBLE-LAYER BREAKWATERS (SAND ALONE)	78
4.2.1 Wave runup studies	79
4.2.2 Wave rundown studies	81
4.2.3 Wave reflection analysis	86
4.2.4 Stability and Damage analysis	88
4.3 STUDIES ON GSC BREAKWATERS FILLED WITH CEMENT AND SAND	102
4.3.1 Wave runup studies	103
4.3.2 Wave rundown studies	104
4.3.3 Reflection Analysis	106
4.3.4 Stability and Damage Analysis	106
4.4 COMPARISON OF CEMENT FILLED CONFIGURATIONS	112

4.4.1	Comparative analysis of wave runup	112
4.4.2	Comparative analysis of wave rundown	114
4.4.3	Comparative analysis of reflection	114
4.4.4	Comparison of stability	115
CHAPTER 5		
CONCLUSIONS		117
5.1	GENERAL CONCLUSIONS OF EXPERIMENTATION ON BREAKWATERS ARMOURED WITH SINGLE LAYER GSC UNITS.	117
5.2	GENERAL CONCLUSIONS OF EXPERIMENTATION ON BREAKWATERS ARMOURED WITH DOUBLE LAYER GSC UNITS.	119
5.3	GENERAL CONCLUSIONS OF EXPERIMENTATION ON BREAKWATERS ARMOURED WITH CEMENT-FILLED GSC UNITS.	120
5.4	SUMMARY OF CONCLUSIONS	121
5.5	FUTURE SCOPE	122
REFERENCES		124
PUBLICATIONS		136

LIST OF FIGURES

Fig. No.	Title	Page No.
Fig. 2.1	Geotextile bag seawall at Ispingo, South Africa (Corbella and Stretch 2012)	9
Fig. 2.2	Major failure modes identified for revetments made of GSCs	11
Fig. 2.3	Range of reflection coefficient of GSC revetment (Recio 2008)	14
Fig. 2.4	Variation of K_r with respect to surf similarity parameter (ξ_0)	15
Fig. 2.5	Definition sketch of wave runup (Rasmeemasuang et al. 2014)	17
Fig. 2.6	Wave run down over Articulated concrete block mattress revetment	22
Fig. 2.7	Geotextile tubes at Shankarpur (Sundar et al. 2009).	24
Fig. 2.8	Geotextile reef at INS Hamla, Maharashtra (Tayade et al. 2015)	25
Fig. 2.9	Nearshore reef at Candolim, Goa, (Kudale et al. 2014).	26
Fig. 2.10	Nearshore reef at Dahanu, Maharashtra (Kudale et al. 2014).	26
Fig. 2.11	Construction stages of seawall at Uppada, Andhra Pradesh, (Sundar 2013).	27
Fig. 2.12	Coastal protections using geobags in Ullal, Karnataka (Jackson 2016).	28
Fig. 2.13	Geotube island reclamation, Cheruvattor, Kerala	29
Fig. 3.1	Calculation of theoretical volume of GSC	34
Fig. 3.2	Schematic diagram of GSC breakwater model.	35
Fig. 3.3	Construction stages of geotextile breakwater	38
Fig. 3.4	Dimensions and placement modes of various GSC units.	39
Fig. 3.5.	Schematic representation of GSC breakwater model.	41
Fig. 3.6	Flowchart showing the detailed methodology	43
Fig. 4.1	Single-layer GSC breakwater model after construction	45
Fig. 4.2	Variation of relative runup (R_u/H_0)	46
Fig. 4.3	Variation of relative runup of various configurations	48
Fig. 4.4	Variation of relative runup of different configurations	49
Fig. 4.5	Variation of relative rundown (R_d/H_0) with (d/gT^2)	50
Fig. 4.6	Variation of relative rundown of various configurations	52
Fig. 4.7	Variation of relative rundown with respect to surf similarity parameter (ξ_0)	53

Fig. 4.8 Reflection coefficient (K_r) values with respect to wave steepness	54
Fig. 4.9 Plots showing dependence of wave period on reflection coefficient (K_r)	55
Fig. 4.10 Variation of reflection coefficient (K_r)	56
Fig. 4.11 Variation of K_r with respect to surf similarity parameter (ξ_0)	58
Fig. 4.12 Reflection curves of different configurations of GSC breakwater	59
Fig. 4.13 Stable structure ('Bag 1')	61
Fig. 4.14 Bag 1 configuration	62
Fig. 4.15 Damage of GSC armour units (Bag 1)	63
Fig. 4.16 Variation of stability number (N_s) with surf similarity parameter (ξ_0)	65
Fig. 4.17 Stability curves for various GSC configurations.	67
Fig. 4.18 Percentage damage	68
Fig. 4.19 Comparison of stability curves of Bag 1 and Bag 3 (100% filled bags)	68
Fig. 4.20 Comparison of stability curves of Bag 2 and Bag 4 (80% filled bags).	69
Fig. 4.21 Comparison of contact surface area offered by Bags	69
Fig. 4.22 Comparison of stability curves of structure comprising Bag 1 and Bag 2	70
Fig. 4.23 Comparison of stability curves of the structure comprising Bag 3 and Bag 4.	71
Fig. 4.24 Effect of water depth on the stability of GSC breakwaters	72
Fig. 4.25 Variation of damage level with respect to incident wave heights	73
Fig. 4.27 Variation of damage level with respect to incident wave height	76
Fig. 4.27 Stability nomograms for GSC breakwater	78
Fig. 4.28 Constructed model of double-layer GSC breakwater structure.	78
Fig. 4.29 Constructed model of double-layer GSC slope-parallel outer layer.	79
Fig. 4.30 Variation (R_u/H_0) with respect to deep water wave steepness (H_0/gT^2)	80
Fig. 4.31 Variation of relative runup of various configurations	82
Fig. 4.32 Variation (R_d/H_0) with wave steepness (H_0/gT^2)	83
Fig. 4.33 Variation of relative rundown of various configurations	85
Fig. 4.34 Reflection coefficient K_r with respect to wave steepness	87
Fig. 4.35 Effect of various placement modes on reflection	89
Fig. 4.36 Bag 1 Double-layer configuration	90

Fig. 4.37 Total Failure (DC4) after exposure to 0.16 m wave heights.	91
Fig. 4.38 Readjusted primary layer forming slope-parallel arrangement for Bag 1	91
Fig. 4.39 Effect of armour unit size on stability of GSC breakwaters	92
Fig. 4.40 Graphs showing comparative analysis of the stability	94
Fig. 4.41 Stability curves of GSC breakwaters with varying water depth	95
Fig. 4.42 Damage levels exhibited by various test configurations.	96
Fig. 4.43 Graphs representing non-damaging incident wave height	98
Fig. 4.44 Graphs representing non-damaging incident wave height	99
Fig. 4.45 Graphs representing comparative analysis of stability curves	100
Fig. 4.46 Stability nomograms for GSC breakwaters of different relative water depths.	101
Fig. 4.47 Relative runup of all tested configurations	103
Fig. 4.48 Relative runup vs wave height to depth ratio (H_0/d)	104
Fig. 4.49 Relative rundown of all tested configurations	105
Fig. 4.50 Relative rundown vs wave height to depth ratio (H_0/d)	105
Fig. 4.51 Calculated K_r values for all the tested cases	106
Fig. 4.52, Image showing sand container filled to 15% cement	107
Fig. 4.53 Incipient motion curves for Bag 3 filled to 15% cement, single layer	108
Fig. 4.54 Incipient motion curves for Bag 3 filled to 20% cement	108
Fig. 4.55 Incipient motion curves for Bag 3 filled to 20% cement, double layer.	109
Fig. 4.56 Stability curves of all experimented configurations	110
Fig. 4.57 Stability curves of all experimented configurations	111
Fig. 4.58 Stability curves of all experimented configurations	111
Fig. 4.59 Comparative analysis of runup behaviour of all the tested configurations	113
Fig. 4.60 Relative wave runup for various placement modes of Bag 3	113
Fig. 4.61 Comparative analysis of rundown behaviour of all the tested configurations	114
Fig. 4.62 Reflection curves	115
Fig. 4.63 Stability curves for Bag 3 with all the tested arrangements	116

LIST OF TABLES

Table No.	Title	Page No.
Table 2.1	Range of K_r for various geotextile structures	16
Table 2.2	Range of relative runup (R_u/H_0) for various breakwater structures	19
Table 3.1	Calculated dimensions of GSC units.	35
Table 3.2	Range of governing variables.	36
Table 3.3	Non-dimensional model and wave characteristics.	37
Table 3.4	Properties of construction materials used.	37
Table 3.5	Porosity of various tested GSC breakwater configurations	40
Table 3.6	Damage classification criteria for GSC structures as proposed by Dassanayake and Oumeraci (2012b).	41
Table 4.1	Maximum limit of non-damaging incident wave heights observed for various GSC configurations	75

NOMENCLATURE

B	Crest width
C_w	Empirical parameter for stability
d	Water depth
D	Armour layer thickness, given by $l_c \cdot \sin \alpha$
DC0	No Damage
DC1	Incipient motion
DC2	Minor damage
DC3	Medium damage
DC4	Total failure
DL	Double-layer
E_I	Incident wave energy
E_T	Transmitted wave energy
g	Acceleration due to gravity
GSC	Geotextile sand container
h	Crest height
H	Wave height
H_0	Deepwater wave height
H_I	Incident wave height
H_T	Transmitted wave height
K_r	Reflection coefficient
K_T	Transmission coefficient
l_c	Length of GSC armour units.
N_s	Stability number
PS	Parallel to slope
r	Roughness height of GSC
R_d	Rundown
R_u	Runup
SL	Single-layer

T	Wave period
t	Tonnes (Weight)
V	Volume of GSC units
α	Slope angle
ξ_0	Surf similarity parameter.
ρ_{GSC}	Density of armour units (2005 Kg/m ³)
ρ_w	Density of seawater (1025 kg/m ³)

CHAPTER 1

INTRODUCTION

Ocean waves can often cause severe damage to the coastline, livelihood, and properties and disturb the tranquillity in ports and harbours, causing threats to berthed ships (Sindhu et al. 2015). Increasing instances of major cyclones, associated storm surges and coastal inundations create havoc in coastal areas (Albert and Bhaskaran 2020; Krishnan et al. 2021; Sreelakshmi and Bhaskaran 2020). Global climate change and sea-level rise can also be fatal to low-lying coastal zone (Parthasarathy et al. 2020). Approximately 20% of the world's coastline constitutes sandy beaches, out of which more than 60% have been experiencing severe erosion over the past decades (Corbella and Stretch 2012). As far as India is concerned, 1200 km stretch of our coastline is under threat of erosion (Kudale et al. 2014). This erosion trend is assumed to be increasing as a repercussion of increasing sea level rise, storm frequency and intensity. Consequently, coastal engineers are forced to emphasise the protection of eroding shorelines to retain our natural beaches, which constitute the first line of coastal defence.

Coastal protection can be classified into two genres: hard and soft solutions. While seawalls, dikes, groins, artificial breakwaters, etc., serve as hard solutions, beach restoration, vegetation, sand bypassing, dune replenishment, etc., are considered soft solutions. Hard solutions or grey solutions mainly involve the construction of breakwaters, usually comprised of natural rocks, artificial armour units, etc., which are challenging to construct and maintain. Moreover, the non-availability of natural stones of the required weight and size and the cost of machinery and equipment required to carry it from the quarry to the construction field aggravates the issue (Kudale et al. 2014). The alarming increase in the cost of natural rock, reduced availability and prohibition of quarrying in many states demand viable alternatives to rock structures (Jackson, 2016). Over the years, there have been tremendous innovations in artificial armour units. Concrete Cubes, Tetrapods, Accropods, Dolos, Core Loc etc., are some notable armour units. Research extended in designing innovative breakwater structures. Some notable contributions in this

regard include semi and quarter circular breakwater (Binumol et al. 2020; Dhinakaran et al. 2010), plate breakwater (Rao et al. 2009), tandem breakwater (Shirlal et al. 2007), floating pipe breakwaters (Hegde et al. 2007; Mani and Jayakumar 1995), pile breakwater (Sathyanarayana et al. 2021; Suvarna et al. 2021) etc. At the same time, these alternatives should be economical and eco-friendly (Shin and Oh, 2007). In this scenario, geosynthetics emerges as a viable alternative.

By the early 1920s, South Carolina Highway Department had used a new construction material comprising high-quality textile for road construction. Later, engineers started effectively using these for coastal engineering applications and began to be known by the name 'Geosynthetics' (Recio and Oumeraci, 2007). Geotextiles are permeable polymeric fabric that allows the flow of water through and retains the material by which it is filled. Geosynthetics find recent applications as revetments (Bezuijen and Pilarczyk 2012), embankments (Nishold et al. 2014), groins, breakwater (Hornsey et al. 2011), clay liners and liquid waste containment systems (Rowe et al. 2010, 2014; Rowe and Shoaib, 2017). Geotextiles are used in various marine applications such as coastal protection structures (Kiran et al. 2015; Kudale et al. 2014; Pilarczyk 2000; Shin and Oh 2007; Sundar et al. 2009).

Geosynthetic sand containers (GSCs) are proved to possess various benefits over conventional rock constructions (Jackson et al. 2008). It can supply a wide range of uniformly sized armour units, which is very difficult in the case of rocks. Cost per unit volume can be reduced when the size of containers is large, reducing construction time significantly. Fill ratio affects stability and shape due to interlocking and flexibility (Steege et al., 2011). It can also be stacked to steeper slopes when compared to conventional structures. Another attractive feature of the geotextile constructions is the insitu filling capability of the tube or containers with locally available materials, making the construction cost-effective and rapid (Pilarczyk 1997). The above-stated advantages make sand-filled geotextile units a viable alternative to the primary and secondary armour units of a conventional rubble mound breakwater. There have been fewer attempts to quantify

the performance of geotextile units in a breakwater structure, motivating one to pursue the present study. To sum up, GSCs offer the following benefits.

- Construction time, work volume and cost can be reduced as GSC structures involve large units stacked to steeper slopes.
- Locally available sand or dredged waste can be utilised instead of massive rock armour units.
- Eco-friendly approach, as it can act as a platform for marine growth, even in case of damage, expelled sand from containers is harmless, and GSCs can be easily removed from the site.
- It can also be used as a temporary construction material to study proposed coastal structures' response and environmental repercussions.
- Ease of modification or reshaping after extreme events.

There may arise queries on how these huge units can be filled, lifted and placed with precision in position. Filling in slurry form can be equipped with pumps (Shin and Oh 2003), whereas filling in dry form can use techniques like J-bin technology (Jackson 2016). Split bottom barges with Global Positioning System can be harnessed to accurately position the geotextile sand containment units (Borrero et al. 2010; Jackson et al. 2012; Recio and Oumeraci 2009).

In spite of these advantages, aspects pertaining to durability, incident and damage resulting from vandalism remains a major challenge. Additionally, GSC structures lack proper design guidelines. There have been successful attempts to construct seawalls, submerged tube breakwaters and coastal revetments using GSCs, but not as breakwater encasing a harbour area. Harnessing the advantages of GSCs and addressing its limitations, the present work involves the feasibility study of an emerged, non-overtopping breakwater armoured with GSC units, which may substitute conventional structures. The current investigation aims to bridge the knowledge gaps in the stability considerations and hydraulic performance (including wave transmission, reflection, runup and rundown) of breakwaters armoured with geotextile sand units and provide design guidelines for field applications.

As a part of proposing a viable alternative for conventional breakwaters, the present study involved a novel approach of using GSCs as the armour units. Initially, GSC units are arranged in a single layer over the core, making an emerged breakwaters. The study analysed the damage by varying the size and sand fill ratio of GSCs, concluding that the bags with the higher dimension and 100% sand fill are more stable than other test cases. Hydraulic performances of single-layer GSC breakwaters were also examined. Further experimentations investigated the variation of stability and hydrodynamic parameters when armour unit layers' number and placement modes are altered. Double layer placement of the armour units in a breakwater structure is examined. In the case of double-layer GSC breakwaters, secondary layer armour units act as a separator for the first layer. The units in the primary layer tend to rock, detach or displace from the structure resulting in core exposure in the absence of a second armour unit layer. In due course of experimentation, some detaching GSC units are observed to readjust themselves parallel to the structure slope, exhibiting higher stability. The present investigation also explored the possibility of such 'slope parallel placement' of GSC units which may help in enormous reduction of construction materials if proved stable. As a pilot study, breakwaters armoured with cement and sand-filled units were also tested and compared with sand-alone GSC units for their stability and hydraulic performance. Collectively the present thesis aims at the following,

- To experiment with the possibility of geotextile sand containers in using as armour units of breakwater structures.
- To provide design guidelines for GSC breakwater structures.
- Investigate stability and hydraulic performance of various GSC breakwater configurations.
- Compare the damage pattern of various configurations of GSC breakwaters
- Investigate the effect of armour unit placement and filling material in determining the stability and hydraulic performance
- Investigate sand and cement-filled geotextile containers being used as breakwater armour units.
- Compare the stability and hydraulic performance of all the tested configurations

- Provide stability curves and design guidelines for GSC breakwaters.

1.1 ORGANISATION OF THE THESIS

The present thesis is organised into five different chapters. Chapter 1 deals with the introductory facts regarding the problem of unavailability of natural resources for breakwater construction. It also discusses a brief timeline of geosynthetics being used as coastal protection structures. A brief discussion on the conducted research is also outlined. Chapter 2 presents the in-depth theoretical background of the research work. Detailed discussions on geotextile materials, its types, fabrication process, sand fill ratio, etc., are provided. Moreover, the stability and hydraulic performance of various conventional protection structures are compared with the existing geotextile protection structures in the same chapter. The global experiences of using coastal geotextile protection structures are briefly discussed, with the Indian experiences being analysed and reviewed in detail. Chapter 3 deals with the adopted methodology of the research work. The detailed design of the GSC breakwater is discussed in this chapter. Information regarding the wave mechanics laboratory and the experimentation techniques appears here. The complete results and analysis of the current research work are included in chapter 4. This chapter is subdivided into four, concerning model studies on single-layer GSC armour unit breakwaters, double-layer GSC armour unit breakwaters, sand-cement-filled armour unit breakwaters and a comparison of the above three. The conclusions and inferences from the extensive research work have been compiled in chapter 5. This includes the general conclusions from the comprehensive model studies on the stability and hydraulic performance of various GSC breakwater configurations.

CHAPTER 2

THEORETICAL BACKGROUND

2.1 GEOSYNTHETICS- AN OVERVIEW

The term Geosynthetics refers to a broad spectrum of synthetic polymer materials that are exclusively fabricated for geotechnical, environmental, transportation and hydraulic engineering. It finds wide application in civil engineering, specifically in separation, filtration, reinforcement, drainage, fluid/gas containment, slope stabilisation and erosion control (Pilarczyk 2000). The polymeric materials generally used for the manufacturing of geosynthetics are Polyester (PET), Polyethylene (PE), Polypropylene (PP) and Polyamide (PA). Geosynthetics can be broadly classified into – Geotextiles, Geogrids, Geonets, Geomembranes, Geocomposites, Geocells, Geofoam etc., based on the method of construction and application (Pilarczyk 1997). Extensive research on geosynthetics is going on, and new types of products are being introduced.

Geotextiles are continuous sheets of fibres that are flexible, permeable and have the appearance of a fabric. Geotextiles are broadly classified into- Woven and Non-woven fabric (Heerten et al. 2000; Jackson 2010; Soysa et al. 2012). Woven geotextiles are made out of polypropylene yarns and are woven using textile looms. They possess uniform and fine textures and have identical apparent opening sizes. Woven geotextiles have large tensile strength and low elongation. Non-woven geotextiles are made like felts, where a conveyor belt takes a mass of fibres through a machine that binds them into a single fabric. The binding process can be chemical bonding, heat bonding or needle punching, where barbed needles are used to entangle the fibres. Non-woven geotextiles are thicker than woven geotextiles, they perform well with regard to filtration and puncture resistance but have lower tensile strength and more elongation.

An extensive literature survey revealed that ‘Geotextile sand containment’ systems used for marine applications can be tubes, containers and bags. Geotextile tubes are massive structures, usually ranging from 1 m to 10 m in diameter and can be up to 200 m in length.

They are filled at the site, using hydraulic pumping of a sand slurry. These massive tubes are generally used to construct detached submerged breakwaters, nearshore reefs, seawalls etc. (Borrero et al., 2010; Kim et al., 2018; Kudale et al., 2014; Lawson, 2008; Oh and Shin, 2006; Shin and Oh, 2007; Steeg et al., 2011; Zornberg, 2013). Oh and Shin (2006), Kudale et al. (2014), and Kiran et al. (2015) discuss the use of locally dredged sand-water mixture to fill the geotubes, whereas Lawson (2008) describes the use of contaminated sediments and waste materials in filling geotubes.

When the volume of units is sufficiently large, i.e. in a range of 100 m³ to 700 m³, they are termed geotextile containers (Hornsey et al., 2011 and Lawson, 2008). These containers are filled onshore and are transported to the site using split-bottom barges for the construction of artificial reefs, containment dikes and submerged breakwaters. Tubes are generally used in shallow water conditions, whereas containers require deep water as the barges must be able to sail over the required dumping location (Bezuijen, 2013). However, there are issues and challenges on how these huge units are lifted, transported and placed with precision in the site. Split bottom barges with Global Positioning System can be harnessed to accurately position the geotextile sand containment units (Borrero et al. 2010; Jackson et al. 2012; Recio and Oumeraci 2009).

Lastly, Geotextiles bags are small units in the range of 0.05 m³ to 5 m³ and are extensively used for temporary coastal protection structures like seawalls. Structures made of Geobags have been discussed by Akter et al. (2013) and Jackson (2016). Additionally, tubes and bags are even used as the core of breakwater structures (Fowler et al., 2002; Nasar et al., 2004 and Oumeraci and Kortenhaus, 2011). An example of a geotextile seawall is shown in Fig. 2.1. In all these geotextile sand encapsulated structures, the percentage of sand filling plays a vital role in the stability and is discussed in detail in the following section.



Fig. 2.1 Geotextile bag seawall at Ispingo, South Africa (Corbella and Stretch 2012)

2.1.1 Sand fill ratio

Geotextile coastal protection systems commonly use sand as a major filler material. According to Koffler et al. (2008), sand is considered the best fill material. According to Faraci (2018), sand fill ratio is defined as the “ratio of volume of fully inflated bag to the actual volume of filled bag”, whereas Bezuijen (2013) defines sand fill ratio as “cross-sectional area of sand filled container or tube divided by maximum theoretical cross-sectional area, that is possible for a given circumference of the geotextile”. The theoretical maximum area is attained when the container is in the form of a perfect circle. In the field, sand fill ratio is often calculated by the ratio of the actual height of the tube and theoretical maximum height. Sand can be filled both in dry form and slurry form. Geobags and containers (Bezuijen et al. 2002) are filled using dry sand, as this process is simple and usually carried out from land. Various innovative techniques have been adopted to simplify the sand filling process, such as the ‘Grab Units’ to fill the 1 m³ bags at Ullal berm, Mangaluru, Karnataka, India (Jackson, 2016) and ‘J-Bin’ Technology to fill the 2.5 m³ geobags in Maroochydore Beach Groynes, Australia (Hornsey et al., 2011). While geobags and geocontainers use dry sand, geotubes are filled using sand slurry, generally pumped at the site (Borrero et al., 2010 and Mead et al., 2010). Apart from sand, sand-cement mortar

and dredged waste are also used for filling in some cases (Pilarczyk, 1997; Plaut and Klusman, 1999 and Shin and Oh, 2003).

According to Bezuijen et al. (2002), sand fill ratio of tubes should be 70 – 80%. When Permanent International Association of Navigation Congresses (PIANC, 2011) recommends a sand fill ratio of 80%, studies conducted by Dassanayake and Oumeraci (2013) on geobags show 36% higher stability for 100% filled bags compared with 80% filled bags. Faraci (2018) carried out experimental studies on submerged geotextile containers with 94% sand fill ratio. Shirlal and Mallidi (2015) conducted studies on 100% filled sandbags. Both authors report improved stability for highly filled bags. However, Faraci (2018) specifies a lower reflection for bags filled with fine sand. It has to be noted that filling bags to 100% in model studies is comfortable but in actual practice, attaining a 100% sand fill ratio is a herculean task. All the investigations lead to the general conclusion that the degree of sand fill should be between 70 - 100% and should not be less than 60%. Migration of sand inside the geotube due to a low filling percentage (less than 60%) is indicated as ‘Caterpillar mechanism’, as it resembles the movement of a caterpillar (Steeg et al., 2011). This mechanism causes higher instability of geotubes and geocontainers. The authors specify that Froude’s scaling cannot be applied for structures observed with caterpillar mechanism. Caterpillar mechanism is not observed when the fill percentage is higher. In such cases, Froude’s scaling laws are applicable. Kriel (2012) specifies 80% to be the maximum practical filling percentage that can be attained by geotubes in the field. Therefore, it may be concluded that to ensure the stability of geotubes, a safe sand fill ratio of 70-100% may be practised.

2.2 STABILITY AND DAMAGE ANALYSIS OF GSCS

2.2.1 Structural damages of GSCs

Major failure modes or wave-induced damages of GSC structures are identified to be pullout, sliding, overturning, puncturing and toe scour (Jackson et al., 2006; Recio and Oumeraci, 2009 and Akter et al., 2013) (see Fig. 2.2). Overturning of GSC units is observed in the crest layers, while pullout and sliding instability is reported in units within

critical layers. In most reviewed cases, failure is due to the horizontal or vertical displacement of the containers and is subjected to interface friction, contact surface area, vertical restoring load etc. The percentage of sand filling is identified as another guiding parameter. Dassanayake and Oumeraci (2012b) reports higher pullout and sliding in 80% filled containers than 100% filled ones. This is due to the increased free spaces and reduced restoring force forces of 80% filled containers. Toe scouring occurs at the GSCs located at the seabed, scour aprons and anchor tubes are suggested for minimising scouring and undermining (Jones et al., 2006 and Lawson, 2008). Interface friction is identified to be a significant contributor to the hydraulic stability of GSC units (Recio and Oumeraci 2008). It has to be noted that the effect of interface friction is not yet fully examined.

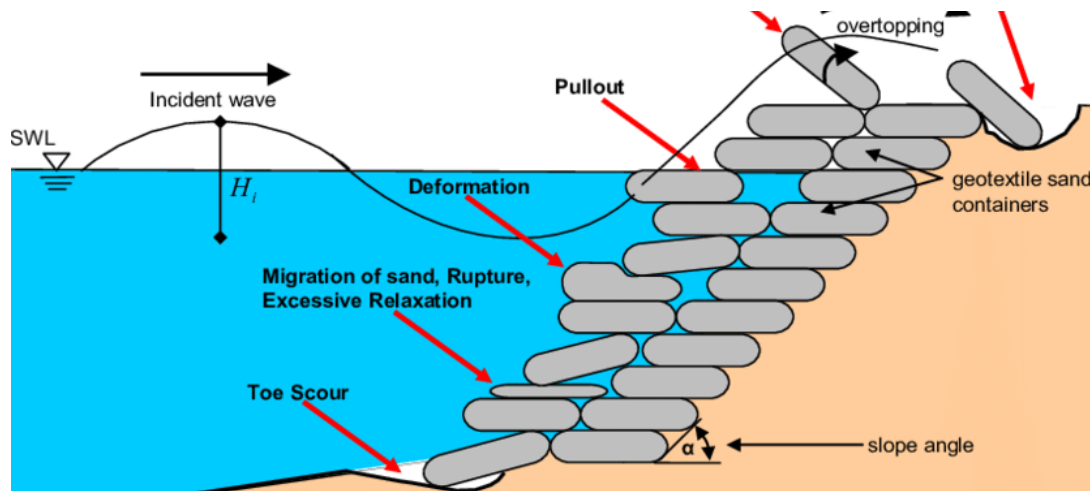


Fig. 2.2 Major failure modes identified for revetments made of GSCs (Recio and Oumeraci 2008)

2.2.2 Anthropogenic Damages

Exposed GSC structures are susceptible to damage by anthropogenic causes (Hornsey et al. 2011). They can be categorised as,

- Vandalism
- Incidental Damages
- Biological Damages

Vandalism or deliberate destruction of GSC structures is a major concern and remains a prime disadvantage. GSCs, when designed as exposed structures, attract the curiosity of the local population and consequently cutting it with sharp tools have been reported. Knife cut vandalism has led to the failure of Kirra Groyne (Gold Coast, Australia), St Clair revetment (Dunedin, New Zealand), Submerged Reef at Kovalam, Kerala etc. (Hornsey et al. 2011 and Corbella and Stretch 2012). Once the containers are cut, the sand fill leaks out due to waves leading to total deflation and failure.

Incidental damages are mainly due to boats making a direct impact or anchoring on the structure. Certain fishing activities involving sharp rods can tear the geotextiles, leading to sand loss (Borrero et al. 2010). Ice and driftwood also cause incidental damages (Hornsey et al. 2011). Incidental damages depend upon the site and may vary from place to place. Seawalls are less susceptible to incidental damage compared to a structure constructed adjacent to a boat landing facility.

Corbella and Stretch (2012) point out the incident of rats and rodents nesting around the GSC structures and is grouped as biological damage. Food waste encourages the colonisation of rats resulting in the tearing of geotextiles using their tooth. All the above damages are attributed to the textile nature of geosynthetics. When appropriately strengthened, it can attain vandal-resistant properties. Literature suggests the usage of various coatings improving the vandal resistance of geotextiles from the 1990s. Polyurethane spray is one such coating, which improved the properties to a limited extent while having a higher cost (Hornsey et al. 2011). Saathoff et al. (2007) suggested a composite vandal-deterrent geotextile, which has a layer entrapped with 3 kg of sand per square meter. This improved the durability and life of GSC. However, these textiles fail to resist when deliberately punctured with extremely sharp tools. GSCs used in dune protection should be covered with sand, promoting vegetation growth over it. This not only stabilises backshore morphology but improves vandal resistance as well. An additional cover layer of rock gabions proves effective in vandal resistance, as implicated in the construction of saline embankment at Penth Coast, Odisha, and seawalls at Uppada,

Andhra Pradesh (Nishold et al. 2014; Kiran et al. 2015 and Nishold et al. 2018). Rajagopal et al (2013) describes the use of cement-sand mortar in filling geotextile bags. Cement and sand are mixed together and filled in a dry form. Water contact helps in the hydration and setting of mortar-filled bags, making them hard and vandal-resistant units. It may alter the behaviour of geobags and is yet to be comprehensively analysed.

2.3 HYDRODYNAMIC STUDIES ON GSC STRUCTURES

The shoreline response of a breakwater depends on various factors, from which wave transmission and reflection play a vital role (Hanson and Kraus 1990). Based on these parameters, a Tombolo, Salient or Null response can be observed on the shoreward side of the reef structure. Model studies revealing wave transmission, reflection, runup and rundown behaviour are inevitable before implementing a new reef structure. A brief discussion about the hydraulic performance of GSC structures is provided.

2.3.1 Wave transmission

Since the prime objective of a breakwater is to lessen the wave energy on the lee-side, the efficiency of such structures depends upon their transmission characteristics. According to Shore Protection Manual (1984), wave transmission coefficient K_T is defined as the ratio of the wave height directly shoreward of the breakwater to the height directly seaward of the breakwater. K_T generally takes a value between 0 and 1 see eqn. (2.1), with 0 representing no transmission (highly impermeable) and 1 representing full transmission, as if no breakwater is present (Pilarczyk 2003).

$$K_T = \frac{H_T}{H_I} = \sqrt{\frac{E_T}{E_I}} \quad (2.1)$$

Where K_T is the coefficient of transmission, H_T is the height of transmitted waves in the leeward side of the breakwater, H_I is the incident wave height seaward of the structure. It can also be expressed as the square root of the ratio of transmitted wave energy (E_T) to incident wave energy (E_I) (Nishold et al. 2019). The major parameters that govern the wave transmission include – crest height and width, the slope of the structures, core and armour material, tidal and design water level, wave height and period (Pilarczyk 2003).

2.3.2 Wave Reflection

Wave reflection from coastal structures may severely affect structural stability by increasing bed scour. It may also increase the foreshore's erosion and the neighbouring coastlines (Oumeraci and Kortenhuis 2011). Wave reflection over GSC structures has been discussed by various researchers, including Pilarczyk (2003), Recio (2008), Oumeraci and Kortenhuis (2011), Soysa et al. (2012), Kriel (2012) etc. It has to be noted that wave reflection is bound to large uncertainties as it cannot be directly measured (Kriel 2012). An experimental investigation on a double layer GSC revetment revealed a reflection coefficient (K_r) ranging from 0.5 to 0.7 (Recio 2008) See Fig. 2.3.

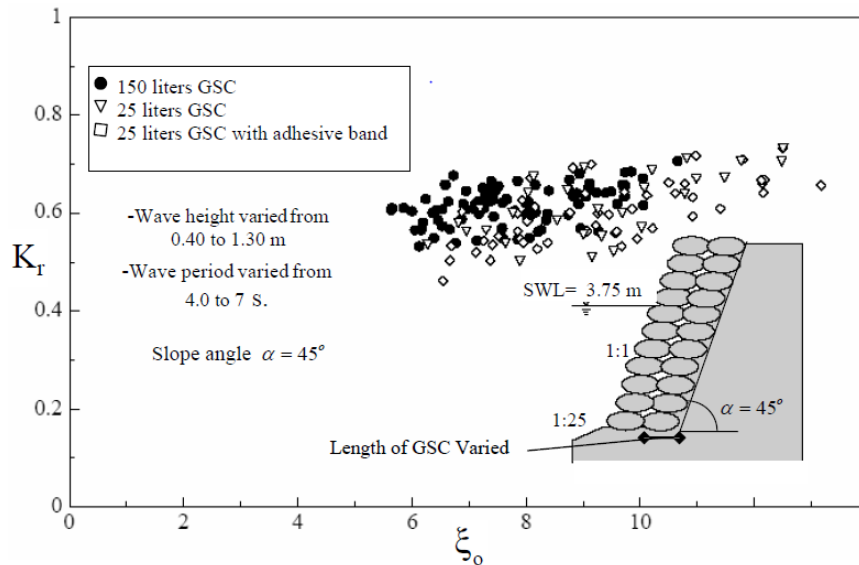


Fig. 2.3 Range of reflection coefficient of GSC revetment (Recio 2008)

Neves (2011) reports reflection studies on geotextile sand encapsulated systems at a 28 m long, 12 m wide and 1.2 m high piston type, movable bed wave basin at the Department of Civil Engineering, University of Porto, Portugal. The study reveals that K_r is directly related to the wave period, thereby with wavelength and surf similarity parameter and inversely related to wave height and wave steepness. The range of K_r is identified to be 0.26 to 0.57. When geosynthetic tubes are used as the core of breakwaters, no significant changes are observed in reflection characteristics with respect to a conventional rubble mound breakwater (Oumeraci and Kortenhuis 2011). K_r was found to be ranging from

0.22 to 0.54. In contrast, a study conducted by Nasar et al. (2004) observed 7 to 8% more reflection in geo-core breakwaters than rubble-core ones. The increase in the reflection is because of the dense sand-filled geobags in the core. In conventional breakwaters, water waves encounter a porous core soon after they penetrate the primary armour units, this will create additional absorption and energy dissipation by the core, unlike in the case of geo-core breakwaters. Experimental investigations by Nishold et al. (2019) reveal a K_r value of 0.15 to 0.45 for a tested geotube embankment system. A 50 to 70% decrease in K_r is reported when the geotube structure is supplemented with rock gabion boxes. These porous boxes effectively aid in wave dissipation on the structure.

Experimental investigations by Faraci (2018) on submerged reefs made of GSCs, report a reflection coefficient (K_r) increase up to 0.6. K_r values are found to be decreasing with increasing relative water depth and wave height. As water depth increases, more waves can be transmitted without breaking over the submerged structure. Using fine sand also helps in the reduction of the reflected wave energy from the GSC reef structure. The study also reports that there is no significant difference in the response of GSC structure to regular and random waves, as shown in Fig. 2.4. Ordered and disordered placement techniques

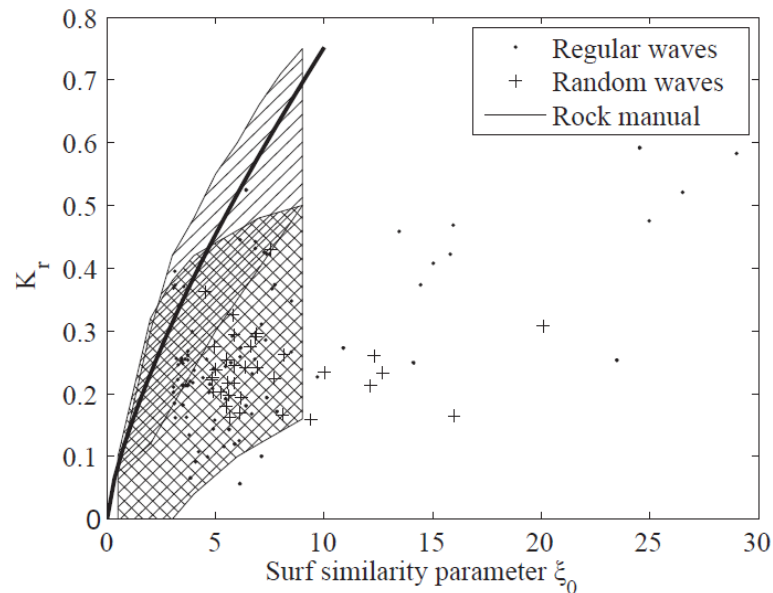


Fig. 2.4 Variation of K_r with respect to surf similarity parameter (ξ_0) for submerged GSC reef (Faraci 2018)

have been tested, with orderly configuration with higher roughness exhibiting lower reflection values. The structure behaves similar to traditional low-crested structures, in terms of reflection. A summarised form of existing reflection studies conducted on geotextile containment systems is outlined in Table 2.1. From the literature survey, it has been identified that most geotextile structures behave similarly to conventional structures from a reflection point of view.

Table 2.1 Range of K_r for various geotextile structures

Sl no	Contributor(s)	Year	Model details	Range of reflection coefficient (K_r)
1	Oumeraci	2002	Geotextile revetment	0.5 to 0.7
2	Juan Recio	2008	Geotextile revetment	0.5 to 0.7
3	L. Neves	2011	Geotextile sand encapsulated systems	0.26 to 0.57
4	Oumeraci and Kortenhuis	2011	Geo-core breakwater	0.22 to 0.54
5	Carla Faraci	2018	Submerged reef with GSCs	0.05 to 0.6
6	Nishold et al	2019	Geotube embankment system	0.15 to 0.45

2.3.3 Wave Runup

Wave runup is the vertical distance between the still water level and the point of the maximum uprush of water on the structure (Fig. 2.5). Study on wave runup is crucial as it decides the maximum crest elevation of a coastal structure. When runup exceeds the crest elevation of the structure, water overtops, resulting in its transmission towards the leeward side; as a result, runup knowledge is required to design a structure either overtopping or non-overtopping. Attempts for quantifying runup on sandbag structures are significantly

less. However, some available published resources discussing runup studies on sandbag or geotextile containers are reviewed.

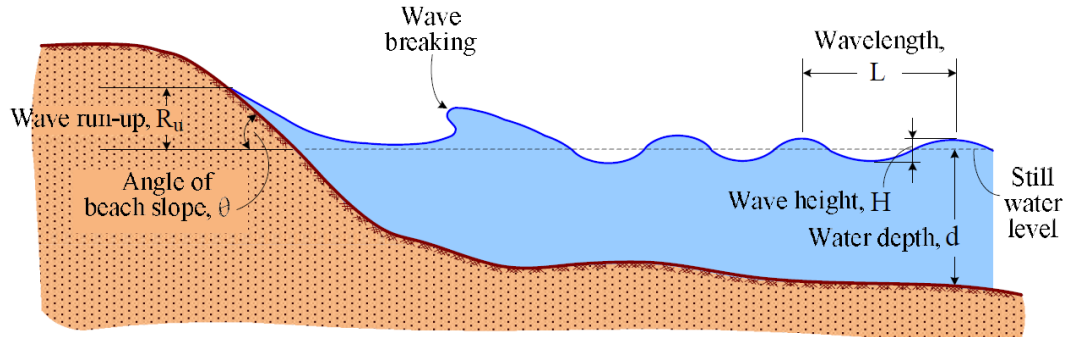


Fig. 2.5 Definition sketch of wave runup (Rasmeemasmuang et al. 2014)

Kobayashi and Jacobs (1985) used empirical equations proposed by Ahrens and McCartney, for predicting runup on sandbag revetments. This equation uses two empirical constants and surf similarity parameter for runup prediction and is found to be unreliable, as thickness and other parameters of sandbags are not considered (Rasmeemasmuang et al. 2014). It is to be noted that, after Kobayashi and Jacobs (1985), a comprehensive study of runup on sandbag structures was reported only by Rasmeemasmuang et al. (2014). During this period, much work related to GSC structures has been done, but most of it focused on stability parameters and wave transmission.

Rasmeemasmuang et al. (2014) carried out extensive experimental analysis on smooth and sandbag slopes and formulated eqn. (2.2), which relates relative runup and surf similarity parameter, along with empirical coefficients and thickness of sandbags. Where, R_0/H_0 is the relative wave runup, a_1 and b are parameters for smooth slopes, a_2 and c are empirical coefficients related to relative roughness height (r/H), where r is the roughness height or thickness. For smooth slopes, roughness height r will be equal to zero; thus, equation (2.2) reduces to (2.3).

$$\frac{R_u}{H_0} = a_1 \xi^b \left[1 - a_2 \left(\frac{r}{H} \right)^c \right] \quad (2.2)$$

$$\frac{R_u}{H_0} = a_1 \xi^b \quad (2.3)$$

The values of parameters are calculated to be, $a_1 = 0.98$, $b = 0.94$, $a_2 = 0.34$ and $c = 0.15$. The equation (2.2) for sandbag slope holds good with experimental results, with a correlation coefficient equal to 0.86. It is concluded that the increase in relative roughness height is beneficial in reducing runup. This attribute is due to increased surface roughness resulting from enhanced friction, that in turn reduces the water onrush over the structure. Relative runup is observed to be 26 to 40% lower for sandbags slopes compared to smooth slopes. In other words, an increase in roughness height reduces runup rates. Relative runup ranged from 0 to 2 for sandbag slopes and up to 2.8 for smooth, impermeable slopes.

As mentioned above, runup studies of sandbag structures are rarely reported. Therefore, it is imperative to note the relative runup values of some conventional coastal structures so that a comparative analysis can be carried out. Shankar and Jayaratne (2003) estimated a relative runup range of 1.2 to 2.8 for the smooth impermeable breakwater, Shirlal et al. (2006) found a range of 0.5 to 1.08 for reef defended breakwater. Physical model studies conducted by Rao et al. (2008) on berm breakwaters revealed a relative runup range of 0.55 to 1.15. In a broad perspective, relative runup values of existing breakwater structures range from 0.5 to 3.1 (Meer and Stam 1992, Schimmels et al. 2012, Diweddar 2016). GSC structures also exhibit runup in a similar range, with higher rates compared to rubble mound breakwaters. An outline of relative runup values for a range of existing coastal structures is provided in Table 2.2. This can be used for comparing runup behaviour of existing structures with the intended GSC breakwater structure. It has to be noted that very high values of relative runup is generally shown by smooth slopes or impermeable slopes. In such cases, wave dissipation over the structure slope is less due to lack of roughness, resulting in increased wave runup.

Table 2.2 Range of relative runup (R_u/H_0) for various breakwater structures

No.	Contributor(s)	Year	Structural details	Range of R_u/H_0
1	Shore protection manual	1984	Conventional rubble mound breakwater	0.64 to 1.04
2	van der Meer and Stam	1992	Rock slopes, revetments and breakwaters.	0.5 to 3.1
3	Shankar and Jayaratne	2003	Smooth and rough rubble mound breakwater.	1.2 to 2.8
4	Shirlal et al.	2006	Breakwater model defenced with submerged reef	0.5 to 1.08
5	Rao et al.	2008	Berm breakwater model	0.55 to 1.15
6	Schimmels et al.	2012	Porous revetments.	2.1 to 3.1
7	Arunjith et al.	2013	Breakwater models with Kolos armour units	0.8 to 1.4
8	Rasmeemasmuang et al.	2014	Sandbag slopes	0.5 to 1.9
9	Binumol et al.	2015	Quarter circle breakwater	0.1 to 0.7
10	Diwedat A. I.	2016	Rubble mound breakwater model.	1 to 2.25

2.3.4 Wave rundown

Wave rundown is the vertical distance between still water level and the maximum extent of the down rush of retarding wave, on the face of the structure. The highest potential for structural damage occurs in this region between ‘still water level’ and point of maximum down rush (Yamini et al. 2018). This is because uplift forces and the head difference will be maximum in this region. This leads to the need for accurate demarcation of rundown limits so that potential damage areas can be easily identified. Additionally, rundown

calculation is essential in computing the required elevation of the structure under still water level (Oumeraci et al. 2010). Foyer (2013) reports that runup and rundown values are nearly identical about still water level. Laboratory investigations and physical model studies of rundown on GSC structures are less compared to runup studies. Relative run down values generally range from 0.5 to 2.5 for conventional porous breakwaters (Battjes and Ary 1976, Pilarczyk 1987, Oumeraci et al. 2010, Foyer 2013, Yamini et al. 2018).

As stated earlier, studies on runup and rundown behaviour of geotextile armour units are less; therefore, a comprehensive analysis of all existing coastal protection structures is carried out to compare the results obtained in the present study. Many researchers reported relative rundown curves with respect to surf similarity parameter (ξ_0) for different coastal protection structures (dikes, revetments and breakwaters). Some important runup curves are discussed. Battjes and Ary (1976) formulated equation (2.4), for wave rundown on rough and permeable slopes with regular wave conditions.

$$R_d = R_u (1 - 0.4 * \xi_0) \quad (2.4)$$

Where R_d and R_u are rundown and runup, respectively, ξ_0 represents surf similarity parameter. Studies of van der Meer (1988) report rundown based on armour layer and core permeability. Wave runup equations of sea dikes have been deduced by Schüttrumpf 2001 (as quoted by Yamini et al. (2018)) using a hyperbolic tangent approach (2.5).

$$\frac{R_{d2\%}}{H_s} = -0.7 [1 + \tanh(\xi_0 - 2.1)] \quad (2.5)$$

Oumeraci et al. (2010) reported on the rundown behaviour of revetments, made of ELASTOCOAST, a highly porous layer made of crushed stones bonded together by polyurethane. These models were tested for their rundown behaviour in a 300 m long, 5 m wide and 7m deep wave flume at Hannover, Germany, for regular and irregular waves. It is observed that smooth, impermeable slopes show higher rundown (Pilarczyk et al. 1995) and revetments made of concrete blocks showed lower rundowns. This was attributed to higher porosity of concrete block revetments. The relative rundown curves of

ELASTOCOAST revetment lies between the values proposed by Pilarczyk et al. (1995) and Coastal Engineering Manual (2008).

Foyer (2013) carried out numerical simulations based on the experimentation on bonded porous revetments conducted at Large Wave Flume (GWK), Hannover, Germany. Numerical modelling is carried out using COBRAS-UC (VARANS – Volume averaged Reynolds averaged Navier-Stokes). Relative rundown and runup values of numerical as well as physical studies were plotted against surf similarity parameter. The runup and rundown values were found to be symmetric about $y=0$. The study also concluded that surface roughness of the revetments plays a much more important role than revetment thickness, as far as wave runup and rundown are considered. Yamini et al. (2018) compiles the relative rundown curves available for a wide range of protection structures. Most of the structures exhibit an increment in relative rundown up to surf similarity parameter equals to 3, and shows a constant value with further increase of surf similarity parameter. Articulated concrete block mattress revetment (ACB Mats) is modelled in the present study with Granular filter layer and geotextile filter layer Fig. 2.6. Rundown values of ACB mats are relatively smaller than the experimental results of other published works. The study revealed that using a geotextile filter layer increased the relative rundown up to 40% compared to ACB mat structures with the granular filter layer. This increase in the rundown is due to the outflow of water from the inside filter. An increase in rundown may result in uplift forces due to wave down rush; this may lead to sliding instability and may be an additional cause of armour displacement in the structure.

To conclude, rundown calculations are essential before implementing a structure in the field. From the review, it is identified that wave height, surf similarity parameter, geometry and surface roughness of the structure and permeability of the structure slope are the key parameters deciding the rundown level (Battjes and Ary 1976, Pilarczyk 1987, Oumeraci et al. 2010, Foyer 2013, Yamini et al. 2018). Since rundown may lead to sliding instability, a good structure should be effective in wave down rush resistance. Additionally, the review

pointed out the need for further experimentation for examining rundown behaviour of GSC structures.

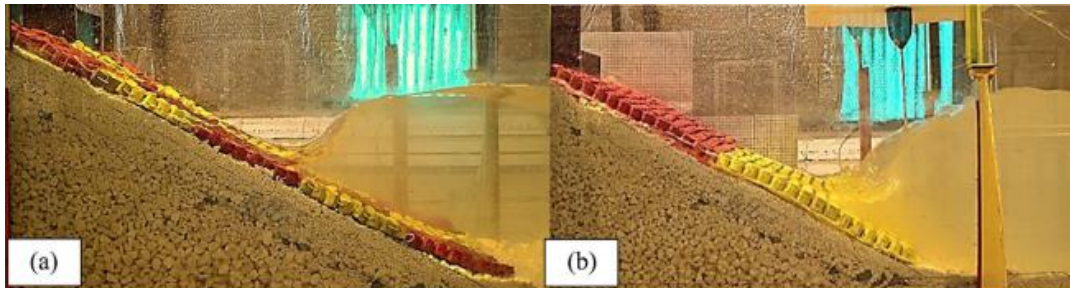


Fig. 2.6 Wave run down over Articulated concrete block mattress revetment (ACB Mats) a. ACB mats with granular filter layer b. ACB mats with geotextile filter layer (Yamini et al. 2018).

2.4 GEOSYNTHETIC STRUCTURES FILLED WITH SAND AND CEMENT

GSC structures are often filled with sand. Dry sand, sand slurry (generally 70% water 30% sand) and even dredged materials are used to fill the containers (Ashis 2015). Cement-sand mortar used in filling the containers are not very novel. Silvester (1986) carried out experiments in filling the geotextiles containers (sausage-shaped) with cement and sand. Cement and sand mixture is considered in the form of a slurry having 100% slump value allowing its easy movement in any parts of the container. These containers, when hardened, should possess the strength of limestone. An extensive study is carried out to obtain optimum mortar mix. According to Silvester, cost of structures made with grout-filled sausages can be as low as 12% compared with limestone counterparts. Rajagopal et al. (2013) describe protection structures using geosynthetics at Pulicat Lake, Tamil Nadu. The breakwater structure constructed at the site is trialled with cement-sand mixture (10% cement). Cement sand mixture is filled into containers in dry form. When immersed in water, hardening takes place within 24 hours, even in the marine environment. This helps in reducing the migration of sand inside the containers, thereby improving the performance. The authors point out the scope for quantifying structure behaviour when the percentage of cement is varied. Geo-mattresses are novel structures pumped with cement and sand slurry to form a mattress cover (Radhakrishnan 2013). They are generally used in slope

protection and river protection in estuarine areas. When cement and sand mortar is used as a filling material, geocontainers transform into a hard substance. Even when the fabric form is degraded, the hardened sand remains intact (Silvester 1986), forming more ‘vandal-resistant’ units.

2.5 GEOTEXTILE SAND CONTAINMENT SYSTEM FOR COASTAL ENGINEERING APPLICATIONS- A GLOBAL PERSPECTIVE.

Since the early 1920s, geotextiles have been used for road construction (South Carolina highway department). Later by the 1950s, geotextiles found its way to coastal engineering applications as it was used to construct an inlet dike in Plumpoint, The Netherlands (Oumeraci and Recio, 2018). Since then, there has been extensive use of geotextile tubes, bags and containers for various coastal protection works. Significant coastal protection works using geotextile containment systems include Russell head groynes (1993), Australia (Saathoff et al. 2007), Maroochydore beach Groynes, Australia (2001) (Hornsey et al., 2011), geotextile tube island protection at Amwaj, Bahrain (2002), geotextile bag seawalls at Umhlanga rock (2011), South Africa (Corbella and Stretch, 2012), submerged geotube reef at Narrowneck, Australia (Jackson et al., 2012 and Saathoff et al., 2007). As evident, geosynthetic containment systems for coastal protection flourished after the 1990s. Global success rates stimulated Indian scientists and coastal engineers to implement alternative protection measures using geosynthetics. Geotextile coastal protection branch flourished in India from 2000 and is discussed in detail in the following section.

2.6 COASTAL PROTECTION WORKS WITH GEOTEXTILE SAND CONTAINMENT UNITS- INDIAN TIMELINE

As discussed, coastal protection works involving geotextile containment units in a global context began in the 1950s (Oumeraci and Recio, 2018). These textiles were used for various other engineering projects even before but were not known by the specific name of geotextiles. Indian experiences in geotextiles coastal protection works date back to the early 1990s, with the same flourishing in India from 2000 to 2010. Over this period,

pioneering works of institutes including Central Water and Power Research Station (CWPRS) Pune, National Institute of Ocean Technology (NIOT) Chennai and Indian Institute of Technology, Madras (IITM) have contributed to the growth of GSC structures. It is imperative to understand the behaviour of such structures implemented in the field. Some of the major projects on the east and west coast of India are reviewed in the present section.

2.6.1 Geotextiles tubes, Shankarpur, West Bengal

Shankarpur is a village in West Bengal, situated on the east coast of India. Many parts of its coastal stretch were subjected to severe erosion and a 900 m long stacked geotextile reef was constructed to protect the eroding coast. The construction of geotube protection structure was completed in 2007 (Sundar et al. 2009). It consisted of two 3 m diameter geotubes at the bottom and one 3 m diameter tube at the top (Fig. 2.7). A non-woven cover of polypropylene is provided for additional UV protection (black colour). The structure is subjected to extreme wave action and got damaged (200 m length) in August 2007, and subsequently (400 m length) in monsoon 2008. In order to provide additional protection, two rows of wooden bullies filled with laterite stones were provided at 20-25 m seaward of the structure. It helped by breaking and reflecting waves in the wooden bullies, thus reducing the effect on the geotubes (Kudale et al. 2014). Post construction, polypropylene protection layer was damaged due to subsequent cyclones and high tide level, but the main tube structure remained intact.



Fig. 2.7 Geotextile tubes at Shankarpur (Sundar et al. 2009).

2.6.2 Nearshore reef at INS Hamla, Mumbai:

INS (Indian Naval Ship) Hamla is a Naval Base located at Malad, Mumbai, Maharashtra State. The beach at Hamla was experiencing serious erosion. As a protection measure, a 900 m RCC vertical retaining wall was constructed on the coast, supplemented with beach nourishment. To hold the nourished sand, a geotube reef was constructed 50 m away from the retaining wall (Fig. 2.8). The reef consisted of a layer of 3 m diameter geotextile tube with the top at mean sea level (+2.6 m) along with a scour protection layer of 1 m diameter geotextile tube at the toe of 3 m tube. The construction and nourishment were completed by March 2010. Beach stabilised after a couple of months, and tubes were buried up to a level of +1.5 m, directly pointing to the efficiency of the structure (Tayade et al. 2015).



Fig. 2.8 Geotextile reef at INS Hamla, Maharashtra (Tayade et al. 2015)

2.6.3 Nearshore reef, Candolim Goa

Candolim beach lies 15 km north of Panjim, Goa. The grounding of a 300 m long ship named 'River Princess' in 2008, 150 m away from the beach, created erosion in the southern part and accretion in the northern part of the beach (Kudale et al. 2014). A nearshore geotextile tube was proposed as the solution to the erosion problem. The reef consisted of two layers of 3 m diameter geotubes and one layer of 1 m diameter tube at the seaside toe of the main tube. Beach nourishment was carried out behind the reef structure (Fig. 2.9). The reef with a length of 800 m and 50 m distance from the coastline was completed in April 2010. Soon after the construction, sand accretion took place on the beach and continued till monsoon 2010. But the monsoon storm and larger waves resulted in the scouring of sand beneath the geotextile tubes. Scattered debris and stones punctured the geotextiles, damaging the structure (Hegde 2010).



Fig. 2.9 Nearshore reef at Candolim, Goa, (Kudale et al. 2014).

2.6.4 Nearshore reef, Dahanu, Maharashtra

Dahanu is located 110 km north of Mumbai, Maharashtra state. Dahanu beach is widely used by tourists. A PCC retaining wall was constructed for a length of 400 m, which is stepped towards the seaside. Beach nourishment was also adopted as a soft protection method. A number of offshore reefs with geo-tubes were constructed to hold the nourished sand. Construction was carried out in the year 2010-2011. It consisted of a 3 m diameter tube supplemented with a 1 m diameter tube as toe protection, placed at 120 m away from the coast (Fig. 2.10). The reef with its top layer placed at the mean sea level helped in arresting the sand on the beach, and its performance was impressive (Kudale et al. 2014).



Fig. 2.10 Nearshore reef at Dahanu, Maharashtra (Kudale et al. 2014).

2.6.5 Seawall, Uppada, Andhra Pradesh

Nearly 1.5 km stretch of coastline in Uppada village, East Godavari District of Andhra Pradesh state had been experiencing severe erosion in last 2 to 3 decades. Since it posed a serious threat to the life of villagers and some important monuments, Irrigation Department, Government of Andhra Pradesh decided to adopt a protection plan for Uppada coast. A seawall constructed with geotextile tubes and bags covered with rock gabions emerged as the solution (Sundar 2013). The core of the sea wall was made of woven polypropylene geotubes of 3 m diameter and 20 m length. 92 geotubes have been used for the entire construction, along with 3,50,000 small geobags placed over the core layer. The

outer layer of the sea wall constitutes rock gabions made of polypropylene ropes (Fig. 2.11).



Fig. 2.11 Construction stages of seawall at Uppada, Andhra Pradesh, (Sundar 2013).

The construction of a 1 km long seawall was completed in the year of 2011. It helped in reducing the erosion rate till 2014, accretion rates showed a positive trend (Kannan et al. 2018). After the Hud Hud cyclone in 2014, studies indicated massive erosion on Uppada coast due to the destruction of the protective structure.

2.6.6 Nearshore Berms, Ullal, Karnataka:

Ullal at Mangaluru in Karnataka state is located on the south coast of India. It lies adjacent to the combined river mouth of Netravathi and Gurupur River. Ullal coast had been suffering from severe erosion over decades. After 2010, erosion was so severe that many of the local fishing communities lost their houses. In order to bring down erosion, a series of shore-parallel berms made of geotextile bags were proposed. As a result, construction started using new methodologies to fill the bags on site. The ‘Grab’ methodology and ‘J-Bin’ technology have been adopted to fill the geobags (Fig. 2.12). These technologies were earlier used to fill bags in various coastal protection projects in Australia (Jackson 2016). Both methods use a crane and specialised equipment to fill and place the bags, with improved precision and pace of construction. Structures stacked with non-woven geotextile bags with 1 m³ and 2.5 m³ volumes were constructed and completed by 2014 (Kannan et al. 2018).



Fig. 2.12 Coastal protections using geobags in Ullal, Karnataka (Jackson 2016).

2.6.7 Geotube and gabion seawall, Pentha, Odisha

The coastal stretch of Odisha state is protected with saline embankment for a length of nearly 475 km made of locally available soil. The erosion of these saline embankments poses a threat to the livelihood of coastal communities. Pentha coast in Kendrapara District, Odisha, is protected by Rajnagar Gopalpur saline embankment. The retarded embankment is also susceptible to erosion, therefore, it has become essential to protect the retarded embankment. Thus, Central Government proposed to construct a geotube embankment at the seaside of the retarded embankment. A stand-alone geotube embankment with a 30 m base width, 675 m length with a design wave height of 5 m was designed by IIT Madras, Department of Ocean Engineering, in 2011 (Sundaravadivelu 2013). The construction was started in September 2013, and soon on October 12th, 2013 Pentha coast was hit by a cyclonic storm, Phailin, accompanied by torrential rain. Pentha coast was severely eroded. As a result, IIT Madras was forced to redesign the geotube embankment because of space limitations. The newly formulated design reduced the length of geotube embankment from 675 m to 505 m. The construction was completed in the year of 2016 (Nishold et al. 2018).

The structure consists of geotubes of 3 m diameter and 20 m length as the core and Polypropylene rope gabions as the outer layer. 16 mm and 9 mm diameter ultraviolet stabilised ropes were used for gabions. Hard granite stones were used to fill the gabions. Finally, gabions boxes of 2 m x 1 m x 1 m size were used. While construction, the structure faced Hud Hud cyclone 2014. The seaside gabion boxes of the embankment were not disturbed even after exposing to huge tidal surges and waves, keeping the structure intact.

Accretion of sand started building up in front geotube tube embankment, and the structure is still serving its purpose (Jugal 2018).

2.6.8 Island Reclamation, Cheruvattor, Kerala

Cheruvattor coastal village is situated in the northern part of Kerala state, in the district of Kasaragod. Cheruvattor fishing harbour is very prominent both in terms of seafood trade as well as tourism. The harbour basin contains a small island formed due to the deposition of sediments supplemented by Tejaswini River and Oripuzha. The island faced severe erosion during the monsoon season, and the government decided to reclaim the island using geotextile tubes. Thus, the island is provided with two layers of geotubes on three sides and one layer of geotubes on the remaining side. Woven geotubes of 3 m diameter and 20 m length were used (Fig. 2.13). Tubes are filled up to 80% of their capacity with a sand slurry containing 30% sand and 70% water. The construction was started in December 2017 (Details collected during Cheruvattor fishing harbour visit, 2018, Department of Harbour Engineering, Kerala state, India).



Fig. 2.13 Geotube island reclamation, Cheruvattor, Kerala (photographs taken during field visit)

It is imperative to consider aspects on coastal processes, soil behavior, extreme events vulnerability on a particular site location at the design stage. Site-specific nature of geotextile coastal protection works makes it very difficult to provide unified codes of design practice. Beginning from 1980s to 2022, the number of geotextile structures used for coastal protection works found an exponential rise. The efficacy and importance of these structures for major protection works across the Indian coast is well documented. In certain instances, various factors have led to the failure of structures, especially in

Candolim Goa. Geotube structure at Shankarapur, in spite of losing its UV protection cover, served its purpose. The review shows a positive approach in India towards geotextile coastal protection in recent years. As evident from the recent examples, geotextiles prove to be a very promising future engineering material, with adequate designs and vandalism control of such structures.

2.7 SUMMARY OF LITERATURE REVIEW

An extensive review of the available literature lights into the emerging possibilities of geosynthetic materials for coastal protection. Despite lacking a generalised design procedure or code regulations, geotextile containment units are favoured from experience. They can be a better alternative, as far as nature friendliness and ease of construction is concerned. Geotubes reefs, groynes and revetments are constructed across the globe, but there have been fewer attempts to quantify its merits when used as armour units. Stability, wave runup, rundown and reflection parameters are reviewed, and it is concluded that there were fewer attempts to quantify GSC structures' hydraulic performance (wave runup, rundown and reflection). Literature also suggests an improvement in the performance of structures when filled with sand and cement. But a comprehensive combination of armour units filled with cement and sand is not fully explored. The present research aims at bridging the above-mentioned knowledge gap.

2.8 OBJECTIVES

The objectives of the present investigation are to;

1. Derive the optimum dimensions of geosynthetic armour units with sand as filler material for an emerged breakwater structure.
2. Analyse the stability and hydraulic behaviour of sand-filled geosynthetic armour units for an emerged breakwater structure.
3. Investigate the stability and performance of sand-cement-filled geosynthetic armour units when used for breakwaters.

CHAPTER 3

METHODOLOGY

The proposed experimental investigation of geosynthetic armour units requires a certain amount of field data for proper simulation. Pertinent data on the seasonal variation of wave parameters at Mangaluru Port are collected and being used. In short, experimentation involves studies on hydraulic performance and stability of sand-filled geosynthetic armour units, arranged in different layers and varying in sand fill ratio. The best performing armour units are then tested with cement-sand fill with regards to its performance.

3.1 LITERATURE SURVEY AND COLLECTION OF INFORMATION:

A comprehensive literature survey is carried out to identify the knowledge gaps in geosynthetic coastal protection works. The extensive literature review obtained the wave parameters, armour unit weight and dimensions, type of geosynthetic material, sand fill ratio limits, and the proportion of cement and sand (for mortar-filled armour). Available experimental data regarding the stability and hydraulic performance of GSC structures have been collected and reviewed. This helped in deciding the wave parameters and aided in designing a concept GSC breakwater.

3.2 STRUCTURAL DESIGN

A comprehensive literature analysis aided in assessing the merits and demerits of geotextile materials and existing GSC structures. This helped in evolving the design of the proposed GSC breakwater. As discussed earlier, there is no unified code of practice for designing GSC structures. Experience and guidelines from various published sources aided in evolving the present structural design, which is being tested in the lab.

3.2.1 Material selection

The prime concern in the structural design is the material selection, i.e. woven or non-woven. High tensile strength and lesser elongation favour woven geotextiles to be used in containers and tube constructions. This facilitates the sand readjustment inside the

containers without causing much elongation. Non-woven geotextiles, on the other hand, offer more puncture resistance (4000 N) than woven textiles (2800 N) (Kriel, 2012). Puncture resistance is crucial as the present structure is more susceptible to human intervention, mechanical damages and vandalism. Non-woven textiles possess a rough surface and increased friction factor, resulting in the slow progress of damage level. The study conducted by Dassanayake and Oumeraci (2012b) revealed a 40% higher stability for structures made with non-woven geotextiles. Additionally, non-woven textiles are self-resistant against abrasive sand attack in the breaker zone by attachment of sand particles into surface pores and its fibrous texture promotes marine growth (Heerten et al., 2000). Non-woven geotextile with less cost, high puncture resistance and friction coefficient is decided to be used in the present study.

3.2.2 Armour unit placement

There have been various investigations regarding the placement of armour units. Shirlal and Mallidi (2015) conducted experiments with four different alignments related to the direction of wave attack (parallel, parallel double layer, Flemish and perpendicular) and concluded that units aligned parallel to the wave direction with two layers in the crest are stable for all the test conditions. Faraci (2018) conducted physical studies on orderly and randomly placed GSC structures and found that orderly placed structures were more stable and less reflective. This, according to the author, is due to the higher surface roughness and porosity of orderly structure, leading to increased wave dissipation on the structure. Most literature suggests a minimum of 50% overlap between units placed at upper and lower layers. Confining to findings from the literature, for the present study, armour units are initially kept with their longer dimension parallel to the direction of wave attack with 50% overlap with units placed above. In the later stage, slope parallel readjustment of armour units is found to exhibit improved stability and is experimented (see section 4.2.4)

3.2.3 Structure slope

For physical modelling, a seaward structure slope of 1:2 is selected. Geotextile containment units can withstand steeper slopes (up to 1:1) than rocks while maintaining

friction and stability (Jackson et al., 2008). According to Oumeraci et al. (2003) and Hornsey et al. (2011), unlike rock structures, GSC structures are stable on steeper slopes as the vertical load from top containers can provide higher confining pressure on steeper slopes. However, to compare its behaviour with other conventional structures, a slope of 1:2 is fixed, as most of the traditional models use a structural slope of 1:2.

3.2.4 Crest width

Shirlal and Mallidi (2015) proved that increased crest width reduces the transmission coefficient for submerged GSC structures. Additionally, the paper suggests a configuration with two layers of GSC units in the crest to be the most stable. The model structure of Dassanayake and Oumeraci (2012b) comprised of two layers, and that of Faraci (2018) consisted of three layers of GSC units at the crest. Most reviewed cases consist of two or more crest layers since Pilarczyk (2000) suggested a single-layered crest to be highly unstable. Thus, the crest width of the present structure is fixed to be the width of two GSC units. Future research may investigate the influence of the increased crest width.

3.2.5 Armour unit layers

The number of GSC armour layers is another crucial parameter involved in structural design. Kobayashi and Jacobs (1985) and Pilarczyk (1997) report a structure with a single GSC armour layer placed over the core. Two-layer placement is reported in the case of beach revetments. Therefore, the present investigation includes single and double layer placement of GSC armour units.

3.2.6 Armour unit weight and size

Stability equations suggested by (Recio and Oumeraci 2008) are given by (3.1).

$$N_{S,Slope} = \frac{H_s}{\left(\frac{\rho_{GSC}}{\rho_w} - 1\right).D} < \frac{C_w}{\sqrt{\xi_{50}}} \quad (3.1)$$

$$\text{Where, } D = \left(\frac{W}{\rho_{\text{GSC}}} \right)^{\frac{1}{3}} \quad (3.2)$$

From equation (3.1), considering a design wave height (H_s) of 3 m of period (T) 8 s (Mangaluru coastal conditions), ρ_{GSC} and ρ_w , 2005 and 1025 Kg/m^3 respectively, C_w , $\tan\alpha$ and ξ_0 as 2.75, 0.5 and 2.884, the thickness of armour unit D is calculated to be 1.956 m. substituting this in equation (3.2), the weight of armour units W is obtained as 15 t or 555 g when converted to a 1:30 scaled model. Dimensions of a bag that can accommodate the calculated weight are computed using the equation suggested by Robin (2004). The equation (3.3) is used for the volume calculation of a fully inflated rectangular bag with dimensions a and b , which cannot stretch or shear (refer Fig. 3.1).

$$V = a^3 \left[\frac{b}{\pi a} - 0.142 \left(1 - 10^{-\frac{b}{a}} \right) \right] \quad (3.3)$$

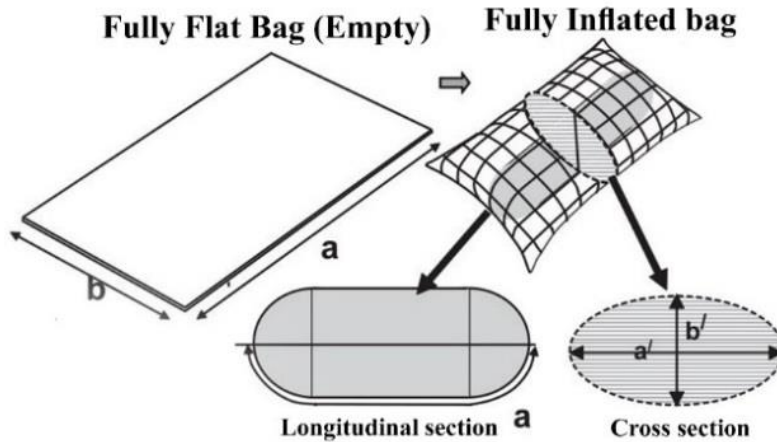


Fig. 3.1 Calculation of theoretical volume of GSC (Dassanayake and Oumeraci 2012b).

For simplification, the length of GSC units is kept double that of its width. Thus, for 500 g GSC units, length and breadth are calculated to be 16 cm and 8 cm, respectively. Shirlal and Mallidi (2015) reported a GSC unit weight of 486 grams. From the range of unit weights identified, physical experimentation is planned to conduct on bags weighing from

400 grams on model scale refer Table 3.1. Considering all the above structural parameters, the final configuration of breakwater structures is evolved (see Fig. 3.2).

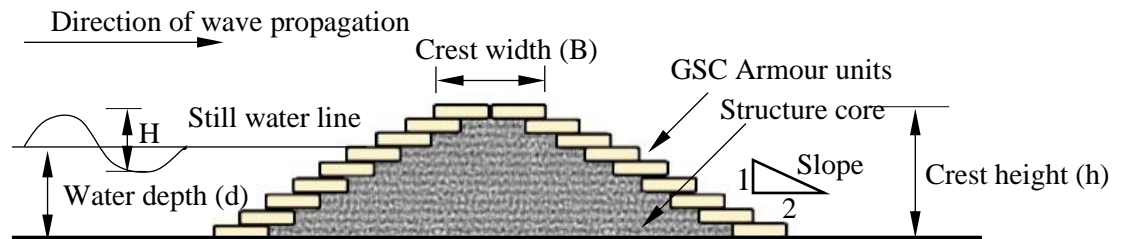


Fig. 3.2 Schematic diagram of GSC breakwater model.

Table 3.1 Calculated dimensions of GSC units.

GSC armour unit model weight (g)	Length of GSC model (cm)	Breadth of GSC model (cm)
400	14.68	7.34
450	15.27	7.6
500	16.00	8.0
600	16.8	8.4

3.3 PHYSICAL MODELLING:

The geotextile sand container armoured breakwater models are subjected to wave attack using Froude's similitude criteria with a 1:30 scale in the Wave Mechanics Laboratory of the Department of Water Resources and Ocean Engineering, National Institute of Technology Karnataka (NITK), Surathkal.

3.3.1 Wave flume

The available monochromatic, two-dimensional, fixed bed wave flume is of 50 m length, 0.74 m width and 1.1 m depth with 25 m length provided with glass panels facilitating model placement, observation and photography. Waves are generated by a 'bottom-hinged flap' located in a chamber, which is 6.3 m long, 1.5 m wide and 1.4 m deep. The other end of the flume comprises a 1:12 sloped beach. The movement of the flap generates waves, controlled by an 11 kW, 1450 rpm induction motor. An inverter drive of 0-50 Hz with

speed of 0-155 rpm regulates the motor. The facility can generate wave heights ranging from 0.02 to 0.20 m and periods of 0.8 to 4 s up to a maximum water depth of 0.50 m.

3.3.2 Instrumentation

Four capacitance-type wave probes with an accuracy of 0.001 m are used for measuring incident, transmitted and reflected wave heights. Total instrumentation facility includes wave probes, amplification unit and computer data acquisition system. The wave probes measure the difference in capacitance between water and copper conductor. This digital voltage input is converted into wave height and period by a wave recorder.

3.3.3 GSC Breakwater Model Construction

GSC breakwater design is explained in detail in section 3.2. Non-woven geotextiles are locally sewn into bags of required dimension and filled with sand collected from the NITK beach. GSC breakwater core made of quarry run is constructed in the flume bed at 12 m from the beach end. Governing wave parameters and properties of model construction materials are discussed in Table 3.2, Table 3.3, Table 3.4.

Table 3.2 Range of governing variables.

Variable	Expression	Range
Wave height (m)	H	0.06, 0.08, 0.10, 0.12, 0.14, 0.16
Wave period (s)	T	1.2, 1.4, 1.6, 1.8, 2, 2.2
Storm duration (Waves)	N	2000
Water depth (m)	d	0.35, 0.40, 0.45
Angle of attack (degrees)	F	90°
Mass density (GSC) (kg/m ³)	ρ	2005
GSC armour weight (g)	W	320 - 500
Slope		1V:2H
Crest height (m)	h	0.70
Crest width	B	0.32, 0.29 m
GSC material		Non-woven

Table 3.3 Non-dimensional model and wave characteristics.

Variable	Range
GSC Breakwater model characteristics	
Slope	1V:2H
Relative height (h/d)	1.55 - 2
Relative crest width(B/d)	0.644 - 0.91
Relative water depth (d/gT ²)	0.007 – 0.023
Wave characteristics	
Wave steepness(H ₀ /gT ²)	0.00126 – 0.0083
Surf Similarity Parameter (tan α /(H ₀ /L ₀) ^{0.5})	2.18 – 5.68

Table 3.4 Properties of construction materials used.

Property	Range
a. Geotextiles	
Type	Non-woven
Material	Polypropylene
Colour	white
Mass (GSM) *	200
Tensile strength (kN/m) *	12
Elongation at max tensile strength*	30%
Permeability (m/s) *	6*10 ⁻²
Thickness (mm) *	1.2
* Specification given by manufacturers.	
b. Sand	
Location	NITK Beach
D ₁₀ (mm)	0.18
Median grain size D ₅₀ (mm)	0.35
Specific gravity	2.65

c. Core	
Material	M-sand
Specific gravity	2.78
D ₁₀ (mm)	0.22
D ₅₀ (mm)	0.45

Once the core is constructed, GSC units are placed (with 50% overlap) with their longer dimensions parallel to the direction of the wave attack. Construction stages and different test configurations are illustrated in Fig. 3.3 and Fig. 3.4.

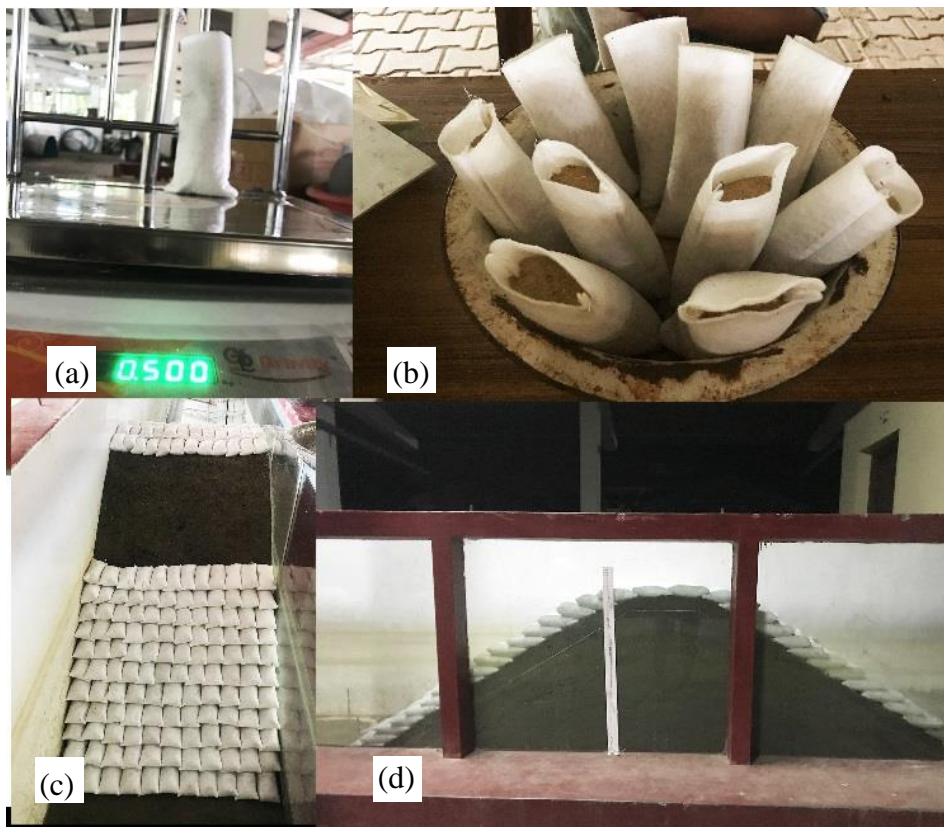


Fig. 3.3 Construction stages of geotextile breakwater, (a) filling calculated amount of sand to bags made with geotextile material, (b) filled bags, (c) stacking stitched bags over the core, (d) final GSC breakwater model after

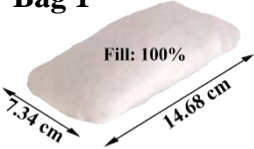

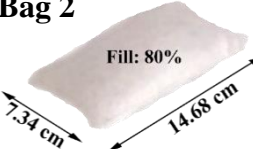

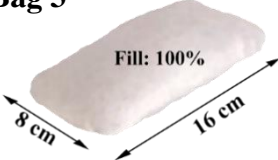

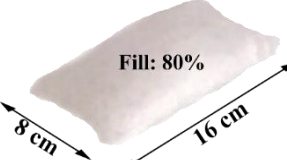

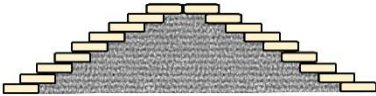

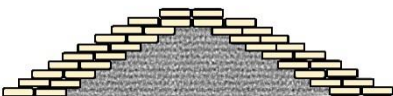

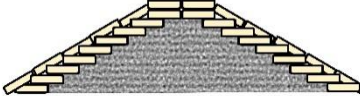

Configuration	Constructed model	Configuration	Constructed model
<p>Bag 1</p>  <p>Fill: 100%</p> <p>7.34 cm</p> <p>14.68 cm</p> <p>Weight: 400 g (Prototype: 10.8 t) Volume: $1.995 * 10^{-4} \text{ m}^3$ Height: 4.5 cm</p>		<p>Bag 2</p>  <p>Fill: 80%</p> <p>7.34 cm</p> <p>14.68 cm</p> <p>Weight: 320 g (Prototype: 8.64 t) Volume: $1.995 * 10^{-4} \text{ m}^3$ Height: 4.3 cm</p>	
<p>Bag 3</p>  <p>Fill: 100%</p> <p>8 cm</p> <p>16 cm</p> <p>Weight: 500 g (Prototype: 13.5 t) Volume: $2.49 * 10^{-4} \text{ m}^3$ Height: 5 cm</p>		<p>Bag 4</p>  <p>Fill: 80%</p> <p>8 cm</p> <p>16 cm</p> <p>Weight: 400 g (Prototype: 10.8 t) Volume: $2.49 * 10^{-4} \text{ m}^3$ Height: 4.4 cm</p>	
  <p>Single Layer Placement</p>	  <p>Double Layer Placement</p>	  <p>Slope Parallel Placement</p>	

Fig. 3.4 Dimensions and placement modes of various GSC units.

When sand cement mixture is used as the filler material, the required quantity of cement (15% and 20% of the bag-weight) sand mixture is filled into the units in dry form. Later these units are kept in water for curing up to 24 hours. Note that configurations are named ‘Bags’ as they look like bags on the model scale, but these units will be huge sand containers in the prototype. After model construction, water is pumped to the desired depth. The porosities of various breakwater configurations are provided in Table 3.5.

Table 3.5 Porosity of various tested GSC breakwater configurations

Armour units	Porosity
Bag 1	39.33%
Bag 2	25.33%
Bag 3	50.3%
Bag 4	37.4%
15% cement-filled units	42.18%
20% cement-filled units	41.7%

3.3.4 Test Procedure

For damage analysis, the model is exposed to waves as per the test conditions. Wave attack is limited to a burst of 10 waves, and the generator is shut off before the reflected wave energy from the structure returns to it and creates an undefined wave condition. Brief intervals are provided between wave bursts to completely dampen the reflected wave energy (Shirlal et al., 2006). The structure was initially subjected to smaller waves of 0.06 m and gradually increased by 0.02 m till it reached the maximum wave height of 0.16 m for a particular wave period. Armour unit displacement and detachment are observed and recorded manually and classified into Damage Categories DC0 to DC4 as given in Table 3.6. In contrast to the reported 100 regular and 1000 random wave tests by Dassanayake and Oumeraci, (2012b), the present structure is exposed to more than 2000 waves to define damage level equivalent to 6-11 hours of actual storm duration (van der Meer and Pilarczyk 1985). The damaged structure is rearranged after every test condition. Once the configuration is investigated for all the test wave conditions, water is drained out from the flume and the core is reconstructed for testing with a new configuration of GSC units. Isaacson (1992) discussed the three probes method to compute the reflection coefficient (K_r). For the same, three wave probes are kept at the leeward side at a distance of L at a spacing of $L/3$ from the breakwater model. Wave amplitudes from the three probes are used to compute the reflection coefficient K_r . Runup and rundown values are computed using the strip charts attached to the glass panels of the wave flume. Maximum limits of uprush and down rush on the structure, measured vertically from the still water level, are

reported as runup and rundown, respectively. The experimental setup is illustrated in Fig. 3.5. Results obtained are analysed in the following sections.

Table 3.6 Damage classification criteria for GSC structures as proposed by Dassanayake and Oumeraci (2012b).

Damage Classification I (Single GSC)				
Considering only a single GSC in the most vulnerable position (Critical GSCs)				
“Stable”	Horizontal displacement < 10% of GSC length (or width) / Upward rotation < 10°			
“Movement”	10% of GSC length (or width) < Horizontal displacement < 50% of GSC length (or width)			
“Detachment”	Horizontal displacement > 50% of GSC length, width, Upward rotation > 45°			
Damage Classification II (GSC-Structure)				
Considering all critical GSC layers of GSC-Structure				
No Damage [DC0]	Incipient Motion [DC1]	Minor Damage [DC2]	Medium Damage [DC3]	Total Failure [DC4]
< 10% of critical GSCs moved. No critical GSCs detached	10% - 50% of critical GSCs moved. < 5% of critical GSCs detached	> 50% of critical GSCs moved. 5% - 20% of critical GSCs detached	20% - 40% of critical GSCs detached	> 40% of critical GSCs detached

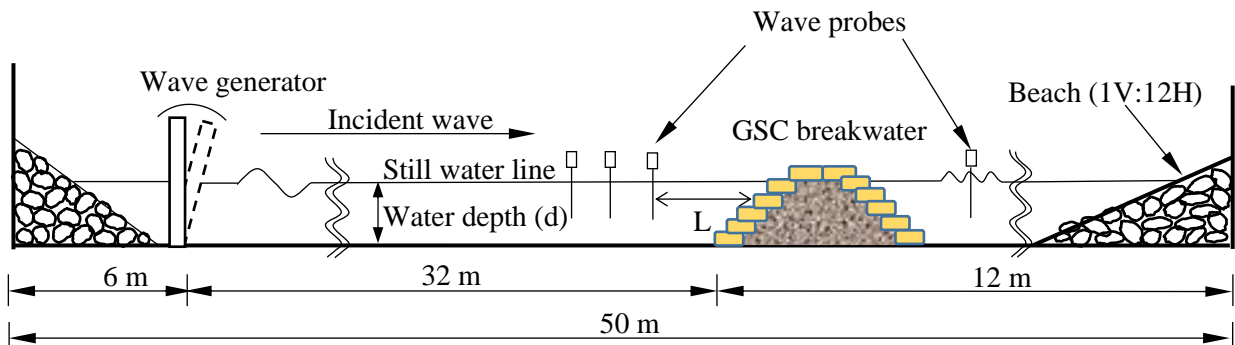


Fig. 3.5. Schematic representation of GSC breakwater model at Wave Mechanics Laboratory, NITK.

3.3.5 Experimental data to be recorded:

Geotextile armour units with varying sand fill and cement sand mortar fill ratios are subjected to wave attack at different water depths, wave heights and wave periods. The following data are computed:

1. Incident wave height
2. Reflected wave height.
3. Wave runup.
4. Wave rundown.
5. Damage level.

3.3.6 Analysis of results:

Relevant non-dimensional parameters are estimated to interpret and analyse the results. Results are graphically represented to establish a relation between non-dimensional parameters. Fig. 3.6 illustrates the workflow of the present investigation.

3.3.7 Assumptions in physical modelling

The replica of field conditions to be generated in the laboratory is often quite a difficult task. Hence the following assumptions are made in this experimental study.

1. The difference in density and other properties of the seawater and the water used in the flume is neglected.
2. The sea bed of the wave flume is horizontal and rigid type; hence sediment movement is not considered.
3. Regular waves are generated in the laboratory, whereas the prototype is always subjected to irregular wave attacks.
4. All the assumptions of Froude's similitude are included as the scaling is done according to it.
5. Geotextiles and sand used in the experiments are not scaled to 1:30.

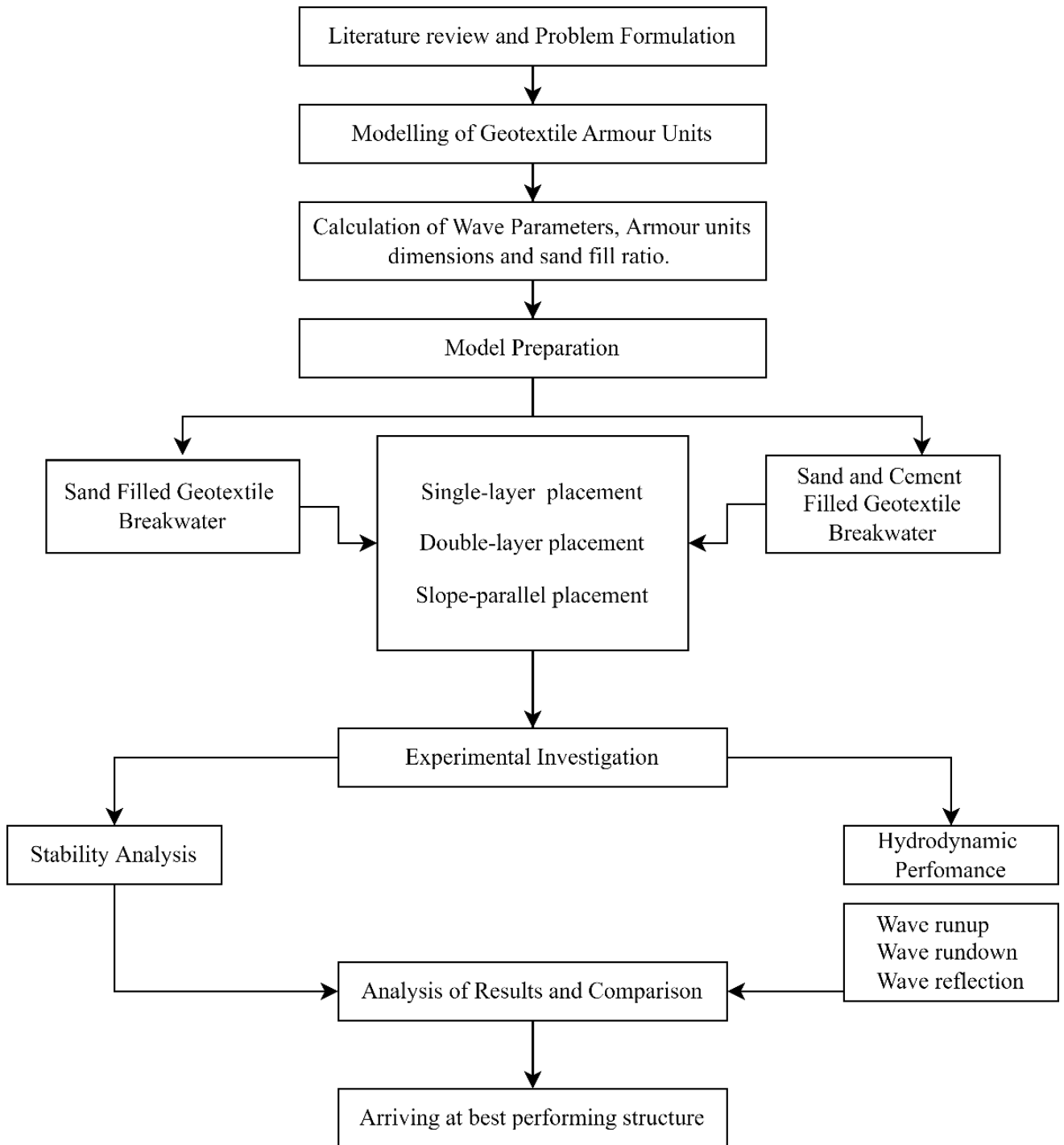


Fig. 3.6 Flowchart showing the detailed methodology

CHAPTER 4

RESULTS AND DISCUSSION

This chapter aims to provide a comparative analysis of all the tested configurations so that the best-performing configuration with respect to various wave responses can be identified. The chapter deals with results regarding the hydraulic performance and damage analysis of GSC structures. Hydraulic performance analysed includes wave runup, rundown and reflection characteristics.

4.1 STUDIES ON GSC SINGLE-LAYER BREAKWATERS (FILLED WITH SAND ALONE)

This section discusses the initial set of experimentation on single-layered, sand-alone filled GSC breakwaters. Breakwaters are constructed with four different GSC armours, namely Bag 1, Bag 2, Bag 3 and Bag 4 (refer Fig. 3.4 for bag dimensions), arranged with their length parallel to the direction of wave attack (Fig. 4.1). The observed results and discussion can be found in the subsequent sections.



Fig. 4.1 Single-layer GSC breakwater model after construction at wave mechanics laboratory

4.1.1 Wave runup studies

4.1.1.1 Effect of deepwater wave steepness (H_0/gT^2) on relative runup (R_u/H_0)

Fig. 4.2 represents the variation of relative runup (R_u/H_0) with respect to deepwater wave steepness (H_0/gT^2) for a relative water depth of d/gT^2 (0.007 to 0.018 (0.35 m water depth), 0.008 to 0.020 (0.40 m water depth) and 0.009 to 0.023 (0.45 m water depth)) for different configurations of geotextile breakwater.

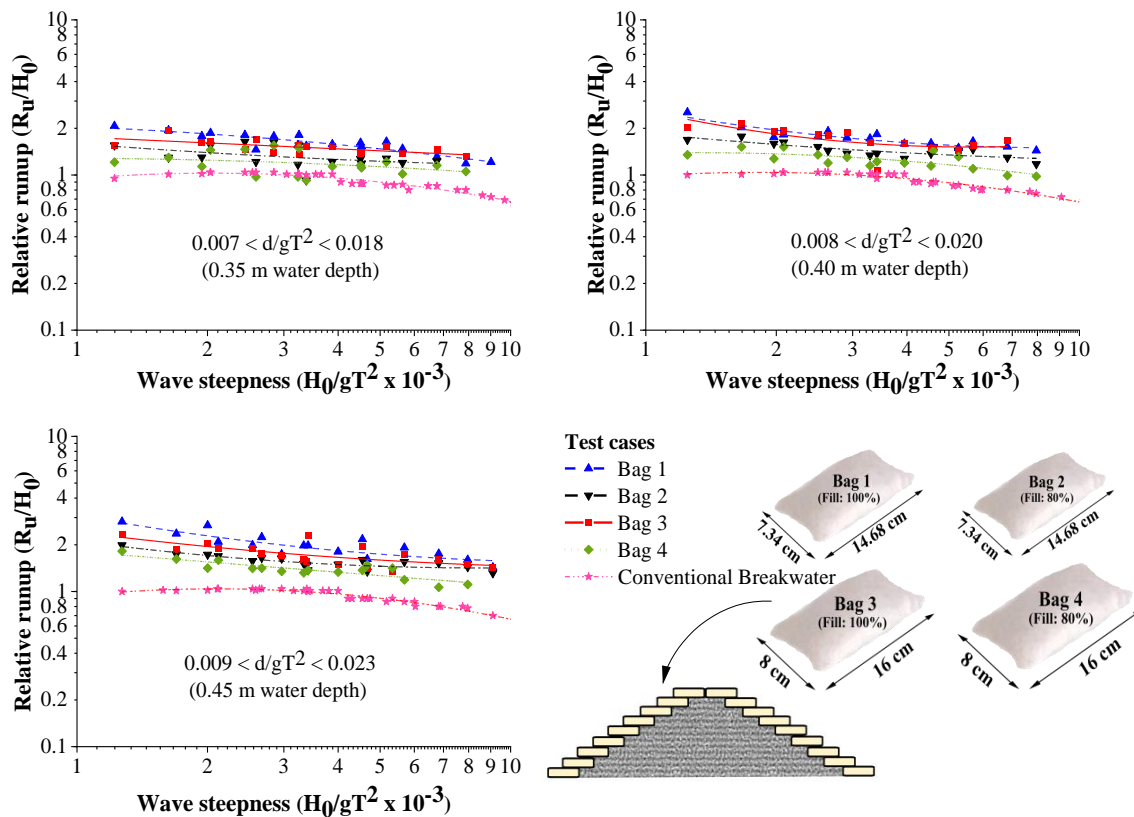


Fig. 4.2 Variation of relative runup (R_u/H_0) with respect to deep water wave steepness (H_0/gT^2) for various relative water depths (d/gT^2) for different configurations of geotextile breakwater.

The maximum and minimum runup observed among all configurations were 2.81 and 0.92 times the deepwater wave heights, respectively and is decreasing with increasing deepwater wave steepness (H_0/gT^2). The trend lines of tested configurations showed higher relative runup than conventional rubble mound breakwaters (Shore Protection Manual

(SPM) 1984) (20.20 to 95.65 %). Wave runup values observed at 0.45 m water depth are up to 17.09% and 48.9% higher than those reported at 0.40 m and 0.35 m water depths, respectively, indicating a rise in runup with increasing water depth. In all water depths, breakwater configuration armoured with 'Bag 1' (100% filled 400 g bags) exhibited maximum relative runup followed by those armoured with 'Bag 3', 'Bag 2' and 'Bag 4' respectively. Relative runup exhibited by 'Bag 1' configuration is 72.5 to 30.47% higher than that of 'Bag 4', i.e. variation between maximum and minimum trend lines. When the geotextile armour units are filled to their maximum capacity, the bags act like solid units, thereby reducing water absorption into these units. This is evident from the graph; Bag 1 showed 12.05 to 56.3% more runup than the same bags filled to its 80% volume (Bag 2). Similarly, a 24.3 to 64.05% increase in relative runup is recorded when the fill of the larger bag is changed from 80 to 100% (Bag 4 to Bag 3). This indicates that filling the bags to its maximum capacity would result in higher wave runup, which may result in overtopping of waves.

Larger bags (Bag 3 and Bag 4), when arranged as primary armour units, produced more inter-unit spaces or pore spaces than smaller bags (Bag 1 and Bag 2). Higher pore spaces aid in absorption and wave energy dissipation, resulting in a 7.4 to 34.48% lesser relative runup for larger bags. Similarly, for 80% filled bags, void spaces between bags and increased space within the bag make them better in absorbing nature therefore, 'Bag 4' showed 4 to 24.2% lesser relative runup.

From the current example, it can be summarised that changing the fill from 100 to 80% resulted in a 12.05 to 64.5% reduction of runup, whereas increasing the size of the bag has helped only up to 34.8% reduction in runup. Reduction in percentage fill reduces wave runup considerably more than changing bag size.

4.1.1.2 Effect of water depth on relative runup (R_u/H_0)

The influence of water depth on wave runup is considered in the present section. Fig. 4.3 shows the variation of relative runup (R_u/H_0) of various configurations for three different relative water depths. Out of the three water depths considered, 0.45 m water depth (0.009

$< d/gT^2 < 0.023$) condition represented higher runup for all four configurations. ‘Bag 1’ at 0.45 m water depth showed 12.5 to 63.37% and up to 11% higher R_u/H_0 than 0.35 m and 0.40 m water depths. Similarly, ‘Bag 2’ at 0.45 m water depth showed 14.3 to 26.11% and up to 17.5% higher R_u/H_0 than 0.35 m and 0.40 m water depths. ‘Bag 3’ at 0.45 m water depth showed 6.25 to 41.66% and up to 3% higher R_u/H_0 than 0.35 m and 0.40 m water depths. ‘Bag 4’ at 0.45 m water depth showed up to 33.58% and 15.8% higher R_u/H_0 than 0.35 m and 0.40 m water depths, respectively. To sum up, relative runup at 0.45 m water depth exhibited 6.25 to 63.37% and 3 to 17.5% higher values than 0.35 m and 0.40 m water depths, respectively. It is observed that runup values increase as depth increases. Increased water depth can sustain higher unbroken waves, leading to increased uprush, resulting in higher runup at 0.45 m water depth.

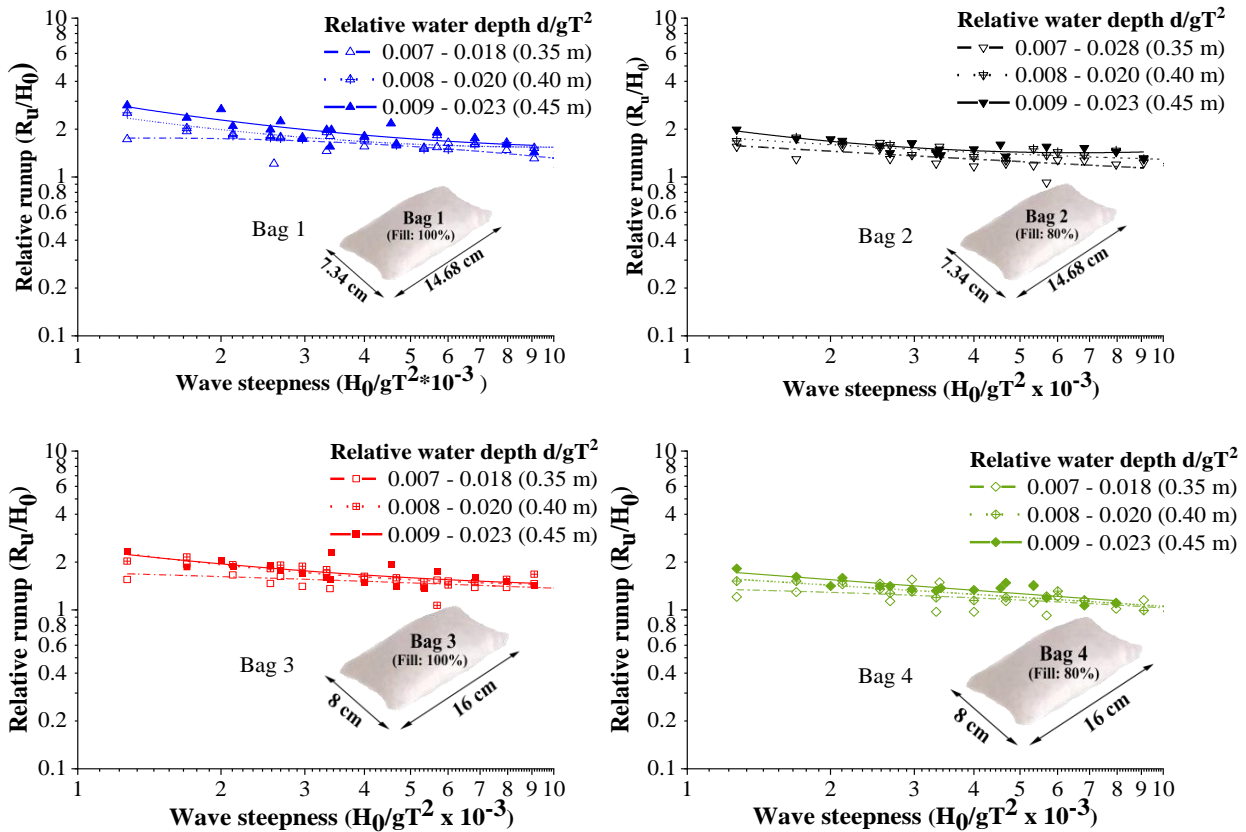


Fig. 4.3 Variation of relative runup of various configurations for different relative water depths (actual water depth is indicated in brackets).

4.1.1.3 Effect of surf similarity parameter (ξ_0) on relative runup (R_u/H_0)

To analyse the relationship, relative runup (R_u/H_0) values are plotted against the surf similarity parameter (ξ_0). ξ_0 for the whole experimental setup ranged from 2.18 to 5.6. Representation with respect to ξ_0 gives additional information regarding the breaking of waves. It is observed that the relative runup value increases with an increase in ξ_0 . According to SPM (1984), collapsing or surging waves are observed after a ξ_0 value of 3.3. As a result, waves breaking on the structure tend to uprush, increasing runup on the structure slope. This is observed from the progressive R_u/H_0 value in Fig. 4.4. The trend observed by different configurations of GSC structure is attributed to the difference in fill percentage and GSC size, as discussed in section 4.1.1.1.

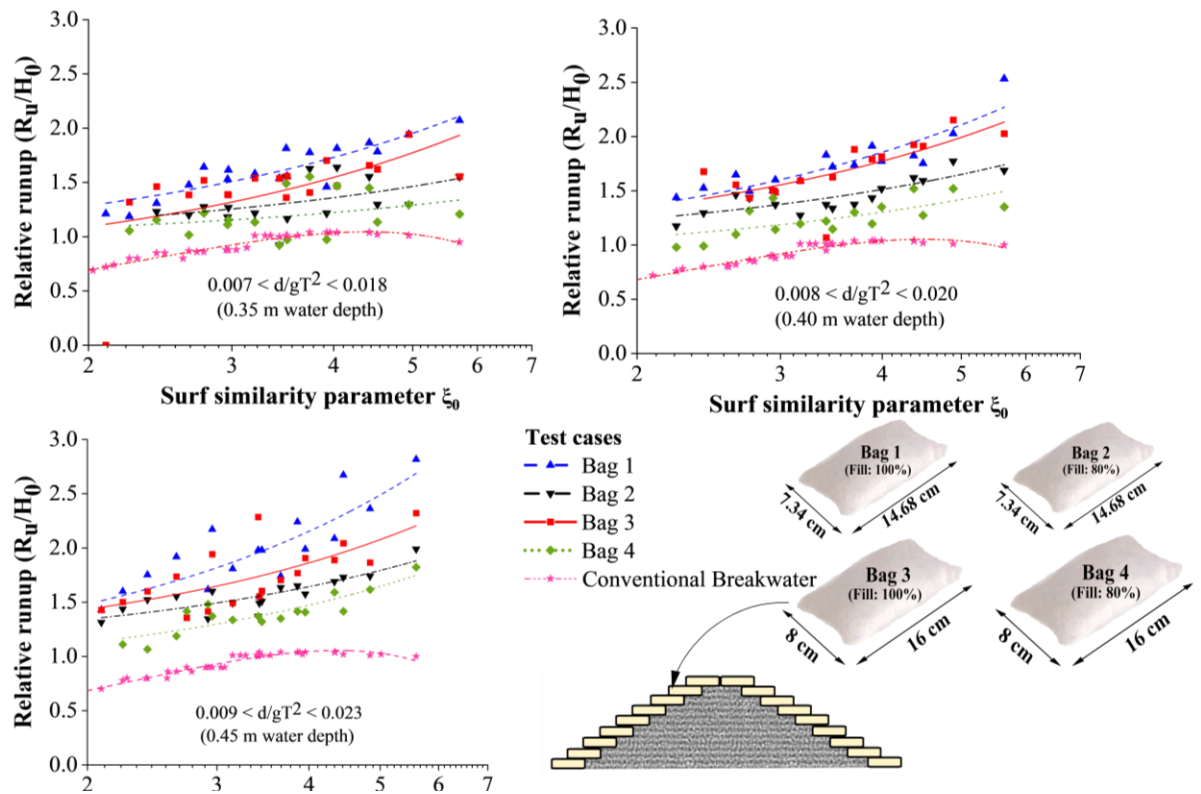


Fig. 4.4 Variation of relative runup of different configurations with surf similarity parameter

4.1.2 Wave rundown studies

4.1.2.1 Variation of relative rundown (R_d/H_0) with deepwater wave steepness (H_0/gT^2)

Fig. 4.5 represents the variation of relative run down (R_d/H_0) with respect to deepwater wave steepness (H_0/gT^2) for a relative water depth of d/gT^2 , (0.007 to 0.018 (0.35 m water depth), 0.008 to 0.020 (0.40 m water depth) and 0.009 to 0.023 (0.45 m water depth)) for different configurations of geotextile breakwater.

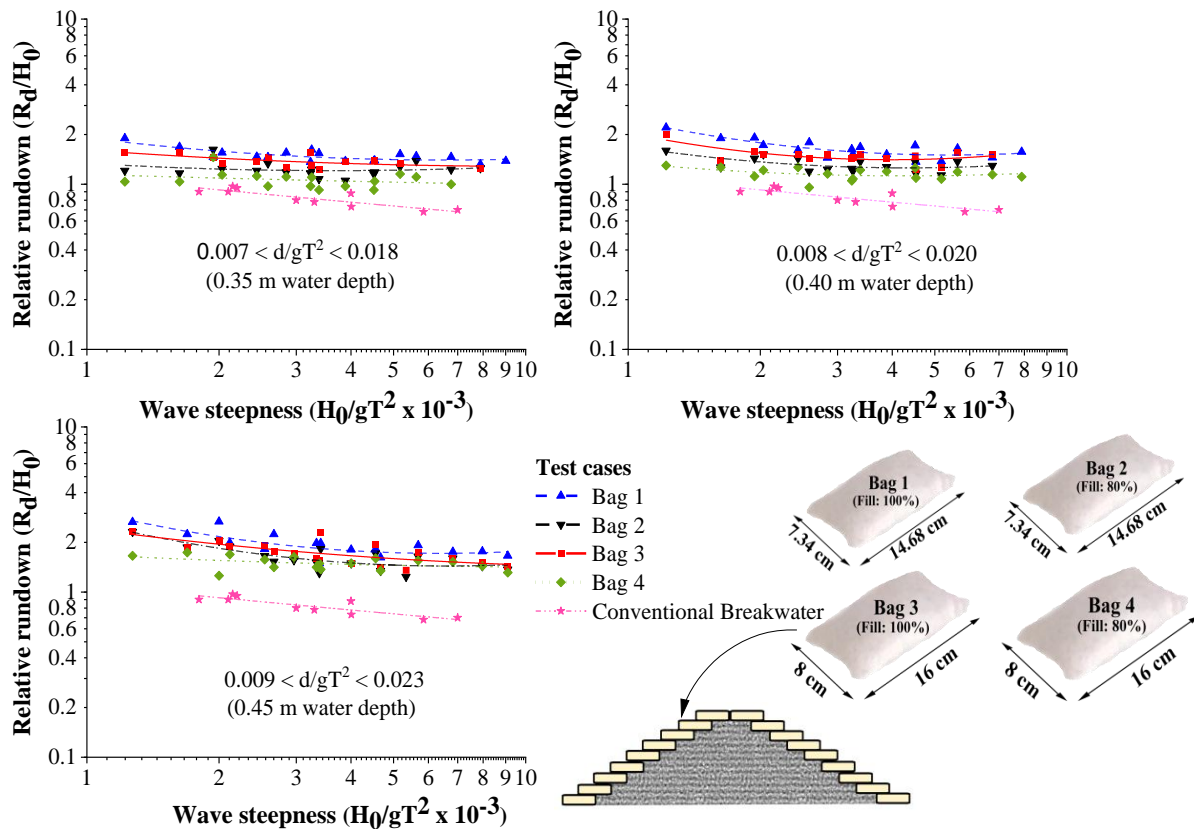


Fig. 4.5 Variation of relative rundown (R_d/H_0) with respect to deepwater wave steepness (H_0/gT^2) for various relative water depths (d/gT^2) for different configurations of geotextile breakwater.

Relative rundown (R_d/H_0) of all configurations shows a wide range varying from 0.91 to 2.81 and is decreasing with increasing deepwater wave steepness (H_0/gT^2). The trend lines of tested configurations showed higher relative rundown than conventional rubble mound

breakwater. The rundown data for conventional breakwater is adopted from the experimental studies conducted by Shirlal et al. (2006). Breakwaters armoured with 'Bag 1' exhibited maximum relative rundown, followed by those with 'Bag 3', 'Bag 2' and 'Bag 4'. When the geotextile armour units are filled to its full capacity, the bags act like solid units, thereby reducing the absorption of water into these units. This is evident from the graph, as Bag 1 showed 5.4 to 36.40% more rundown than the same bags filled to its 80% volume (Bag 2). Similarly, a 10.9 to 45.23% increase in the relative rundown is recorded when the fill of the larger bag is changed from 80 to 100% (comparison between Bag 4 and Bag 3). This indicates that filling the bags to their maximum capacity would result in a higher wave rundown.

When arranged as primary armour units, larger bags (Bag 3 and Bag 4) produced more inter-unit spaces or pore spaces than smaller bags (Bag 1 and Bag 2). Higher pore spaces aid in absorption and wave energy dissipation, resulting in 10.20 to 44.04% lesser relative rundown for 100% filled larger bag (Bag 3) than 100% filled smaller bag (Bag 1) configuration. In case of 80% filled bags, the void spaces between bags and increased free space within the bag makes the Bag 4 a better choice in terms of energy absorption. . As a result, 80% filled bags control the down rush of water. Therefore Bag 4 showed 9.73 to 34.5% lesser relative rundown than Bag 2. The maximum reduction percentage is more (up to 30%) in bigger bags, as 80% filled bigger bags (Bag 4) have more space within the bags than 80% filled smaller bags (Bag 2), leading to improved absorption.

From the mentioned trials, it can be summarised that changing the fill from 100 to 80% resulted in 5.45 to 45.23% reduction of rundown, whereas increasing the size of bags has helped only up to 34.5% reduction in rundown. Thus, a decrease in percentage fill reduces wave rundown considerably more than changing bag size.

4.1.2.2 Variation of relative rundown with water depth.

Fig. 4.6 shows the variation of relative rundown of various configurations for three different relative water depths, $0.007 < d/gT^2 < 0.018$ (0.35m), $0.008 < d/gT^2 < 0.020$ (0.40 m) and $0.009 < d/gT^2 < 0.023$ (0.45 m) with respect to deep water wave steepness.

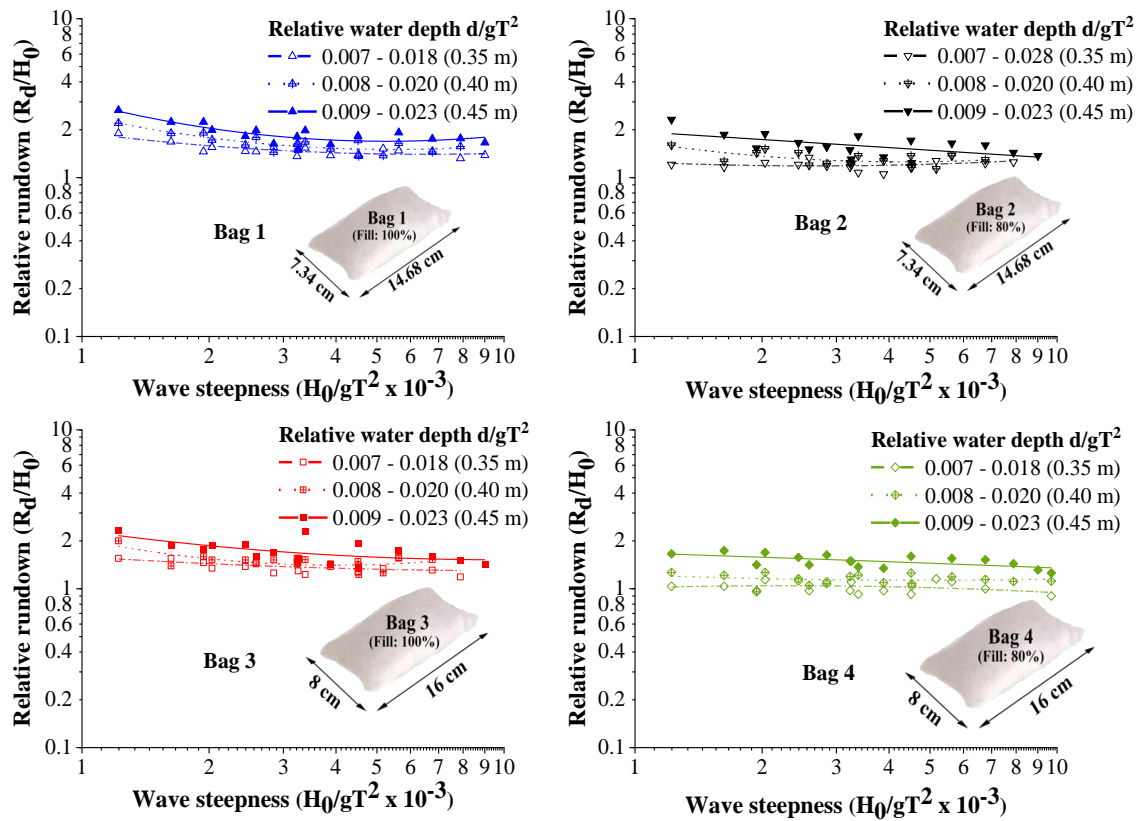


Fig. 4.6 Variation of relative rundown of various configurations for different relative water depths (actual water depth is indicated in brackets).

Out of the three water depths considered, 0.45 m water depth ($0.009 < d/gT^2 < 0.023$) condition represented higher rundown for all four configurations. Breakwater armoured ‘Bag 1’ at 0.45 m water depth showed 19.58 to 49.14% and up to 17.8% higher relative rundown than at 0.35 m and 0.40 m water depths. Similarly, breakwaters armoured with ‘Bag 2’ at 0.45 m water depth showed 9.58 to 54.48% and up to 28.6% higher relative rundown than 0.35 m and 0.40 m water depths. Breakwaters armoured with ‘Bag 3’ at 0.45 m water depth showed 15.9 to 45.03% and up to 11.11% higher relative rundown than at 0.35 m and 0.40 m water depths. Breakwaters armoured with ‘Bag 4’ at 0.45 m water depth showed up to 62.6% and 33.57% higher relative rundown than at 0.35 m and 0.40 m water depths, respectively. To sum up, relative rundown at 0.45 m water depth exhibited 9.58 to 62.6% and 8.5 to 33.57% higher values than 0.35 m and 0.40 m water depths, respectively.

It is observed that rundown values increase as depth increases. This may be because waves possessing higher energy result in a higher rundown. Increased water depth can sustain waves with larger heights (consequently higher wave energy), resulting in increased downrush in higher water depths.

4.1.2.3 Effect of surf similarity parameter (ξ_0) on relative rundown

Relative rundown values are plotted against ξ_0 to analyse the relationship. ξ_0 for the whole experimental setup ranged from 2.18 to 5.6. It is observed that relative rundown increases with increasing ξ_0 . According to SPM (1984), collapsing or surging waves are observed after a surf similarity value of 3.3. As a result, waves breaking on the structure tend to uprush, increasing runoff on the structure slope. This is observed from the progressive relative rundown value in Fig. 4.7.

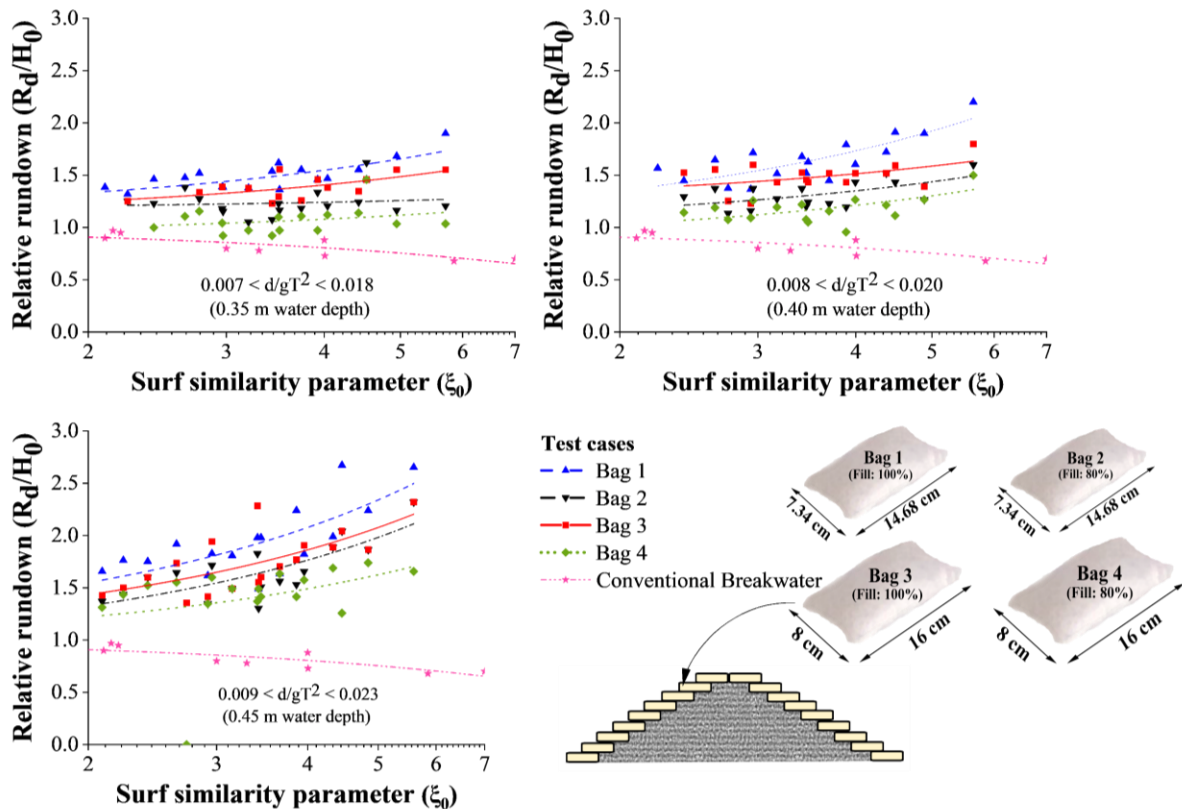


Fig. 4.7 Variation of relative rundown with respect to surf similarity parameter (ξ_0) for different GSC configurations.

The trend observed by different configurations of GSC structure is attributed to the difference in fill percentage and GSC size, as discussed in section 4.1.1.1. Relative runup and rundown show nearly identical ranges, but deviations from conventional breakwater are found to be more for relative rundown values than runup. It has to be mentioned that, due to continuous interaction of consecutive waves, measurement of rundown values of faster waves ($T < 1.8$) showed up to 9% variation.

4.1.3 Wave reflection studies

Wave reflection analysis of GSC structures has been carried out confining to the three probe method proposed by Isaacson (1992). Fig. 4.8 represents the reflection coefficient values with respect to wave steepness for all the test cases conducted for breakwaters armoured with Bag 1.

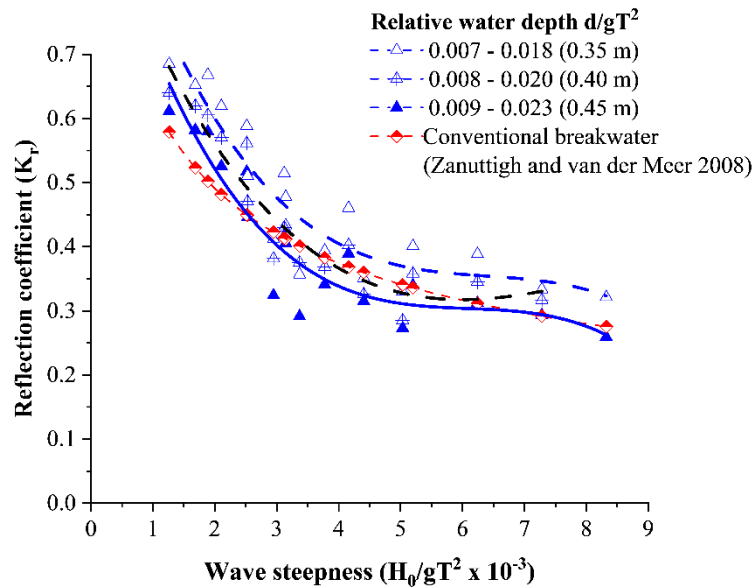


Fig. 4.8 Reflection coefficient (K_r) values with respect to wave steepness for all the test cases conducted for Bag 1.

This type of representation is essential for deducing an overall impression of the reflection behaviour of the structure. From Fig. 4.8, the values of K_r appear to scatter over a range of 0.26 to 0.68. This representation is quite difficult in comprehensively analysing the results but helps in understating the entire K_r range. In general, it is noted that K_r reduces with

increased wave steepness. But these trends can be clearly understood from further detailed analysis.

Fig. 4.9 represents the variation of K_r with respect to wave steepness, keeping the periods fixed to 1.4, 1.8 and 2.2 seconds. Fig. 4.9 clearly indicates the effect of the incident wave period on reflection. For the relative water depths considered, wave steepness reduces with increasing wave period. It is also observed that K_r increases with progressing wave periods.

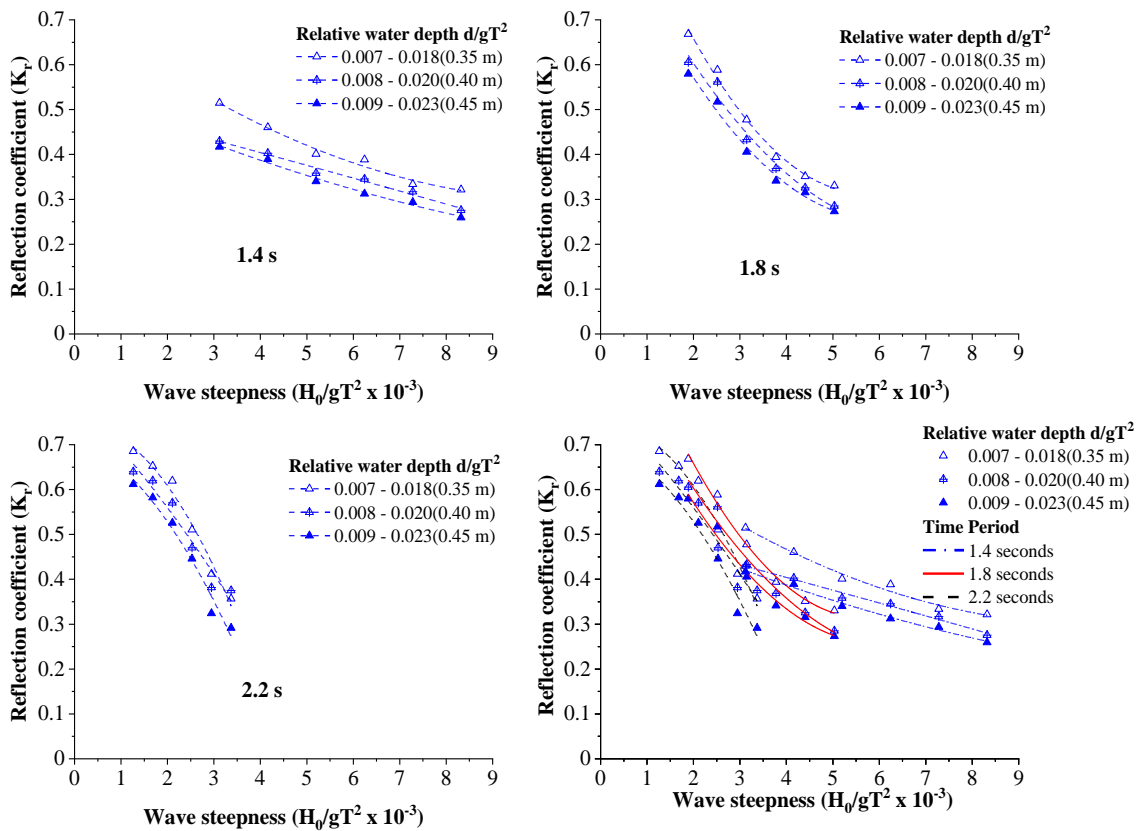


Fig. 4.9 Plots showing dependence of wave period on reflection coefficient (K_r) for different configurations of GSC breakwaters.

Out of all the tested cases for breakwaters armoured with ‘Bag 1’, 2.2 s waves exhibited 1.49 to 3.57% and 11.53 to 33.33% higher reflection coefficients than 1.8 and 1.4 s waves, respectively. We can conclude that for a particular configuration, there exists an inverse relationship between the wave period and K_r . 11.53 to 33.33% reduction in K_r is observed when the period of waves is altered from 2.2 s to 1.4 s.

Considering the effect of water depth, K_r reduced from 0.61 to 0.29, 0.64 to 0.37 and 0.69 to 0.36 for relative water depths 0.007 to 0.018 (0.45 m), 0.008 to 0.020 (0.40 m) and 0.009 to 0.023 (0.35 m) respectively. Out of the three water depths considered, structure kept at 0.45 m water depth showed 4.68 to 21.62% and 11.59 to 19.44% less reflection than 0.40 m and 0.35 m water depths, respectively. A possible reason for decreasing reflection with increasing water depth is the high runup at higher water depths (as concluded in section 4.1.1.2). When runup increases, up-rushing water comes in contact with more GSC units, resulting in the increased absorption of water. As a result, reflected wave energy is reduced.

4.1.3.1 Effect of incident wave height on wave reflection

Fig. 4.10 shows wave reflection of configuration with ‘Bag 1’ for minimum and maximum incident wave heights used in physical modelling (0.06 m and 0.16 m). K_r of 0.06 m waves varied from 0.42 to 0.68, while that of 0.16 m waves vary from 0.26 to 0.36.

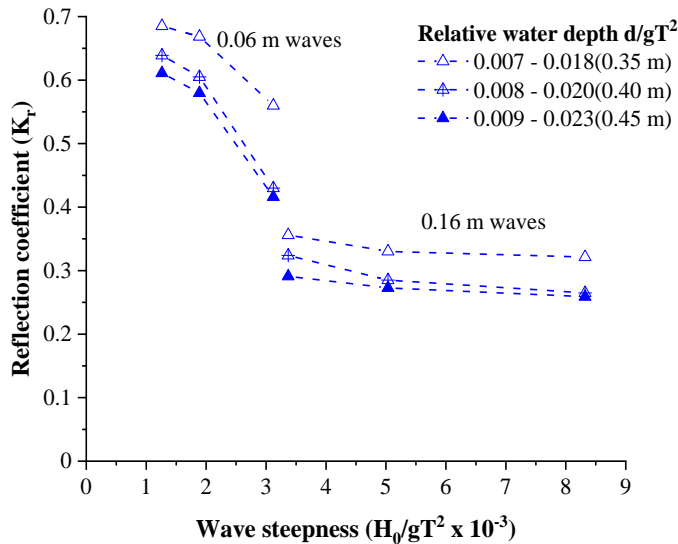


Fig. 4.10 Variation of reflection coefficient (K_r) with respect to wave steepness (Incident wave height 0.06 m and 0.16 m) for different relative water depths.

It is observed that K_r reduces as the incident wave height increases. 0.06 m waves were 38.09 to 47.05% more reflective than 0.16 m high waves. Existing literature like Kriel (2012) points out a decreasing trend of K_r (10 to 15%) with increasing incident wave

heights. But in the present study, the effect of incident wave height is very prominent on reflection behaviour. As wave height increased from 0.06 m to 0.16 m, a decrease of up to 47% was reported. This range is higher than expected and can be due to higher waves interacting more with GSC units. Unlike stone or other concrete armour units, GSC units are highly absorbing in nature. As incident wave height increases, more runup occurs, leading to higher water absorption into the structure.

From previous sections, the dependence of wave period and incident wave height on reflection behaviour has been identified for configuration with Bag 1. On a general note, K_r tends to increase with increasing wave period and decrease with increasing incident wave height. To be precise, there is a 10.35 to 25% decrease in K_r when the wave period is varied from maximum to minimum in the experimental range. Similarly, a 38.09 to 47.05% decrease in reflection coefficient is observed when the incident wave height is varied from 0.06 m to 0.16 m.

4.1.3.2 Influence of surf similarity parameter (ξ_0) on reflection coefficient (K_r)

The reflection coefficient (K_r) is plotted against the surf similarity parameter (ξ_0) to analyse the relationship. ξ_0 for the whole experimental setup ranged from 2.18 to 5.6. Representing the reflection coefficient (K_r) with respect to ξ_0 gives additional information regarding the breaking of waves. According to SPM (1984), collapsing or surging waves are observed after a surf similarity value of 3.3. As a result, waves breaking on the structure reflects more energy as it cannot be effectively absorbed. This is observed from the progressive reflection value in Fig. 4.11. The trend observed by different configurations of GSC structure is attributed to the difference in fill-percentage and GSC size, as discussed in the above sections.

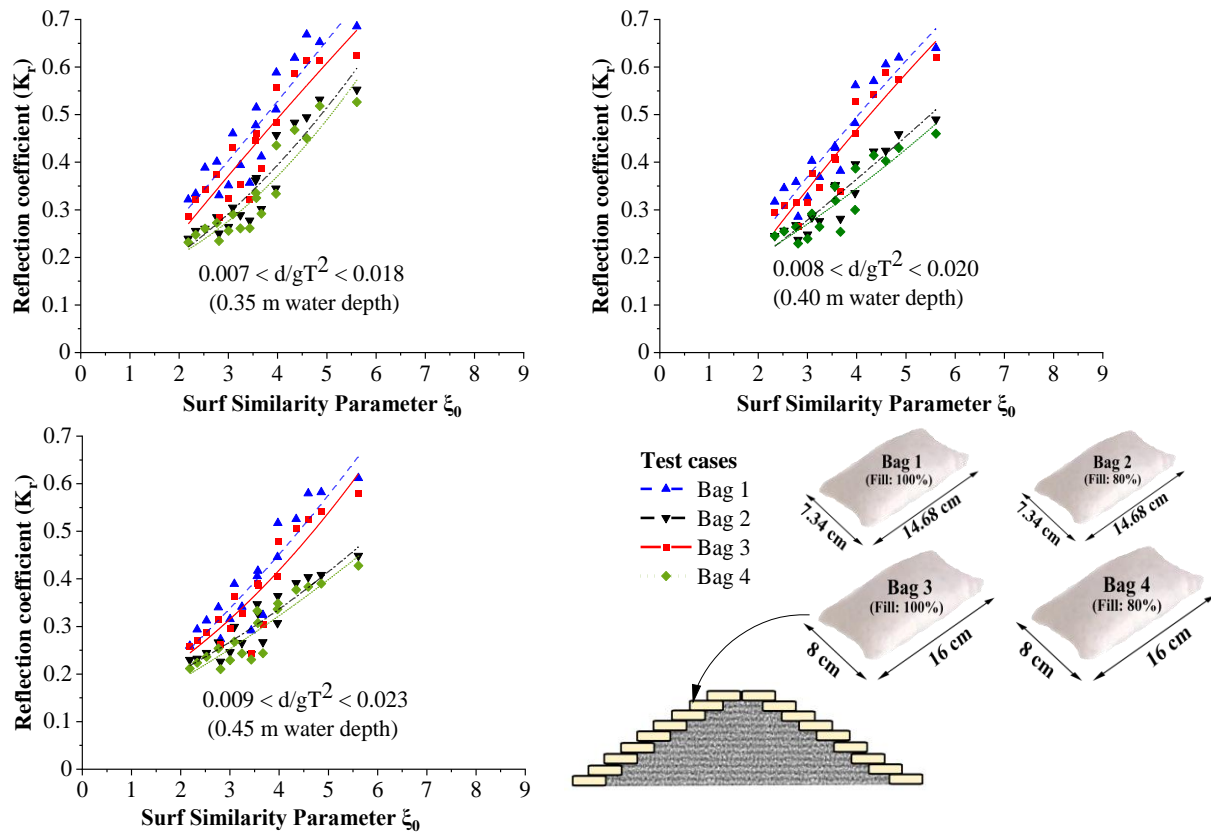


Fig. 4.11 Variation of K_r with respect to surf similarity parameter (ξ_0)

4.1.3.3 Reflection curves

A comprehensive analysis of all the configurations would light more on the response of each configuration to different incident characteristics of waves. Fig. 4.12, shows the reflection behaviour of all the four tested configurations for varying relative water depths. The maximum K_r observed is 0.69 for breakwaters armoured with Bag 1 and the minimum is 0.21 for those with Bag 4. Out of the four configurations, breakwaters armoured with Bag 1 show the highest reflection, followed by those with Bag 3, Bag 2 and Bag 4. This is due to the fact that the dimensions of Bag 1 and Bag 2 (0.148 m length * 0.073 m breadth * 0.05 m height) is smaller than Bag 3 and Bag 4 (0.16 m length * 0.08 m breadth * 0.05 m height), resulting in the lesser inter-bag spaces when packed as the outer layer of geotextile breakwater. This reduces the wave energy dissipation due to the turbulence caused by the interaction of water waves with the pore spaces on the outer surface of the structure. As a result, more water particles get reflected, resulting in increased wave

reflection. Absorption of water into the bags being the same for both the cases, structure with more pore spaces succeeds in energy dissipation leading to a lesser reflective behaviour. Therefore, configuration comprising bigger bags with more pore spaces showed up to 10.07% lesser reflection than smaller bags when both filled to their maximum capacity.

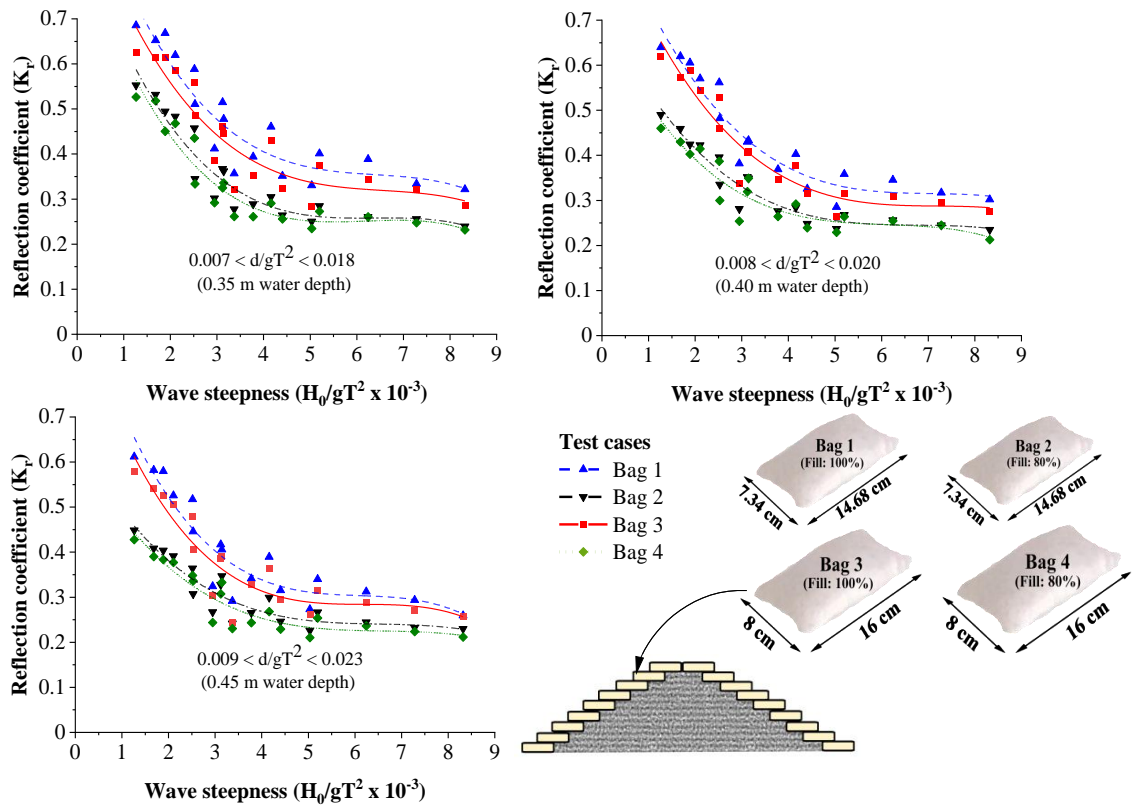


Fig. 4.12 Reflection curves of different configurations of GSC breakwater for different relative water depths

Bags filled to 100% exhibit higher reflection than the same bags filled to 80%. Breakwaters armoured with Bag 1 and Bag 3 (100% filled bags) showed 16.30 to 43.7% and 18 to 37.67% higher reflection than their respective 80% filled counterparts, Bag 2 and Bag 4. This is mainly because of the fact that 80% filled bags have 20% empty spaces within the bag. This leads to additional absorption of water particles into the bag, owing to lesser reflection. Therefore, 80% filled bags tend to be less reflective in nature. Thus reducing the

fill percentage is beneficial in lowering the reflection from the structure. At the same time, the reduction in filling percentage reduces the stability of the structure, pointing to the need for a thorough optimisation. It can be concluded that for particular water depth, Bag 1 and Bag 4 showed maximum and minimum reflections, respectively. This trend is followed in all the tested relative water depths. Out of the three depths, 0.35 m depth represents the higher reflection. That implies in higher depths, waves tend to be less reflective in nature due to increased absorption of uprushed waves. From all the cases, it has been understood that reflection behaviour shows 16.3 to 43.7% decrease when the fill is reduced from 100 to 80% and up to 10.07% when the bag size is increased. It is concluded that lowering the fill percentage reduces reflection (40-20%) than increasing bag size.

4.1.4 Stability and Damage analysis

Stability tests for breakwater with GSCs are carried out in the wave mechanics laboratory of the National Institute of Technology Karnataka, Surathkal. The stability of the structure is well understood by analysing the level of damage exhibited by each configuration. Since the present model of GSC breakwater is different from that of a conventional rubble mound breakwater, damage analysis is carried out based on the methodology proposed by Dassanayake and Oumeraci (2012). This type of classification involves the calculation of displaced or detached units from critical layers. Damage classification is carried out by identifying critical layers and quantifying the amount of bags displaced and detached from those layers. Based on this, each case is categorised from DC0 to DC4. Those cases which showed very high stability (less than 5% of the GSCs in critical layer moved) is classified as 'No Damage' case and is termed DC0. For concluding a test case (with particular wave height and period) to be DC0, the structure is exposed to at least 2000 waves with similar characteristics. Dassanayake and Oumeraci (2012) report the exposure of 100 regular waves for each test case; however, for more conservative results, a minimum of 2000 waves are used in the present study. Test cases are classified into DC1, DC2, DC3 based on the conditions in Table 3.6, after exposure to 2000 waves. In higher damage cases, washing out of the core occurs, which in turn forces one to stop wave exposure and is

marked as ‘Total Failure’ or DC4. In such cases, the total number of waves exposed to the structure need not be 2000.

As a typical example of analysis, only the case of model response for a water depth of 0.40 m is discussed in this section. Experimentation is carried out by first fixing the wave period and then ranging wave heights. For better understanding, prototype wave parameters are indicated in brackets for the following discussions. Waves of 2.2 s (12 s in prototype) period and heights ranging from 0.06 to 0.16 m (1.8 to 4.8 m) are initially tested. 2.2 s is the maximum wave period selected; therefore, waves of this period will be very gentle and less damaging compared to other wave periods. Experimentation showed that for the waves of 0.06 and 0.08 m, the structure remained stable up to 2000 waves (Fig. 4.13).



Fig. 4.13 Stable structure ('Bag 1') subjected to attack of 3000 waves of time period 2.2 s, (a) wave height 0.06 m and (b) wave height 0.08 m, for relative water depth $0.008 < d/gT^2 < 0.020$ (i.e. 0.40 m water depth).

Keeping the wave period fixed at 2.2 s, 0.12 m (3.6 m) waves are tested in the next trial. In this case, the initial 1000 waves could not make considerable deformations to GSC units. After 1200 waves, two units started rocking from 12th row (from the crest). Rocking represents a very minute to and fro motion. But as wave attack progressed, rocking increased and uplift force resulted in the outward motion of these units. This deformation

left its vertically upper units from 11th row in similar outward movement (Fig. 4.14). After 2000 waves, 13 units from 11th and 12th row showed displacements up to 4 cm with no units detached. There are 24 units in 11th and 12th rows, out of it, more than 50% of units got displaced. Therefore, this case is considered to be ‘Minor Damage’ (DC2) according to the adopted damage classification (Table 3.6).



Fig. 4.14 Bag 1 configuration subjected to 0.12 m high waves with 2.2 s time period for a relative water depth of $0.008 < d/gT^2 < 0.020$ (i.e. 0.40 m water depth). Highlighted armour units exhibited sliding instability due to uplifting.

For higher incident waves, the structure showed higher levels of damage. Structure subjected to 0.16 m incident waves (maximum wave height selected for physical modelling) started displacement just after the first 100 waves, and rocking of units from 9th, 10th, 11th and 12th layers could be observed. These layers lie close to the still water line; therefore, increased wave-structure interaction occurs in this region. Since the wave height is maximum, the increased energy of the incident waves accelerated the rocking process resulting in the pullout of the armour units. Since layers around the still water line settled down, a complete downward motion has been observed. This resulted in the pullout of 3rd

and 4th layers (Fig. 4.15, a. and b.). These movements continued till 500 waves, afterwards, the core got exposed (Fig. 4.15, c). The exposed core marks the extreme level of damage, and the present case is categorised as ‘Total Damage’ or DC4, even when there is no complete detachment of GSC units.

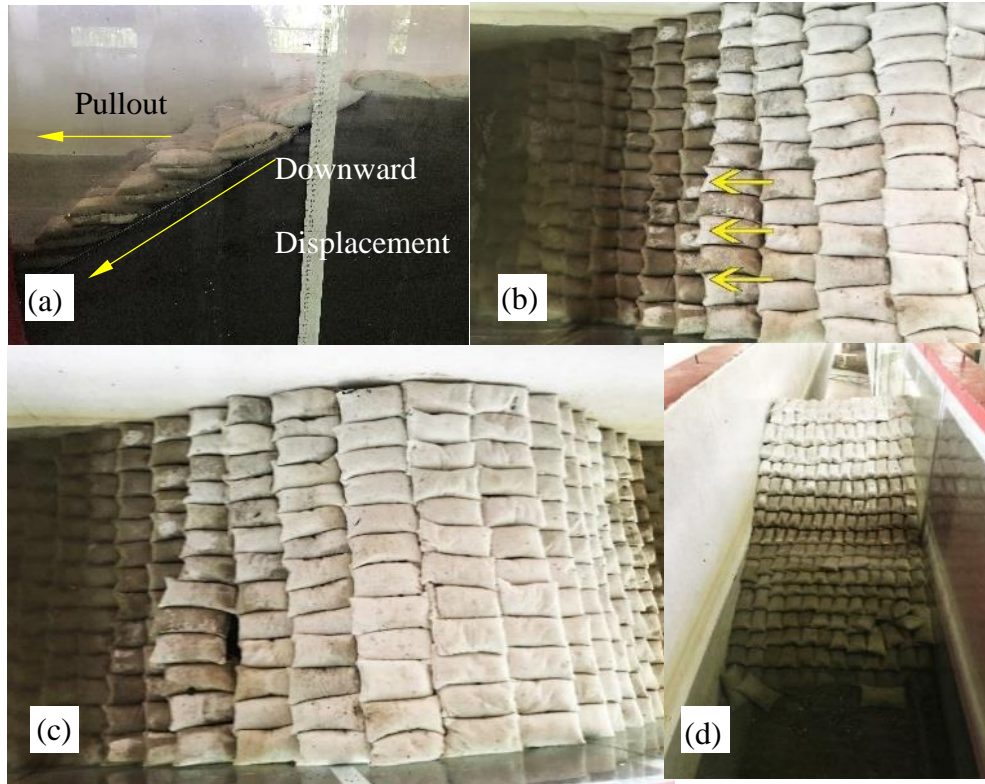


Fig. 4.15 Damage of GSC armour units (Bag 1) in response to 0.16 m (max wave height) waves, 2.2 s wave period, (a),(b) settling down and pullout of 3rd and 4th layer after 200 waves; (c) exposed core after 500 waves; (d) ‘Bag 1’ subjected to 1.4 s (T) and 0.16 (H) waves, all experiments are carried out in a relative water depth of $0.008 < d/gT^2 < 0.020$ (i.e. 0.40 m water depth). This can be considered for the future studies.

Considering the typical case of a wave period of 1.4 s (7.7 s), the structure exhibited stable conditions in response to waves of 0.06 m (1.8 m) and 0.08 m (2.4 m) height. Waves of 0.10 m (3 m) and 0.12 m (3.6 m) produced minor damage and 0.14 m (4.2 m) and 0.16 m (4.8 m) waves totally damaged the structure. It has to be noted that, 1.4 s waves are more

critical than 2.2 s waves, as the smaller wave period will increase the frequency of wave attack on the structure, results in greater damage. This is evident as 2.2 s waves caused ‘total damage’ only in the case of 0.16 m waves, whereas 1.4 s waves with both 0.16 m and 0.14 m wave heights caused ‘total damage’ to the structure as illustrated in Fig. 4.15, c and d. Further, 1.4 s waves resulted in 52.77% damage within the first 50 waves, whereas 2.2 s waves showed sliding down and core exposure only after 500 waves. Therefore, a general conclusion can be drawn that, as the wave period decreases, the structure is subjected to the attack of more waves within a unit time. Increased wave energy incident on structure within short period results in upliftment and detachment of armour units.

Observations of model studies are used to plot a number of graphs. Graph shows the relationship between stability number (N_s) and surf similarity parameter (ξ_0) for a GSC breakwater model with Bag 1 for a relative water depth d/gT^2 ranging from 0.018 to 0.0073 (35 cm water depth in the wave flume)(Particular case is selected to explain the process of stability curve development. Tests with other bags in various water depths are discussed in subsequent sections). Stability number (N_s) is calculated using (4.1).

$$N_s = \frac{H_s}{\left(\frac{\rho_{GSC}}{\rho_w} - 1\right).D} = \frac{C_w}{\sqrt{\xi_0}} \quad (4.1)$$

where, $D = l_c \cdot \sin\alpha$.

N_s is the stability number

H_s = Incident wave height

ρ_{GSC} = density of armour units (2005 Kg/m³)

ρ_w = density of seawater (1025 kg/m³)

D = armour layer thickness, given by $l_c \cdot \sin\alpha$

C_w = empirical parameter

ξ_0 = Surf similarity parameter.

l_c = length of GSC armour units.

The stability number (N_s) of each test case is calculated and is classified into various damage levels using physical modelling. The relationship between the surf similarity parameter (ξ_0) and stability number (N_s) is identified in the graph. For the present case, ξ_0 varies from 2.08 to 5.71. The Lowest ξ_0 (2.08) is exhibited by cases with a wave height of 0.16 m and a wave period of 1.4 s, which is the highest wave height and lowest wave period among all the input wave parameter ranges. The Highest ξ_0 (5.71) is exhibited by case with a 0.06 m wave height and 2.2 seconds period, which is the lowest wave height and highest wave period among the input wave parameter range. Stability number (N_s) is ranged from 0.87 to 2.63. Fig. 4.16 represents the relation between surf similarity parameter (ξ_0) and stability number (N_s) for a set of test cases. A total of 30 test series were conducted to study the stability of the structure in this particular water depth by varying wave height and period. Of these, 33.33% of cases are reported as ‘No Damage’ or DC0.

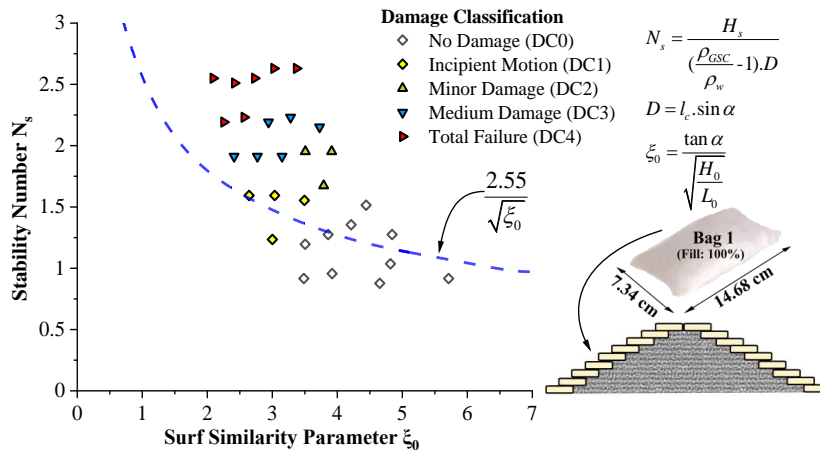


Fig. 4.16 Variation of stability number (N_s) with surf similarity parameter (ξ_0) for structure armoured with Bag 1 at a relative water depth (d/gT^2) ranging from 0.018 to 0.0073 (0.35 m actual depth)

13.33% showed ‘Incipient Motion’ (DC1), 10% showed ‘Minor Damage’ (DC2), 20% showed ‘Medium Damage’ (DC3), and 23.33% showed ‘Total Failure’ or DC4. The incipient motion curve is drawn from the relation (4.3)

$$N_s = \frac{C_w}{\sqrt{\xi_0}} \quad (4.2)$$

$$C_w = N_s \cdot \sqrt{\xi_0} \quad (4.3)$$

C_w value for all the ‘Incipient Motion’ cases is calculated, and its average is used in (4.2) to draw the curve. In the present case, the curve is represented by $2.55/(\xi_0)^{0.5}$, where 2.55 is the average C_w value of 4 reported ‘Incipient Motion’ cases. The importance of this curve is that it represents the boundary of stability cases. All the points below the curve are considered to be stable and can be used for engineering applications. All the points above the curve represent a set of unstable cases which cannot be suggested for field applications.

In general, the graph can be used to draw some additional information. The rows of points in the graphs coincide with wave height, i.e. all the cases with the lowest wave height of 0.06 m will be in the lowest row and the highest wave height of 0.16 m in the topmost row. Other rows are in the order of increasing wave height from bottom to top. Similarly, columns are represented in the order of wave period, with the left-most column showing the minimum period (1.4 s) and the right-most column showing the maximum wave period (2.2 s). In the present case, the structure is stable for 0.06 m and 0.08 m waves for all wave periods except for 1.4 s and 0.08 m. From 0.10 m onwards, the structure remains unstable, with all 0.16 m (highest wave height) cases showing total damage.

4.1.4.1 Comparison of damage levels exhibited by different GSC armour units

Stability analysis for ‘Bag 2’, ‘Bag 3’ and ‘Bag 4’ configurations are carried out. 2.61, 2.38, 2.68 and 2.52 are obtained as empirical parameters (C_w) for ‘Bag 1’, ‘Bag 2’, ‘Bag 3’ and ‘Bag 4’, respectively, refer Fig. 4.17. Results of experimentation in other water depths are discussed in section 4.1.4.4. The increasing value of C_w signifies an increase in the stability of the structure. 100% filled bags show higher stability than their 80% filled counterparts. For the particular water depth considered, Bag 3 showed maximum stability,

followed by Bag 1, Bag 4 and Bag 2. Fig. 4.18 discuss the levels of damage and its percentage exhibited by structure for different armour unit configurations. As the fill percentage varies from 100 to 80, ‘Total Damage’ (DC4) cases increase considerably (up to 25%). This can be attributed to the difference in size and filling percentage of the bags. These parameters are separately analysed in the following sections.

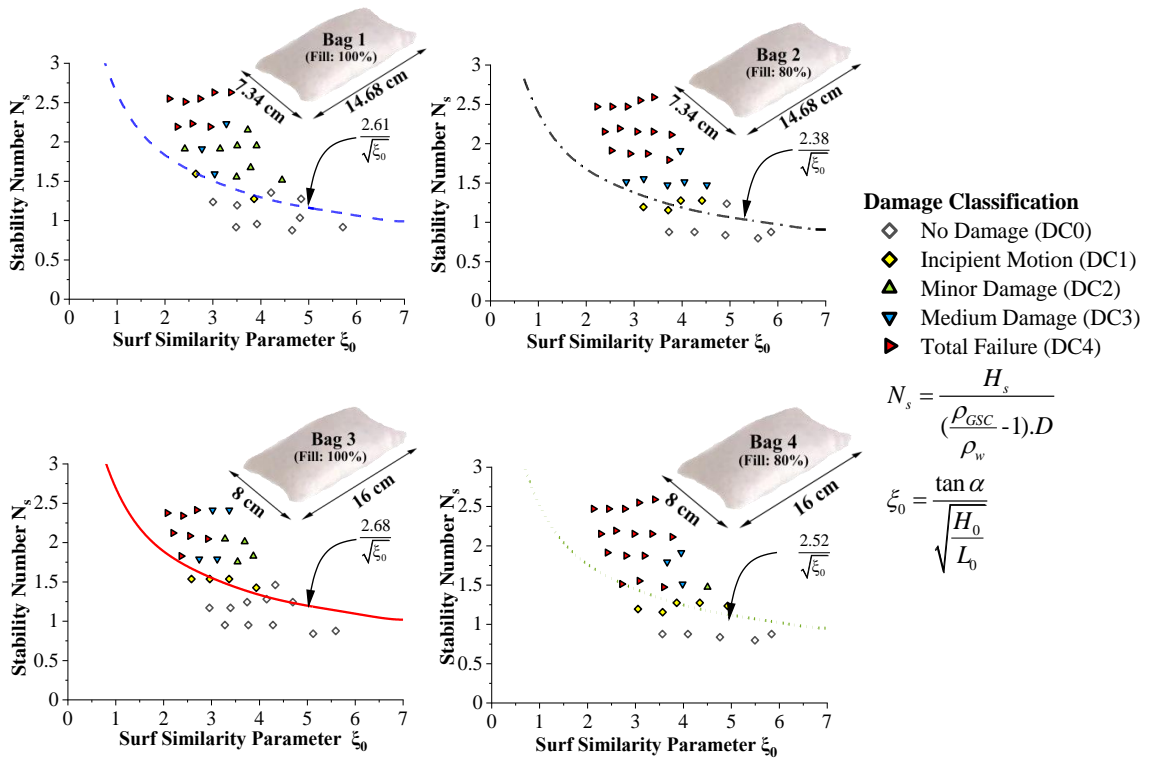


Fig. 4.17 Stability curves for various GSC configurations.

4.1.4.2 Effect of armour units size

As far as armour unit size is considered, Bag 1 and Bag 2 are of the same dimensions. Similarly, Bag 3 and Bag 4 also share identical dimensions. Bag 1 and Bag 3, when filled to 100% resulted in 400 g and 500 g bags, respectively. As discussed, using 500 g bags (Bag 3) as armour units resulted in 3.13 to 4.2% higher stability (Fig. 4.19.). Similarly, Bag 4 showed up to 8% higher stability than Bag 2 (both bags are filled to 80%) (Fig. 4.20.). This is obtained by the comparison of the incipient motion curves deduced for each

configuration. Additionally, a drastic increase in total failure cases ($\approx 50\%$) is reported for 80% filled bags (Compare 'Total Failure' (DC4) points in Fig. 4.19 and Fig. 4.20).

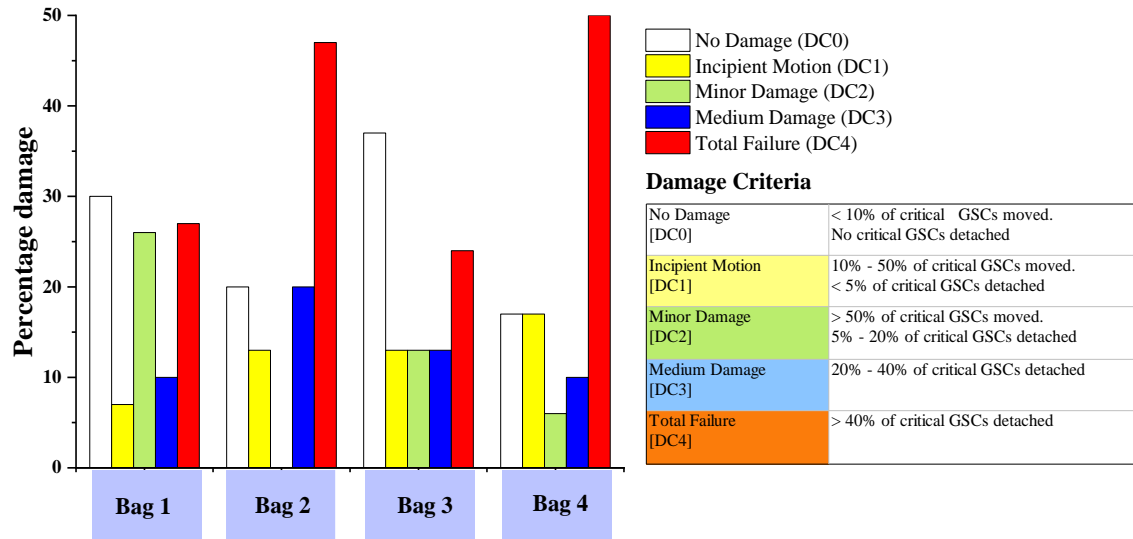


Fig. 4.18 Percentage damage (concerning damage levels) exhibited by different configurations of GSC breakwater structure.

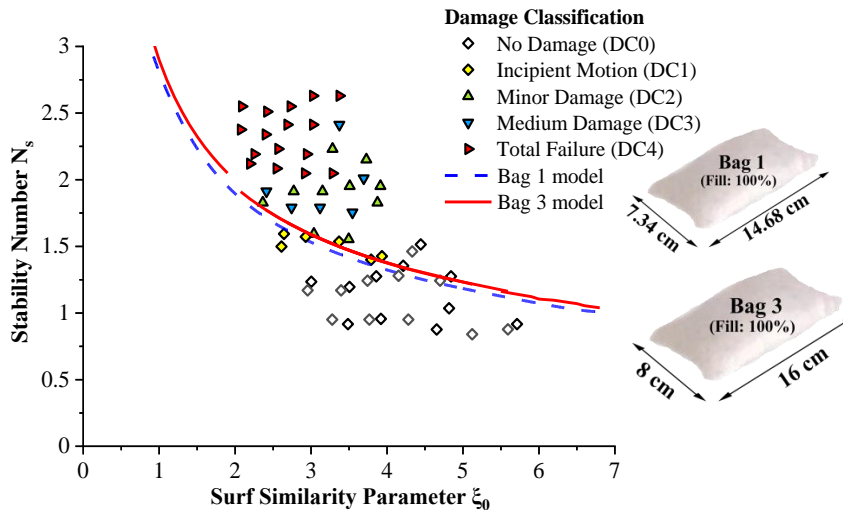


Fig. 4.19 Comparison of stability curves of Bag 1 and Bag 3 (100% filled)

Variation in C_w values is found to be more for 80% filled bags than 100% filled bags. Bag 3 (500 g) has more self-weight than Bag 1 (400 g), which contributes to the higher stability

of the structure. Since the percentage of overlap is kept constant at 50%, bags with larger dimensions (Bags 3 and 4) offers more area of overlap. This contributes additional stability for Bag 3 and Bag 4, as it comprises up to 18.8% more surface area in each bag for the gravitational force to act (refer Fig. 4.21). Moreover, structures armoured with bigger bags comprise more pore spaces, which results in increased energy absorption contributing to higher stability of the configuration.

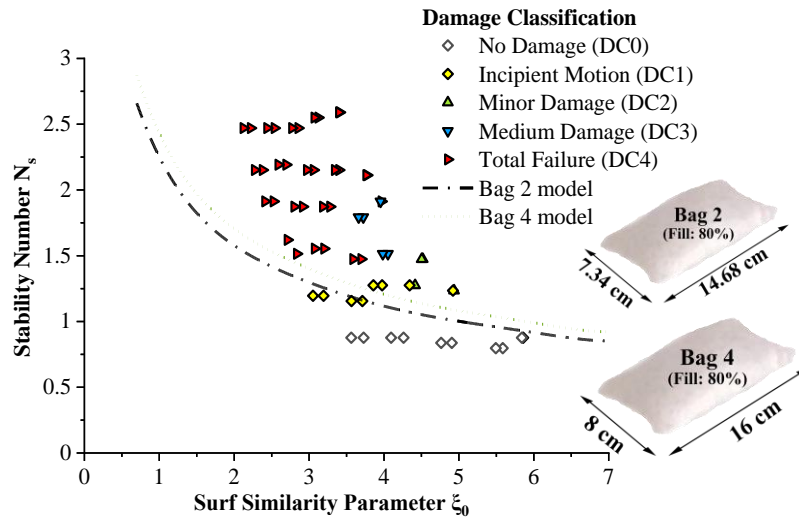


Fig. 4.20 Comparison of stability curves of Bag 2 and Bag 4 (80% filled bags).

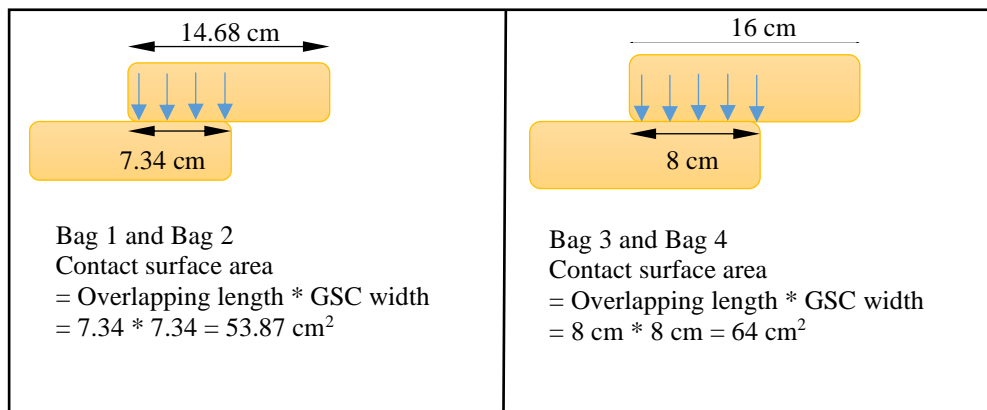


Fig. 4.21 Comparison of contact surface area offered by Bags when placed in GSC breakwater model with 50% overlap.

4.1.4.3 Effect of sand fill ratio

The significance of the sand fill ratio is examined in the current section. When the fill percentage of the smaller bags is varied from 100 to 80, a decrease of 12.2 to 14% is observed in the stability number (N_s) (Fig. 4.22). Similarly, up to a 7% decrease in stability is observed when the larger bags are filled to 80% from 100% (Fig. 4.23). This has resulted in increased movement of GSC units in the form of sliding and mostly 'pullout'. When the sand fill percentage of bags is reduced, the weight of individual units reduces, more empty spaces are created in the bag, and internal migration of sand takes place. Dassanayake and Oumeraci (2012a) report that the required pullout force increases with increasing sand fill ratio. i.e. 90 – 100% filled sandbags require higher force for the pullout, thus remaining stable than lesser sand-filled ones. This fact is validated in the present study, as 100% filled containers showed 7-14% higher stability than 80% filled counterparts. Failure of 80% filled bags was prominently due to pullout and can be because of increased empty spaces, reduced self-weight and sand migration within the bag.

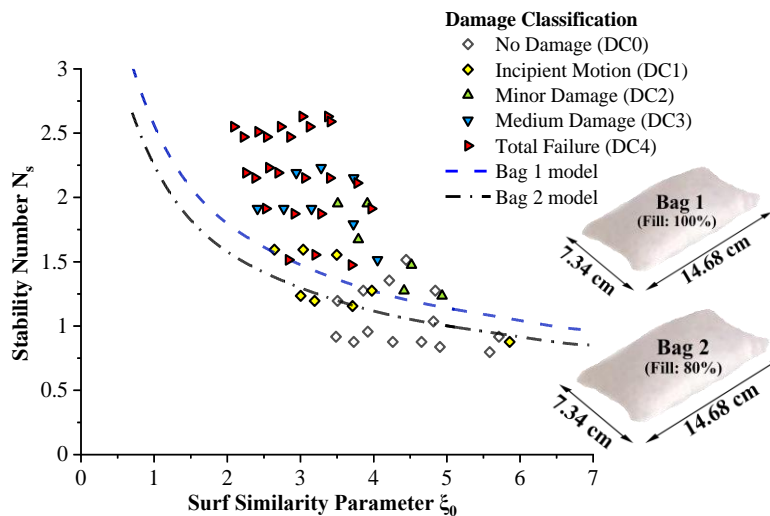


Fig. 4.22 Comparison of stability curves of structure comprising Bag 1 and Bag 2 (same bag dimensions with 100% and 80% fill respectively).

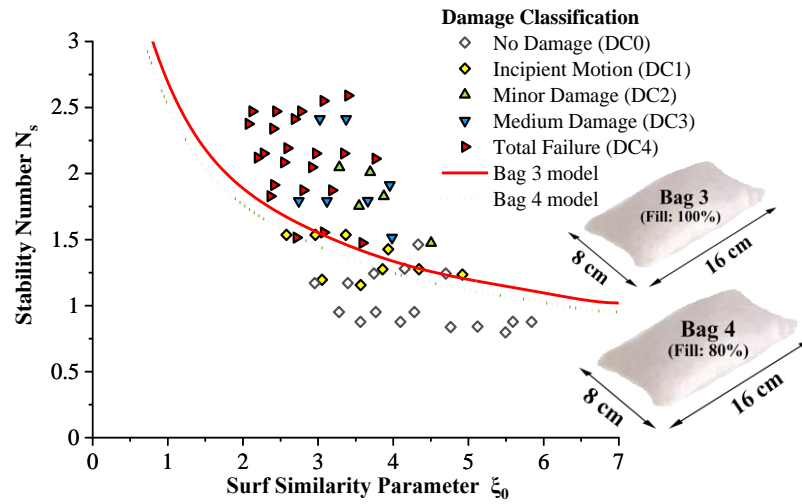


Fig. 4.23 Comparison of stability curves of the structure comprising Bag 3 and Bag 4.

4.1.4.4 Effect of water depth

Each configuration is tested for different water depths in order to attain various field depth conditions. In the present study, three different relative water depths are considered (actual water depth is indicated in brackets),

1. $0.007 < d/gT^2 < 0.018$ (0.35 m)
2. $0.008 < d/gT^2 < 0.020$ (0.40 m)
3. $0.009 < d/gT^2 < 0.023$ (0.45 m)

Fig. 4.24 depicts the incipient motion curves of different GSC breakwater configurations for three different relative water depths described above. The initial examination suggests that stability number (N_s) does not depend on relative water depth. Stability curves for all the three configurations align together, indicating a very slight dependence of water depth on stability. As water depth increases, other parameters like runup and overtopping increase, but the stability of the structure remains identical. However, the trend shows a minute increase in N_s (3.9 to 4.4%) as the water depth increases from 0.35 m to 0.45 m. when the water depth is increased from 0.35 m to 0.40 m, an increase of 1.7 to 2.2% is observed in N_s .

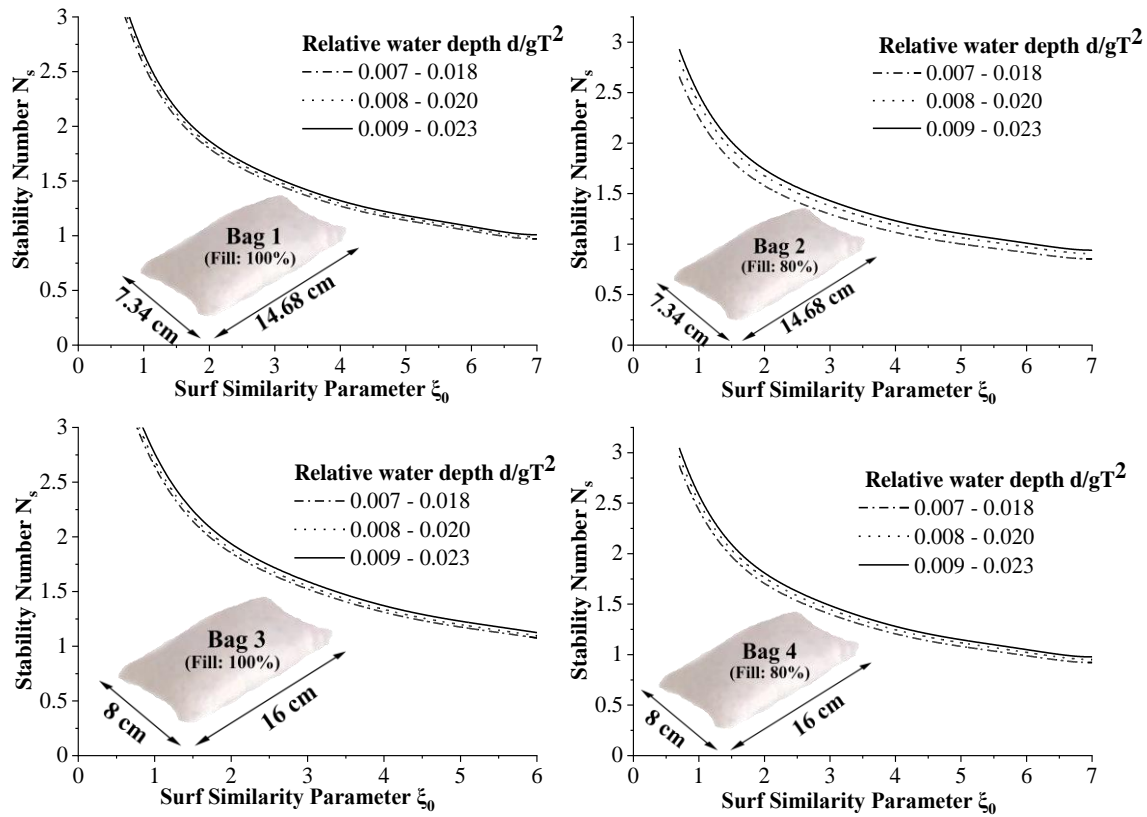


Fig. 4.24 Effect of water depth on the stability of GSC breakwaters with different configurations.

Similarly, a 2 to 2.2% increase in stability number (N_s) is also observed when the water depth is increased from 0.40 m to 0.45 m. Even if the values appear to be insignificant, it is worth understanding the trend in variation of stability curves. It has to be noted that the structure tends to be a little more stable in higher water depths. This disagrees with the general conclusions of various studies, reporting increased instability in higher water depths. A possible reason can be the upward shift of still water level in higher water depth cases (0.45 m). It is seen that critical damaging layers are observed near to the still water level. Layers lying above 'critical layers' tend to slide and displace, causing higher instability. Relative row height, the ratio of damaged row height to water depth, is calculated to identify the trends. When water depth is 0.35 m, critical layers are observed at a relative row height of 0.77 to 0.51 (in the present investigation, GSC row 13 to 15 from

the crest). As water depth is increased to 0.45 m, critical layers are observed at a relative row height of 0.8 to 1.1 (11 to 8th row from the crest), indicating an upward shift of ‘critical layers’. As critically damaging layers are observed in the top region, the number of affected layers (lying above critical layers) is less in higher water depths. As seen, the number of unstable layers which lie above ‘critical layers’ is nearly 40% less, owing to higher stability in 0.45 m water depth.

4.1.4.5 Effect of incident wave height

The study on the influence of surf similarity parameter (ξ_0) and wave steepness (H/gT^2) helps in understanding the response of different types of waves on GSC structures. But for a grass root level of physical interpretation, it is imperative to identify the impact of incident wave heights on GSC structures. Most of the conventional design formulae like Hudson’s, relate design wave height to armour unit weight. This helps in identifying the limit of wave heights that a structure can withstand. This section aims to identify the limits of permissible wave heights for a GSC breakwater and investigate its response to varying incident wave heights. Fig. 4.25 represents the variation of damage level for different test cases, in accordance with the increasing incident wave heights.

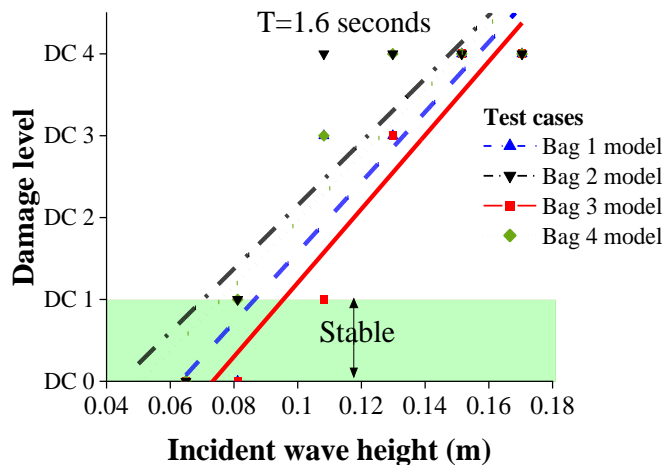


Fig. 4.25 Variation of damage level with respect to incident wave heights for different test cases of GSC breakwater (T= 1.6 s, water depth = 0.40 m).

The sample graph chosen is of waves of period 1.6 s (8.76 s) and tested at a relative water depth, $0.008 < d/gT^2 < 0.020$ (i.e. 0.40 m) for wave heights ranging from 0.06 m to 0.16 m. This graph is randomly chosen to explain the typical model behaviour and its trends. It is clearly identified from Fig. 4.25 that the increase in incident wave height results in a significant rise in damage level. As we know, the transition from DC0 to DC4 represents conditions with ‘no damage’ to ‘total failure’, with DC1 (incipient motion) being the limit of permissible damage (Dassanayake and Oumeraci, 2012b). Therefore, the green area in Fig. 4.25 represents cases which are totally stable or have minor movements of the armour units, which are permissible for field applications. Considering different test cases, ‘Bag 2’ shows the minimum and ‘Bag 3’ shows the maximum abscissa value of the DC1 line. In other words, cases with ‘Bag 2’ exceeds stability limits for smaller incident wave heights than any other configurations. ‘Bag 2’ cuts the line of incipient motion at an incident wave height value of 0.07 m, followed by ‘Bag 4’, ‘Bag 1’ and ‘Bag 3’ at 0.076 m, 0.086 m and 0.095 meters of incident wave heights respectively. This implies that when a particular relative water depth $0.008 < d/gT^2 < 0.020$ (i.e. 0.4 m) and wave period (1.6 s) is considered, ‘Bag 2’ will withstand waves up to 2.1 m, ‘Bag 4’ up to 2.28, ‘Bag 1’ up to 2.58 and ‘Bag 3’ up to 2.85 meters in prototype scale. Analysing the results, it has been identified that bag size and percentage fill are the two crucial parameters affecting stability.

As bag size increases, the self-weight of each bag increases, resulting in additional restoring gravitational force. Literature also suggests that higher pullout force is required to detach bags with higher weight. This is evident from Fig. 4.25, as ‘Bag 3’ with a higher weight (500 g when fully filled) can withstand up to 2.85 m waves than ‘Bag 1’ (400 g when fully filled), which cannot withstand waves more than 2.58 m in prototype scale. In other words, when the bag weight changed from 400 grams to 500 grams, the structure could tolerate up to 10.14% higher waves.

Regarding percentage fill, 100% filled bags can withstand 22.85 to 25% higher incident waves than their 80% filled counterparts. This is due to the fact that 100% filled bags possess more self-weight than 80% filled bags. In addition, in 80% filled bags, sand particles experience more mobility than in bags filled to its maximum capacity, resulting

in additional instability. More empty spaces inside the bag lead to the intrusion of water during wave down rush, resulting in additional internal pullout force leading to the detachment of sandbags. According to the experimental results of Dassanayake and Oumeraci (2012a), as percentage fill increases, more pullout force is required to detach GSC units. They also reported 90-100% filled bags to possess higher stability against pullout. This fact is validated in the present study, as 100% filled bags withstood 25% higher waves than 80% filled bags.

Fig. 4.26 represents the relationship between incident wave height and damage level for all model configurations investigated at a relative water depth of (d/gT^2) 0.008 to 0.020 (0.40 m). As discussed in the above section, ‘Bag 3’ withstands higher waves, followed by ‘Bag 1’, ‘Bag 4’ and ‘Bag 2’. When the period of the waves is considered, short-period waves cause greater damage compared to longer-period waves. To appreciate the effect of the wave period, permissible non-damaging wave heights for each configuration for extreme values of the model wave period are analysed in Table 4.1.

Table 4.1 Maximum limit of non-damaging incident wave heights observed for various GSC configurations for extreme cases of wave periods (relative water depth (d/gT^2) 0.008 to 0.020 (0.40 m).

Configurations	Limit of non-damaging incident wave heights (m)			
	(1.4 seconds)		(2.2 seconds)	
	Model	Prototype	Model	Prototype
Bag 1	0.091	2.732	0.093	2.79
Bag 2	0.065	1.95	0.067	2.01
Bag 3	0.099	2.97	0.104	3.12
Bag 4	0.069	2.07	0.076	2.28

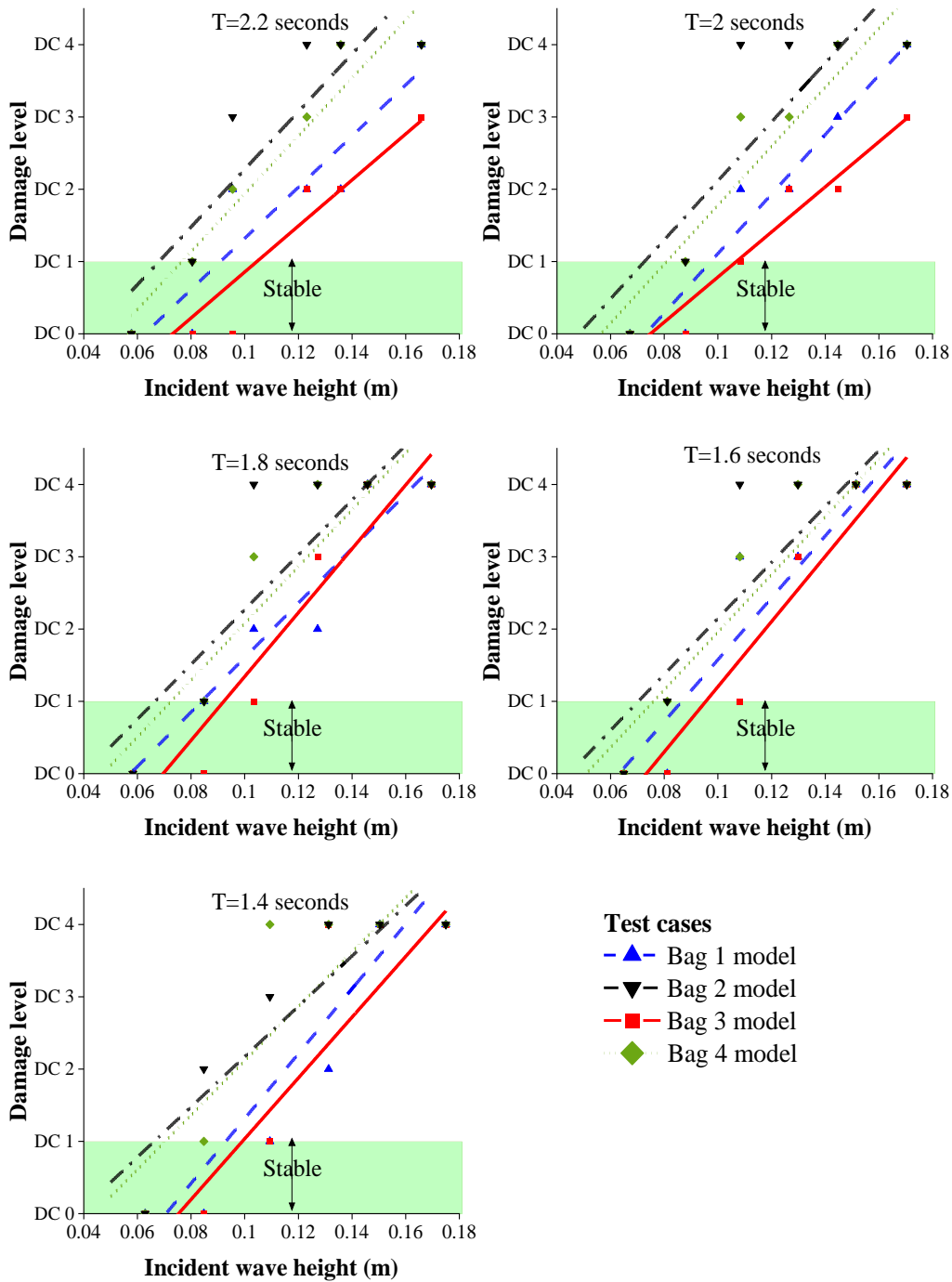


Fig. 4.26 Variation of damage level with respect to incident wave height for all tested cases of GSC breakwaters for relative water depth (d/gT^2) 0.008 to 0.020 (i.e. 0.40 m water depth).

Considering all the cases, when the wave period is varied from 1.4 s to 2.2 s, the structures can withstand 5 to 10.14% higher waves. This is due to the fact that waves with larger periods are gentle and possess less energy. 80% filled bags experience damage at much lower wave heights. As discussed earlier, this is due to the fact that 80% filled bags possess less self-weight and has more empty spaces, which leads to the mobility of internal sand particles owing to the higher instability of those bags. It may also be noted that most of the test cases lie outside the stable region. This may lead to a perception that GSC breakwaters are inconsistent and highly unstable. But from experimental results, it has been concluded that ‘Bag 3’ can be used up to an incident wave height of 0.099 m on the model scale, which would be 2.97 m when converted to the prototype scale. A structure withstanding 2.97 meters of incident wave heights is highly sufficient for small fishing harbours and coastal protection structures. This serves the purpose of study, wherein the use of GSC breakwaters on a large scale like port structures are not considered.

4.1.4.6 Stability Nomograms

Stability curves for all the test cases are outlined in Fig. 4.27, and can be projected as one of the major research outcomes. The lines represent the ‘incipient motion’ curves (DC1), which mark the extent of stability. Individual data points or test cases are not shown in the graph, as the data points for four cases (i.e.120 data points), when represented in one diagram, would result in overcrowding. Fig. 4.27 represents the conclusions of all discussions from previous sections. One can quickly identify the lower stability of 80% filled bags and improved stability with increasing bag size through the nomograms. It has to be noted that the breakwaters model with Bag 3 is up to 28% more stable than with Bag 2 configuration. The increased self-weight and porosity are attributed to the highest stability of GSC breakwater structures armoured with Bag 3. Additionally, these nomograms are useful for designing GSC breakwaters confining to the parameters discussed in the present study. It also serves as a guideline for understanding the behaviour of different model configurations in varying water depths.

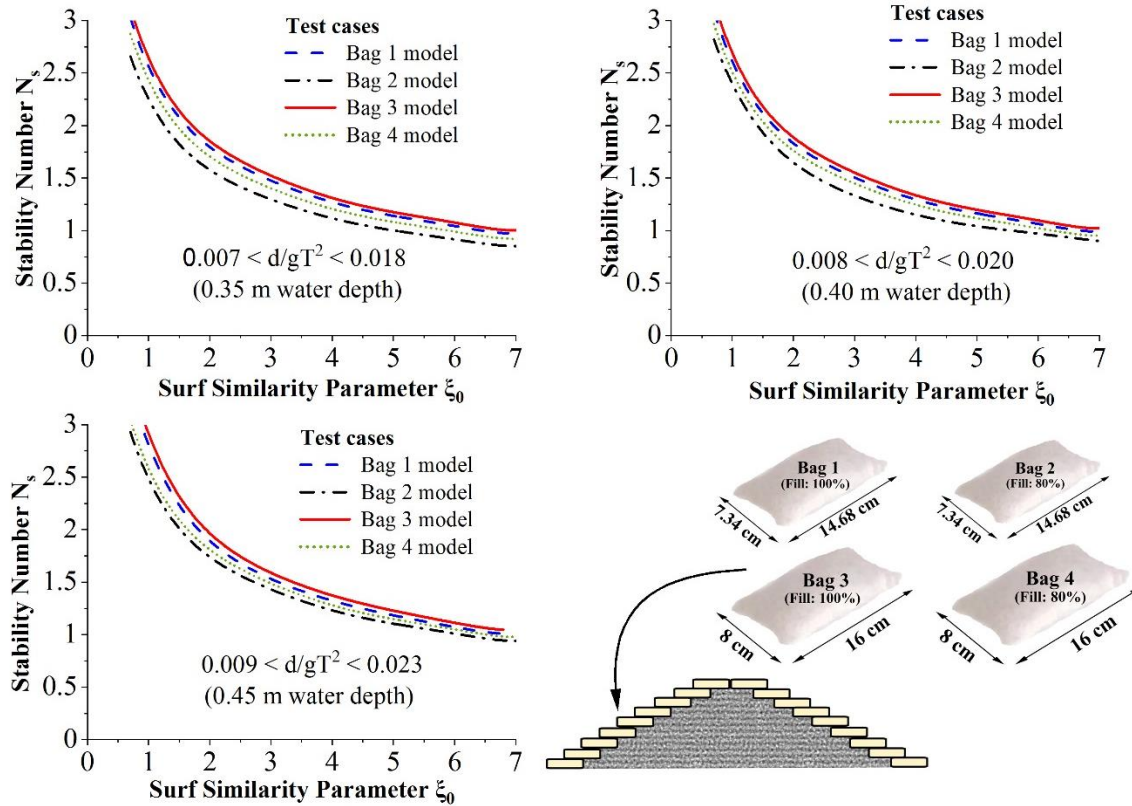


Fig. 4.27 Stability nomograms for GSC breakwater

4.2 STUDIES ON GSC DOUBLE-LAYER BREAKWATERS (FILLED WITH SAND ALONE)

Breakwaters are constructed in two different arrangements, double-layer placement (Fig. 4.28) and slope parallel placement (Fig. 4.29) with four different GSC armours, namely



Fig. 4.28 Constructed model of double-layer GSC breakwater structure.



Fig. 4.29 Constructed model of double-layer GSC breakwater structure with slope-parallel outer layer.

Bag 1, Bag 2, Bag 3 and Bag 4, (refer Fig. 3.4 for bag dimensions and arrangements). Studies conducted on double-layer GSC breakwater structures are detailed in the following sections.

4.2.1 Wave runup studies

4.2.1.1 Variation of relative runup (R_u/H_0) with deepwater wave steepness (H_0/gT^2)

Fig. 4.30 represents the variation of relative runup (R_u/H_0) with respect to deepwater wave steepness (H_0/gT^2) for a relative water depth of d/gT^2 (0.007 to 0.018 (0.35 m depth), 0.008 to 0.020 (0.40 m water depth) and 0.009 to 0.023 (0.45 m water depth) for different configurations of geotextile breakwater. The maximum and minimum runup observed among all configurations were 3.4 and 0.8 times the deep water wave heights, respectively and is decreasing with increasing deep water wave steepness (H_0/gT^2). Wave runup values observed at 0.45 m water depth are higher than those reported at 0.40 m and 0.35 m water depths indicating a rise in runup with increasing water depth. In all water depths, configuration with ‘Bag 3’ (100% filled 500 g bags, parallel to slope) exhibited maximum relative runup followed by ‘Bag 1’ (100% filled 400 g bags, parallel to slope), ‘Bag 1 (DL)’, ‘Bag 3 (DL)’, ‘Bag 2 (DL)’ and ‘Bag 4 (DL)’ configurations. Relative runup exhibited by ‘Bag 3 (PS)’ (100% filled 500 g bags, parallel to slope) configuration is 28% higher than that of ‘Bag 4 (DL)’, i.e. variation between maximum and minimum trend lines. When the geotextile armour units are filled to its maximum capacity, the bags act like solid units, thereby reducing the absorption of water into these units. This is evident from the graph,

Bag 1 (DL) showed 14.28% more runup than the same bags (Bag 2) filled to its 80% volume. Similarly, a 24.3% increase in relative runup is recorded when the larger bag

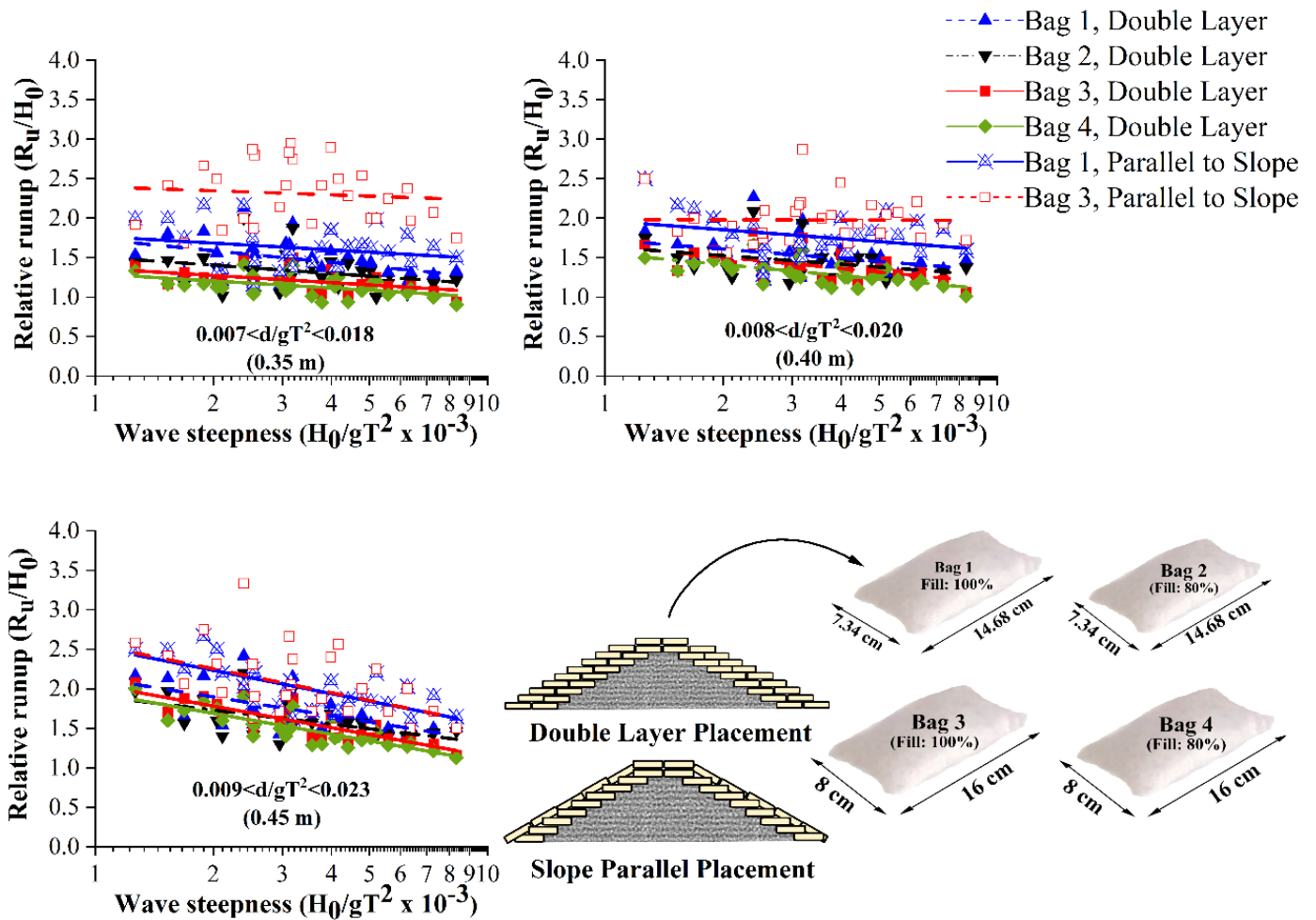


Fig. 4.30 Variation of relative runup (R_u/H_0) with respect to deep water wave steepness (H_0/gT^2) for various relative water depths (d/gT^2) for different configurations of geotextile breakwater.

fill is changed from 80 to 100% (Bag 4 to Bag 3). This indicates that filling the bags to its maximum capacity would result in higher wave runup, which may result in overtopping of waves. Bags with the same fill but different structural configurations have shown a larger variation in the runup values that is ‘Bag 1(PS)’ showed 20% more runup than the same bags arranged in double-layer configuration. This result when

the bags are arranged parallel to the slope. In this case there are limited pore spaces that aids dissipation leading to more water uprush causing increased runup for slope parallel configuration.

4.2.1.2 Effect of water depth

The effect of water depth on the wave runup is studied in the present section. Fig. 4.31 shows the variation of relative runup (R_u/H_0) of various configurations for three different relative water depths. Out of the three water depths considered, 0.45 m water depth ($0.009 < d/gT^2 < 0.023$) condition represented higher runup for all six configurations. “Bag 3 (PS)” at 0.45 m water depth showed 25% and up to 12% higher R_u/H_0 than 0.35 m and 0.40 m water depths. Similarly, ‘Bag 1 (PS)’ at 0.45 m water depth showed 25.15% and up to 16.5% higher R_u/H_0 than 0.35 m and 0.40 m water depths. ‘Bag 3 (DL)’ at 0.45 m water depth showed 9.6 to 46.66% and up to 6.8% higher R_u/H_0 than 0.35 m and 0.40 m water depths. ‘Bag 1 (DL)’ at 0.45 m water depth showed up to 13.58% and 23.8% higher R_u/H_0 than 0.35 m and 0.40 m water depths respectively. To sum up, relative runup at 0.45 m water depth exhibited 16.25 to 30.5% and 9.25 to 26.5% higher values than 0.35 m and 0.40 m water depths respectively. From above statistics it is observed that runup values increase as depth increases. Increased water depth can sustain higher unbroken waves, leading to increased uprush of water resulting in higher runup at 0.45 m water depth.

4.2.2 Wave rundown studies

4.2.2.1 Variation of relative rundown (R_d/H_0) with deepwater wave steepness (H_0/gT^2)

Fig. 4.32 represents the variation of relative rundown (R_d/H_0) with respect to deepwater wave steepness (H_0/gT^2) for a relative water depth (d/gT^2), 0.007 to 0.018 (0.35 m water depth), 0.008 to 0.020 (0.40 m water depth) and 0.009 to 0.023 (0.45 m water depth) for different configurations of the geotextile breakwater. Relative rundown (R_d/H_0) of all configurations shows a wide range varying from 0.8 to

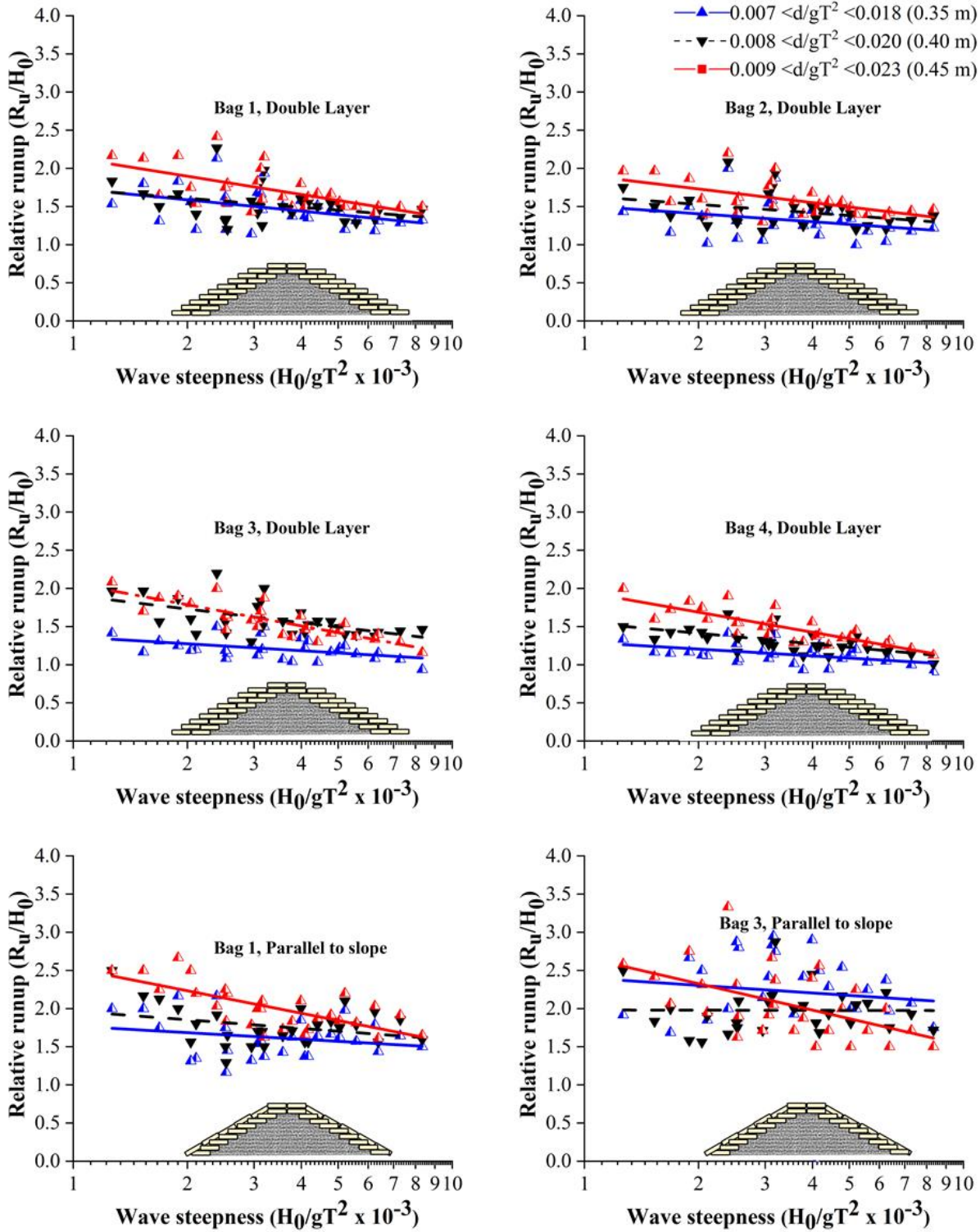


Fig. 4.31 Variation of relative runup of various configurations for different relative water depths (actual water depth is indicated in bracket)

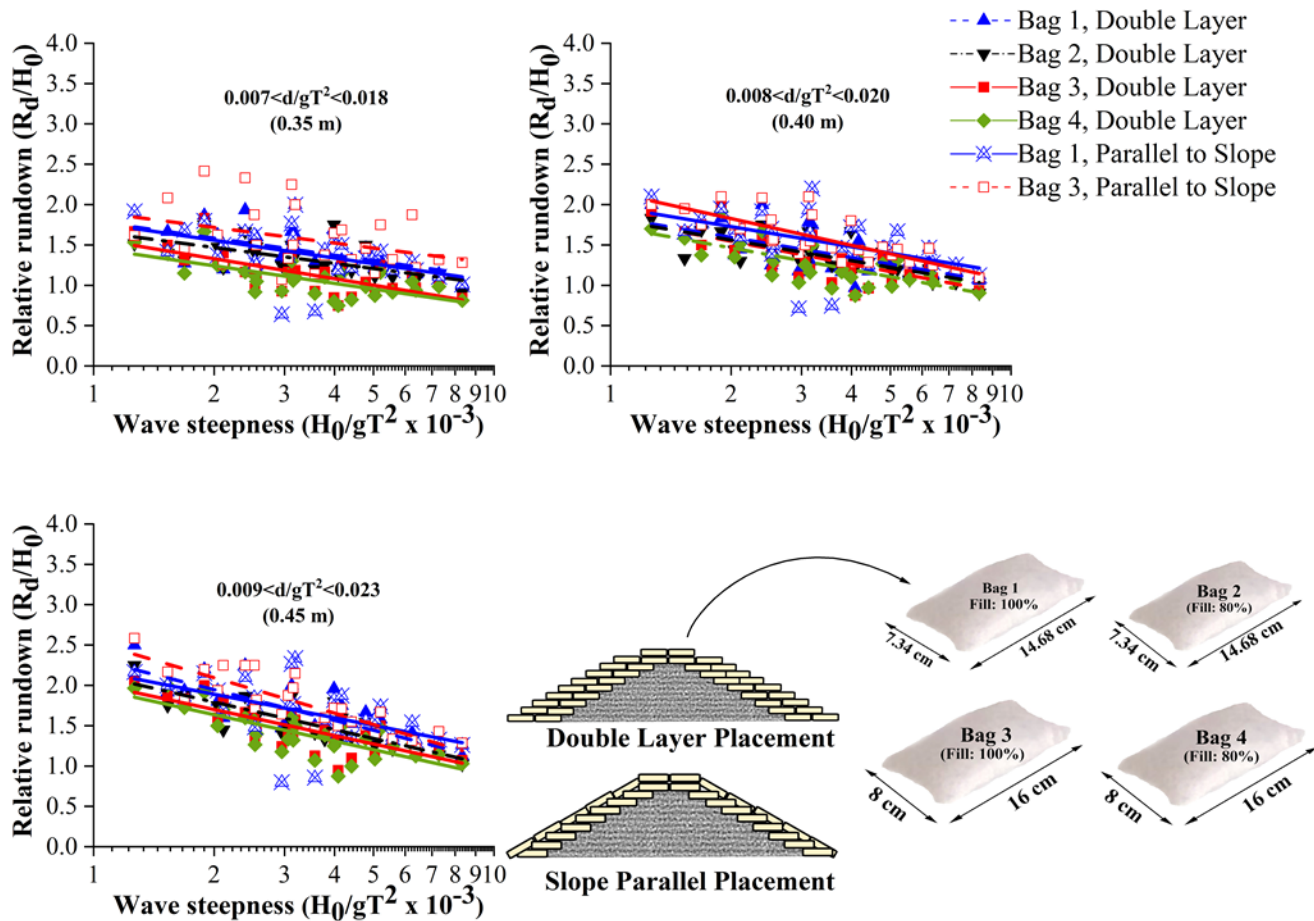


Fig. 4.32 Variation of relative rundown (R_d/H_0) with respect to deepwater wave steepness (H_0/gT^2) for various relative water depths (d/gT^2) for different configurations of geotextile breakwater.

2.6 and is decreasing with increasing deepwater wave steepness (H_0/gT^2). The trend lines of tested configurations showed higher relative rundown for configuration with slope-parallel placement than double-layer placement. Configuration with ‘Bag 3 (PS)’ exhibited maximum relative rundown followed by ‘Bag 3 (PS)’, ‘Bag 1 (DL)’, ‘Bag 2 (DL)’, ‘Bag 3 (DL)’ and ‘Bag 4 (DL)’. When the geotextile armour units are filled to its full capacity, the bags act like solid units, thereby reducing the absorption of water into these units. This is evident from the graph, as ‘Bag 1 (DL)’ showed 18.56% more rundown than the same bags filled to its 80% volume ‘Bag 2 (DL)’. Similarly,

28.88% increase in relative rundown is recorded when the fill of the larger bag is changed from 80 to 100% (comparison between Bag 4 and Bag 3). This indicates that filling the bags to its maximum capacity would result in higher wave rundown.

Larger bags (Bag 3 and Bag 4), when arranged as primary armour units produced more inter-unit spaces or pore spaces compared to smaller bags (Bag 1 and Bag 2). Higher pore spaces aid in absorption and wave energy dissipation, resulting in 21.89% lesser relative rundown for 100% filled larger bag (Bag 3) than 100% filled smaller bag (Bag 1) configuration. Similarly, for 80% filled bags, void spaces between bags and increased space within the bag, make Bag 4 better in absorbing nature. As a result, 80% filled bags control the down rush of water. Therefore, Bag 4 showed 16.8% lesser relative rundown than Bag 2. The maximum reduction percentage is more (up to 30%) in bigger bags, as 80% filled bigger bags (Bag 4) have more space within the bags than 80% filled smaller bags (Bag 2), leading to improved absorption.

From the above-mentioned trials, it can be summarised that changing the fill from 100 to 80% resulted in up to 34.23% reduction of rundown, whereas increasing the size of bags has helped only up to 19.5% reduction in rundown. Thus, a reduction in percentage fill reduces wave rundown considerably more than changing bag size.

4.2.2.2 Variation of relative rundown with water depth.

Fig. 4.33 shows the variation of relative rundown of various configurations for three different relative water depths, $0.007 < d/gT^2 < 0.018$ (0.35m), $0.008 < d/gT^2 < 0.020$ (0.40 m) and $0.009 < d/gT^2 < 0.023$ (0.45 m) with respect to deep water wave steepness. Out of the three water depths considered, 0.45 m water depth ($0.009 < d/gT^2 < 0.023$) condition represented higher rundown for all six configurations.

‘Bag 3 (PS)’ at 0.45 m water depth showed 28.14% and up to 17.8% higher relative rundown than 0.35 m and 0.40 m water depths. Similarly, ‘Bag 1 (PS)’ at 0.45 m water depth showed 21.38% and up to 14.6% higher relative rundown than 0.35 m and 0.40 m water depths. ‘Bag 3 (DL)’ at 0.45 m water depth showed 15.9% and up to 11.11% higher relative rundown than 0.35 m and 0.40 m water depths. ‘Bag 1 (DL)’ at 0.45

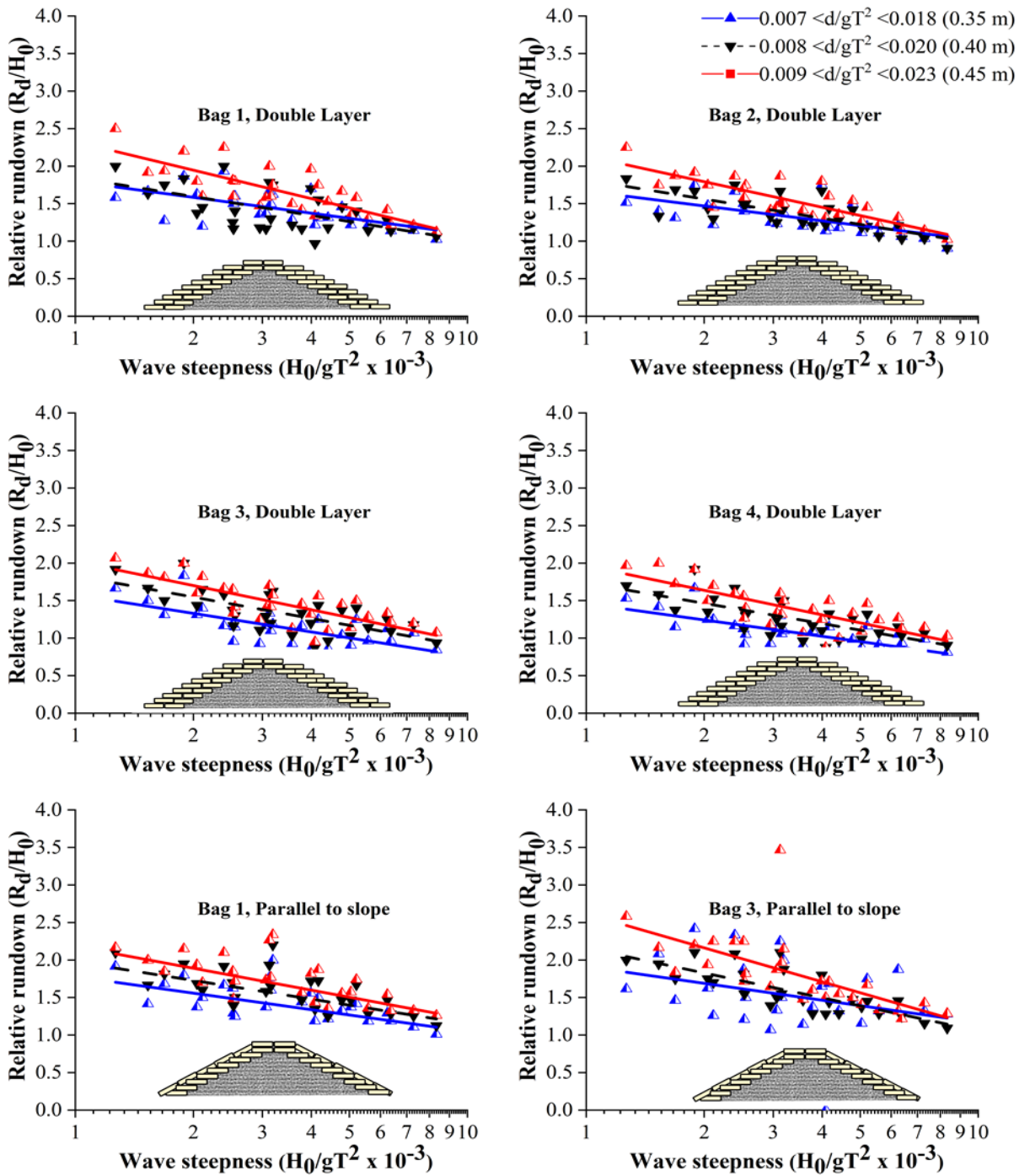


Fig. 4.33 Variation of relative rundown of various configurations for different relative water depths (actual water depth is indicated in bracket)

m water depth showed up to 31.87% and 23.57% higher relative rundown than 0.35 m and 0.40 m water depths, respectively. To sum up, relative rundown at 0.45 m water depth exhibited 32.65% and 23.57% higher values than 0.35 m and 0.40 m water depths, respectively. It is observed that, rundown values increase as depth increases. This can be due to the fact that waves possessing higher energy results in a higher rundown. Increased water depth can sustain waves with larger heights (consequently higher wave energy), resulting in increased downrush in higher water depths.

4.2.3 Wave reflection analysis

4.2.3.1 Effect of water depth on wave reflection

This section discusses the variation of reflection coefficient (K_r) with the change in water depth. Each configuration is tested for different water depths in order to attain various field depth conditions. Fig. 4.34 represents the reflection coefficient values with respect to wave steepness for all the six test cases conducted. This sort of representation is necessary for deducing an overall impression of the reflection behaviour of the structure. From Fig. 4.34 the values of K_r appear to scatter over a range of 0.06 to 0.59. This representation is quite difficult to interpret as a trend but helps in understating the entire K_r range. On a very general note, K_r reduces with an increase in wave steepness. But these trends can be clearly understood from a further detailed analysis.

Out of the three water depths considered, 0.45 m water depth showed 4.68 to 21.62% and 11.59 to 19.44% higher reflection compared to 0.40 m and 0.35 m water depths, respectively. Higher water depth can sustain high energy waves, resulting in increased reflection. However, most of the test cases showed lesser reflection than the conventional breakwater structures as experimented by Zanuttigh and van der Meer (2008). Additionally, Shore Protection Manual (1984) also reveals a range of K_r from 0.25 to 0.5. The decreased reflection rate of GSC breakwaters can be attributed to the increased runup rates compared to the conventional breakwaters. As per SPM 1984, relative runup for conventional breakwater can

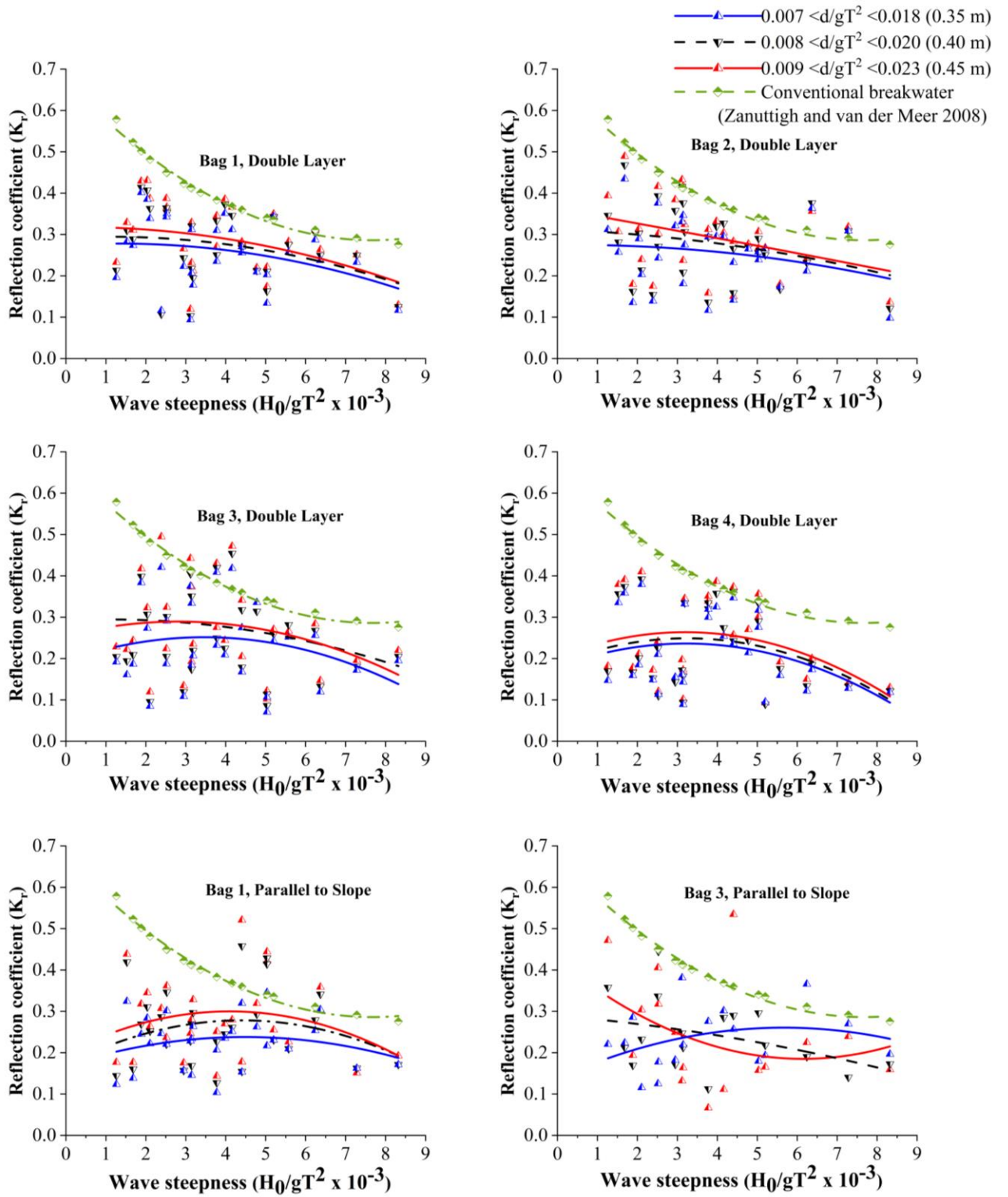


Fig. 4.34 Reflection coefficient K_r with respect to wave steepness

reach up to 1. But for the present investigation, relative runup varies from 0.9 to 2.5. The increased runup of waves over the structure is observed to improve the absorption of water into the structure. This can be the major reason for reduced reflection of GSC breakwater

4.2.3.2 Effect of placement modes on reflection

From Fig. 4.35 it is observed that there is a considerable variation in the reflection coefficient (K_r) for different types of placement modes: single-layer, double-layer and parallel to slope placement. Double-layer placement showed 45 to 52% less K_r when compared to the single-layer placement and 38 to 42% less in the case of the conventional breakwater. From the above graph, it is evident that double layer placement has more pore space compared to single layer placement, absorbing more water and resulting in less reflection. The slope-parallel arrangement also showed up to 50% less reflection than the single-layer structure. This can be due to the higher runup on the slope-parallel arrangement, as water can easily glide to the structure crest, thus improving the absorption of water into the GSCs.

4.2.4 Stability and Damage analysis

Stability tests for breakwaters with GSCs have been carried out in the wave mechanics laboratory of National Institute of Technology Karnataka (NITK), Surathkal. The stability of the structure is well understood by analysing the level of damage exhibited by each configuration. Since the present model of GSC breakwater is different from that of a conventional rubble mound breakwater, damage analysis is carried out based on the methodology proposed by Dassanayake and Oumeraci (2012b). This type of classification involves the calculation of displaced or detached units from critical layers. Damage classification is carried out by identifying critical layers and quantifying the amount of bags displaced and detached from those layers. Based on this, each case is categorised from DC0 to DC4. Those cases which showed very high stability (less than 5% of the GSCs in critical layer moved) is classified as 'No Damage' case and is termed DC0. For concluding a test case (with particular wave height and period) to be DC0, the structure is exposed to

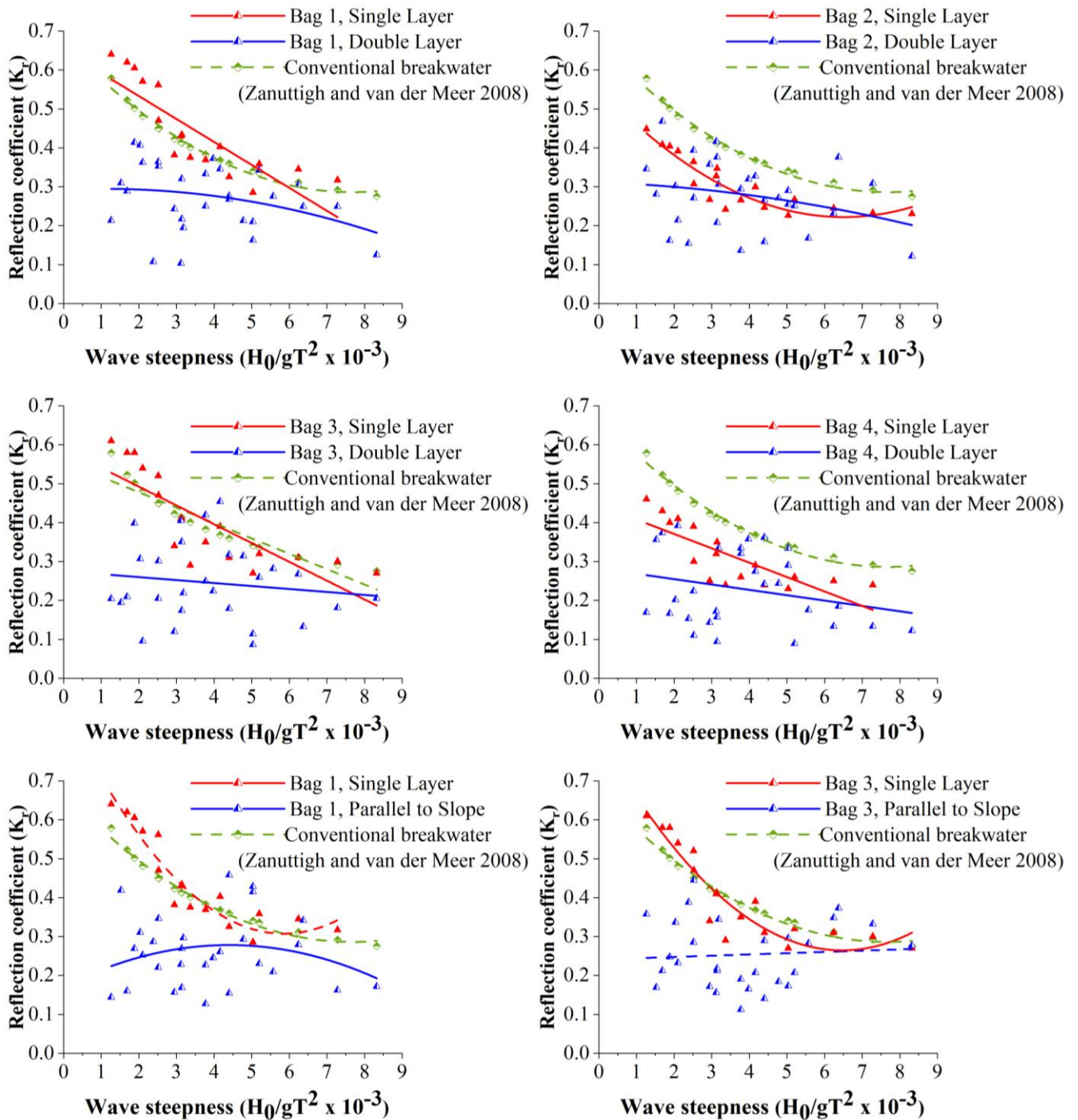


Fig. 4.35 Effect of various placement modes on reflection

a minimum of 2000 waves with similar characteristics. Dassanayake and Oumeraci (2012b) report the exposure of 100 monochromatic waves for each test case; however, for

more conservative results, a minimum of 2000 waves are used in the present study. Test cases are classified into DC1, DC2, DC3 (based on the conditions in Table 3.6.), after the exposure of 2000 waves. In higher damage cases, washing out of the core occurs, which in turn forces one to stop wave exposure and is marked as ‘Total Failure’ or DC4. In such cases, the total number of waves exposed to the structure may be less than 2000. 12th rows, out of it, more than 50% of units got displaced. Therefore, this case is considered to be ‘Minor Damage’ (DC2) according to the adopted damage classification (Table 3.6).

Stability estimations and damage analysis were carried out following the guidelines from various published sources (Dassanayake and Oumeraci 2012a). Initially, the experiments were conducted with double layer of GSC units. The structure was observed to be more stable when supplemented with two GSC layers than a single layer placement (Fig. 4.36).



Fig. 4.36 Bag 1 Double-layer configuration, Stable (DC0) after exposure of 0.06 m wave heights

The primary failure mode observed was the detachment of GSC units. This revealed that the structure can be stable and protected with the second layer, even when the primary layer shows the displacement. The structure generally showed increasing damages with steeper waves exhibiting even complete failure (DC4) as illustrated in Fig. 4.37. It is observed that



Fig. 4.37 Total Failure (DC4) after exposure to 0.16 m wave heights.

the units detached from the primary layer got readjusted themselves to form a layer of slope parallel units (Fig. 4.38).

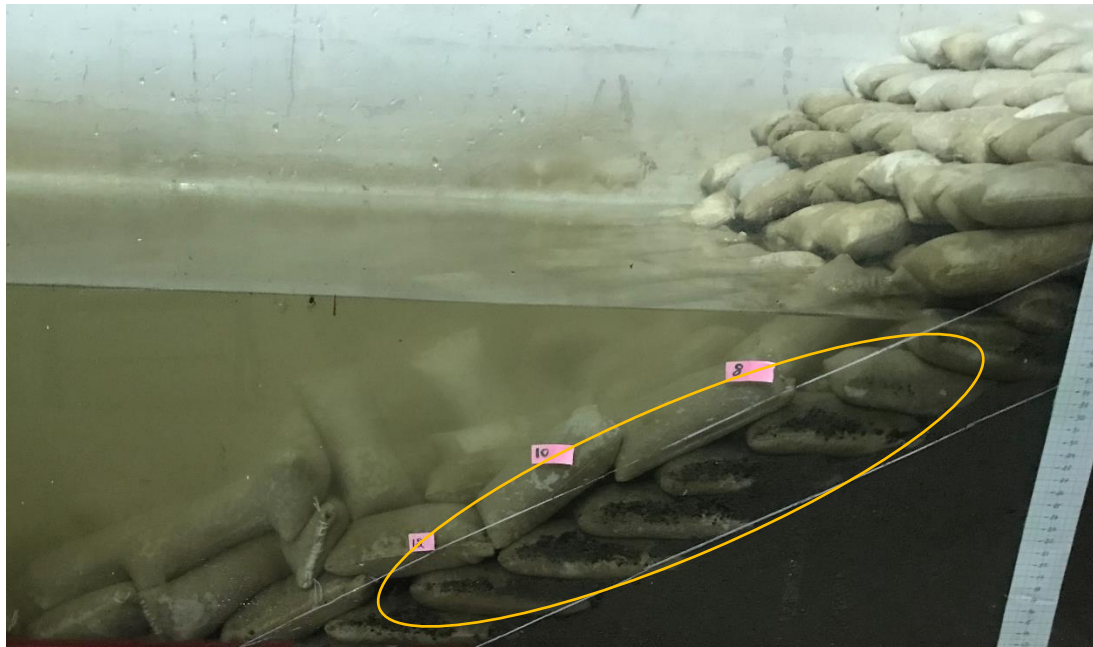


Fig. 4.38 Readjusted primary layer forming slope-parallel arrangement for Bag 1, Double Layer configuration

Those units, in slope parallel condition, were observed to possess higher stability and resist further displacement. This observation lead to experiment with the ‘Slope Parallel’ arrangement in detail. However, damage progression in ‘slope parallel’ placement was observed faster once GSC unit detachment was initiated (more details in section 4.2.4.6). The effect of other structural parameters on the stability of GSC breakwaters has been analysed in the following sections.

4.2.4.1 Effect of Armour Unit Size.

Two different armour unit sizes were examined. Fig. 4.39, Clarifies that Bag 1 and Bag 2 are of smaller size than Bag 3 and Bag 4.

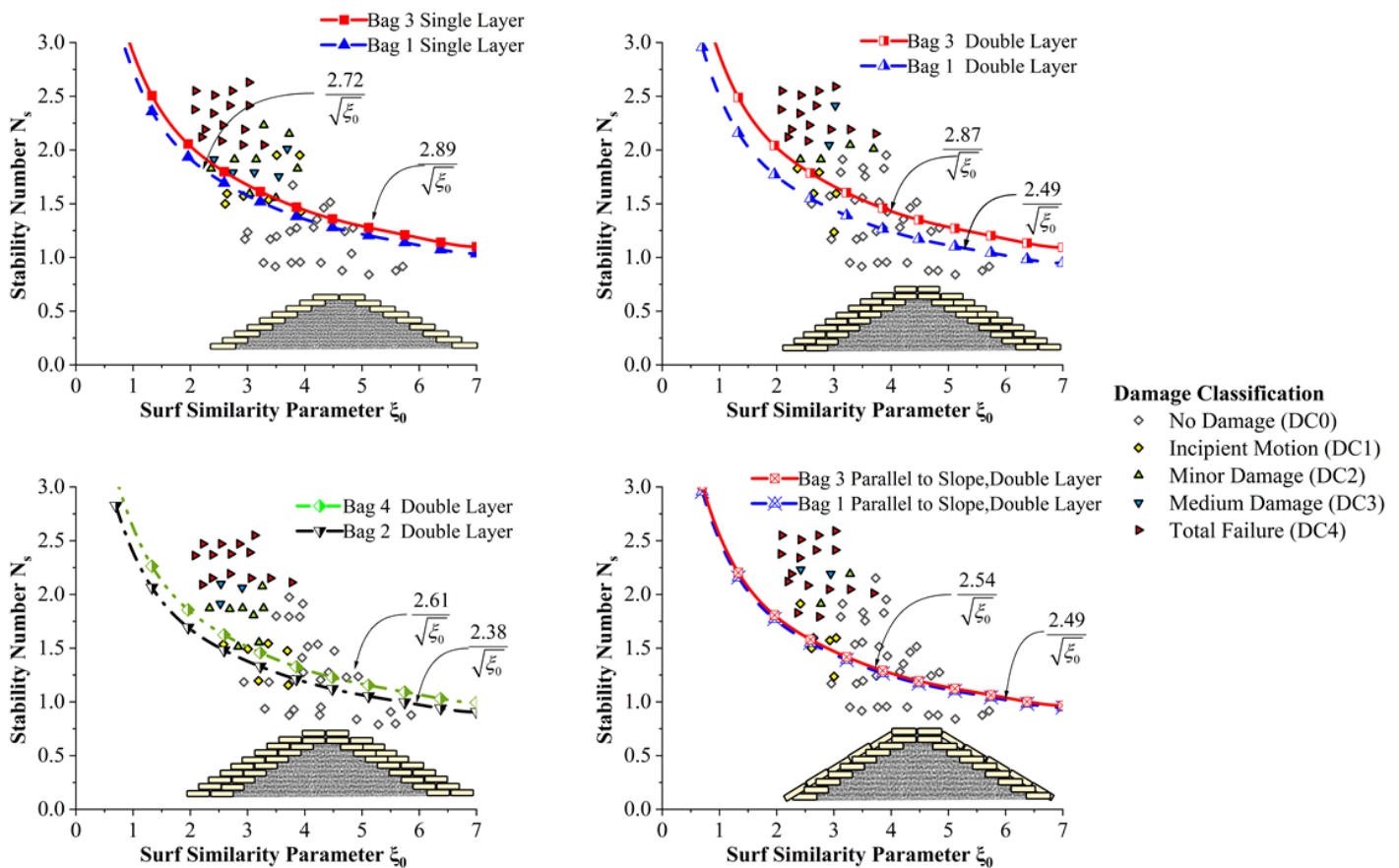


Fig. 4.39 Effect of armour unit size on stability of GSC breakwaters

In all the tested cases, bigger bags exhibited higher stability, with double-layer configuration showing a maximum stability difference of 28.83% and slope parallel

placement showing a minimum difference of 2.62% between bigger and smaller bags. Bag 3 stacked to double layer is observed to have the highest stability, which is 17.8% higher than the same bags stacked to a single layer. Slope parallel placement showed up to 32.3% lower stability compared to all other configurations. Bigger bags possess a higher self-weight resulting in higher stability of the structure. As a result, a more significant wave force is required to overturn or displace bigger armour units (Recio and Oumeraci 2009). However, this effect is less pronounced in slope parallel placement since the curves represented by larger (Bag 3) and smaller (Bag 1) bags are nearly aligned, as observed in Fig. 4.39. Additionally, 80% filled bags showed a variation of 20.5% when armour unit size is increased i.e. from Bag 2 to Bag 4. This can be attributed to the bag weight as it contributes to structural stability for slope parallel placement. 2.6 to 28.83% higher stability is observed for larger bags (Bag 3) due to its increased self-weight. Additionally, it is observed that the chances of sliding down of units are high in the case of slope parallel placement after initial detachments, unlike other placement modes.

4.2.4.2 Effect of Sand-fill ratio

The sand filling percentage of bags is varied from 80 to 100% in order to study the effect of fill percentage on the stability of the structure. In Fig. 4.40, Bag 1 and Bag 3 are fully filled bags, whereas Bag 2 and Bag 4 are 80% filled bags. 100% filled bags exhibited higher stability in all the cases than their corresponding 80% filled ones. An increase in stability of 4.68 to 12.8% is observed when the fill percentage is varied from 80 to 100% in various configurations. 80% filled bags contain a sufficient space, which permits sand movements when exposed to ocean waves. As a result, bags tend to displace and detach much more effortlessly than fully filled units.

4.2.4.3 Effect of water depth

The stability of the structure, in all placement methods, is found to be decreasing with increasing water depth and all the experimental results at minimum water depth exhibited higher stability. According to Khajenoori et al. (2021), geobag revetments experience

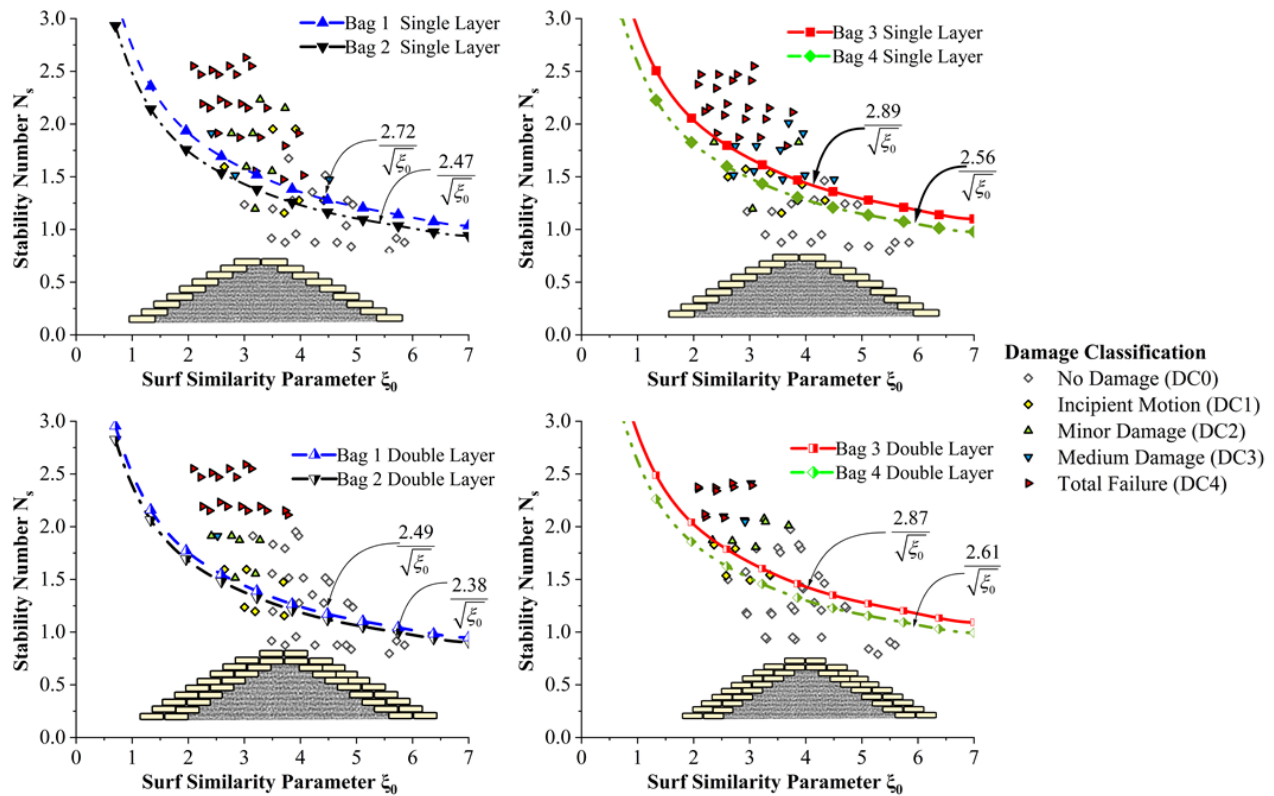


Fig. 4.40 Graphs showing comparative analysis of the stability of 100 and 80% filled GSC units.

increased damage at higher water depths. Increased destabilising forces results in upliftment of units in higher water depths whereas, in lower depths only partial upliftment is reported. All configurations showed a smaller stability difference with water depth (less than 7%) except in the case of bigger bags (Bag 3 and Bag 4) in double-layer placements (up to 21.52%). This is attributed to the aligned nature of stability curves. Similar results showing aligned nature of stability curves have been reported in the previous section, where stability difference was as low as 4.4% with varying water depths.

As observed from Fig. 4.41, bigger bags (Bag 3 and Bag 4) showed up to 21.52% higher stability in lower water depths. This may be because wave runup and rundown are lower in lower water depths, resulting in fewer units getting exposed to wave activity. This reduces the displacement and detachment of units, leading to improved stability at lower

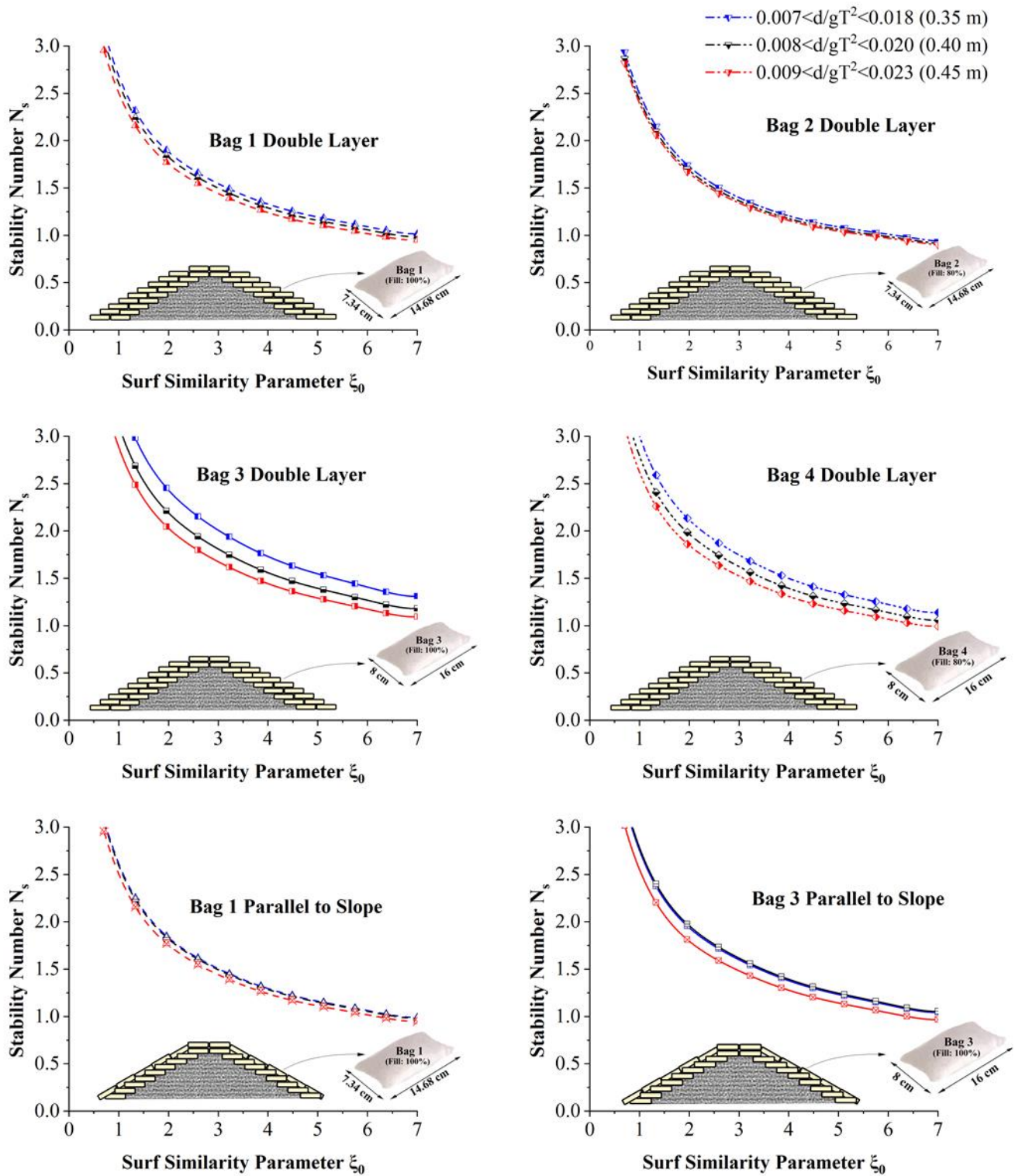


Fig. 4.41 Stability curves of GSC breakwaters with varying water depth

water depths. Additionally, 80% filled bags with lower stability is not examined for slope parallel placement.

4.2.4.4 Damage levels

Fig. 4.42, shows the level of damage exhibited by different armour units for different placement modes. It is observed that single layer and slope parallel placements are highly unstable, as they produced nearly 50% of Total Damage (DC4) cases for 80% filled bags. Double layer arrangement showed fewer DC4 cases (less than 30%) and increased stable cases (40 to 60%) for all armour units. In the case of slope parallel placement, the stable level is high, nearly 60% in certain cases, but damage progresses very fast as unit instability occurs. This is evident from Fig. 4.42, as intermediate damages DC2 and DC3 are less or never reported in slope parallel placement. Damage rapidly progresses to Total Failure DC4 from Incipient Motion DC1 compared to single and double layer placements.

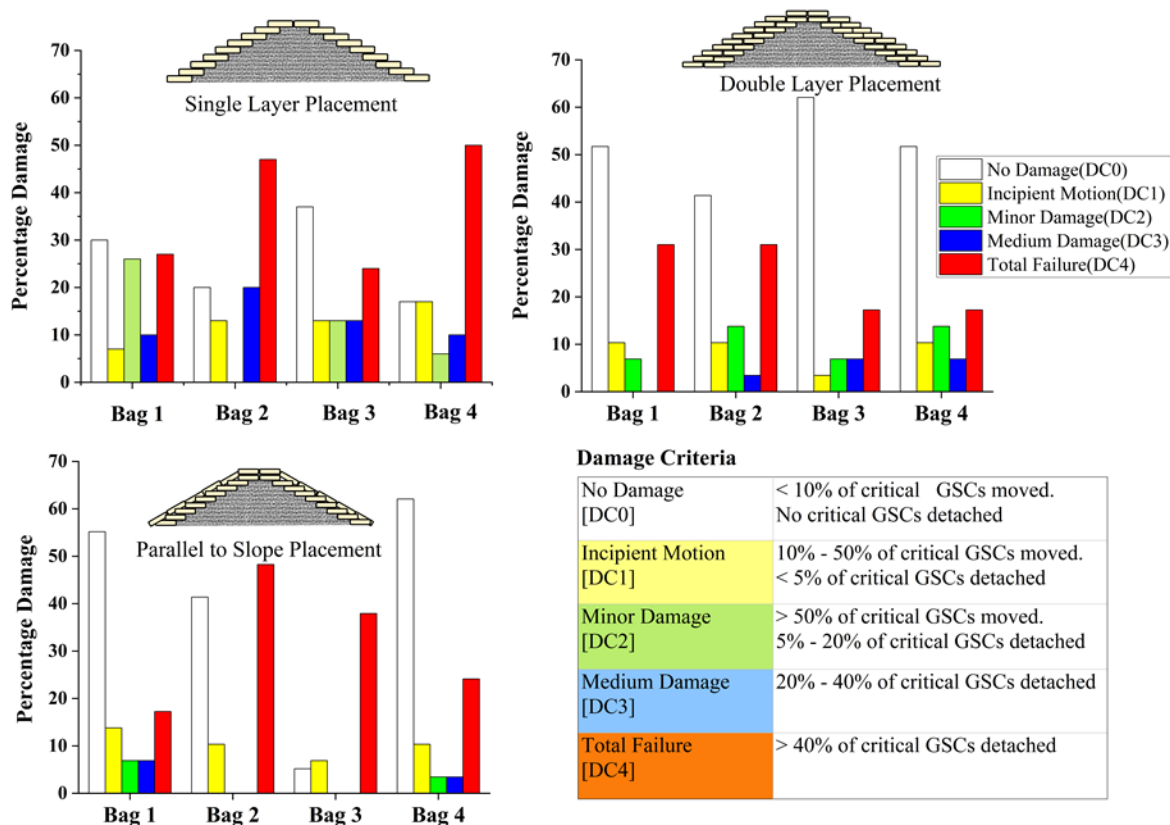


Fig. 4.42 Damage levels exhibited by various test configurations.

4.2.4.5 Effect of Incident Wave Height

Fig. 4.43, shows the plot of the Damage levels with the incident wave height, DCO and DC1 damage levels are considered to be stable according to Table 3.6. Therefore, non-damaging incident wave heights for various arrangements with Bag 1 and Bag 2 have been identified from Fig. 4.43. The breakwater model with Bag 1 stacked to two layers stood stable to waves up to 0.117 m in the model scale, which is 3.51 meters in the prototype. The breakwater model with Bag 2 placed in a single layer exhibited the least performance as it could withstand a maximum of 0.078 m wave in the flume, which would be a 2.34 m wave in the actual sea. All other models exhibited a maximum non-damaging wave heights between 1.98 m and 3.3 m. Additionally, in all cases, damaging wave heights are found to be decreasing up to 22.2 % with reducing wave periods.

Fig. 4.44, shows the plot of damage level with the incident wave height. DCO and DC1 damage levels are considered to be stable according to (Dassanayake and Oumeraci 2012a). Therefore, non-damaging incident wave heights for various arrangements with Bag 3 and Bag 4 have been identified from Fig. 4.44. Double layer placement with Bag 3 is found to be stable up to a wave height of 0.132 m in model scale, which will be 3.96 m in the prototype. Bag 4 single layer exhibited the worst behavior, as it could only withstand waves up to 0.08 m in the flume, indicating a 2.4 m wave in the prototype. The best performing model showed a 22.2% increase in zero-damage wave height when the wave period is varied from 1.4 to 2.2 s, complimenting the gentle and less destructive nature of long-period waves.

4.2.4.6 Effect of number of layers of bags

Fig. 4.45, represents a comparative analysis of various placement modes for all the armour units. It can be observed that curves for double-layer placement have 2.6 to 17.8% higher stability in all the tested cases compared to the single-layer placement. Higher stability can be attributed to the increased self-weight and porosity. As the porosity of the structure increases, more wave dissipation takes place on the structure slope reducing the disturbing wave forces on the structure. Slope parallel placement is observed to have up to 10%

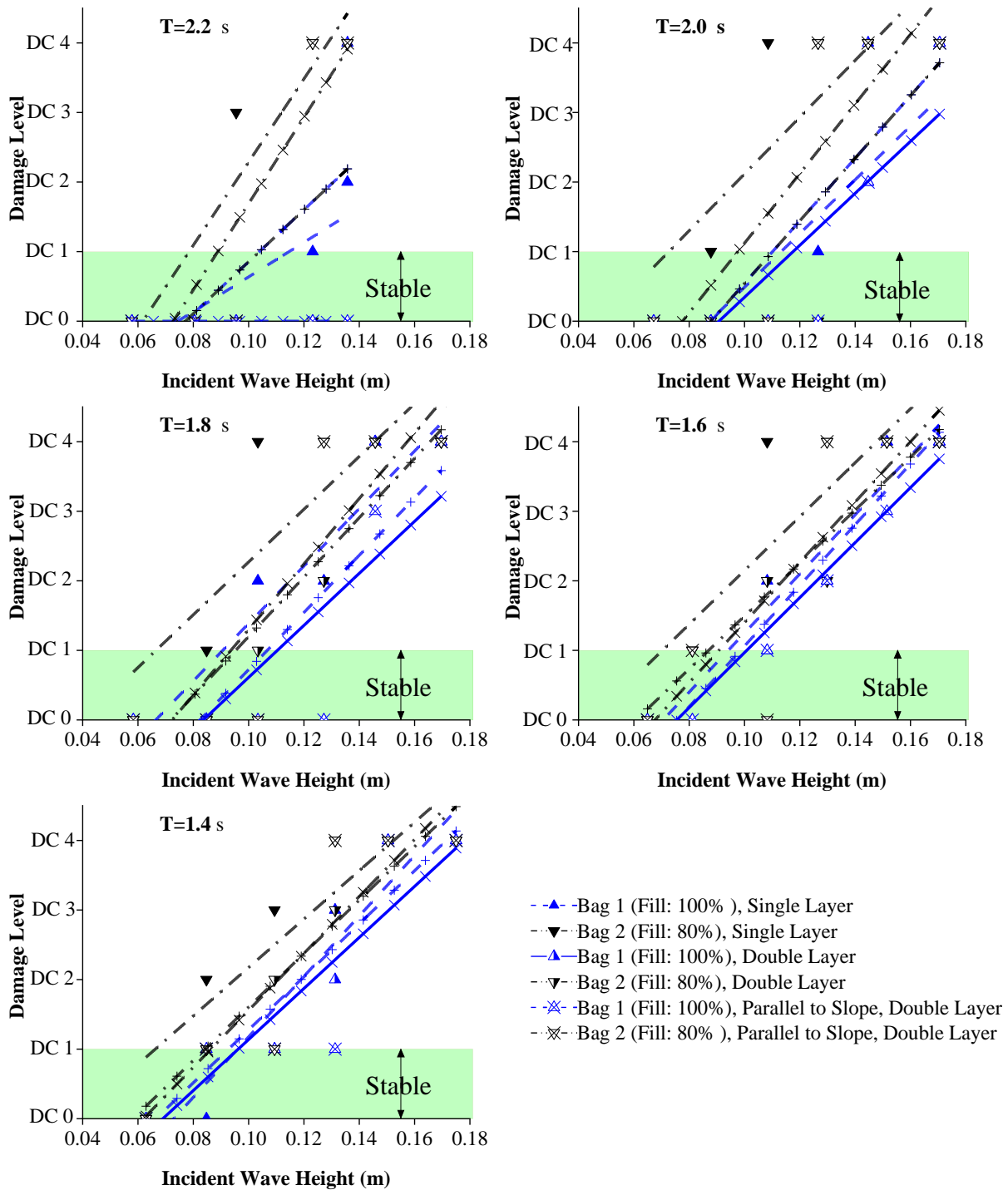


Fig. 4.43 Graphs representing non-damaging incident wave height showed by various configurations involving Bag 1 and Bag 2.

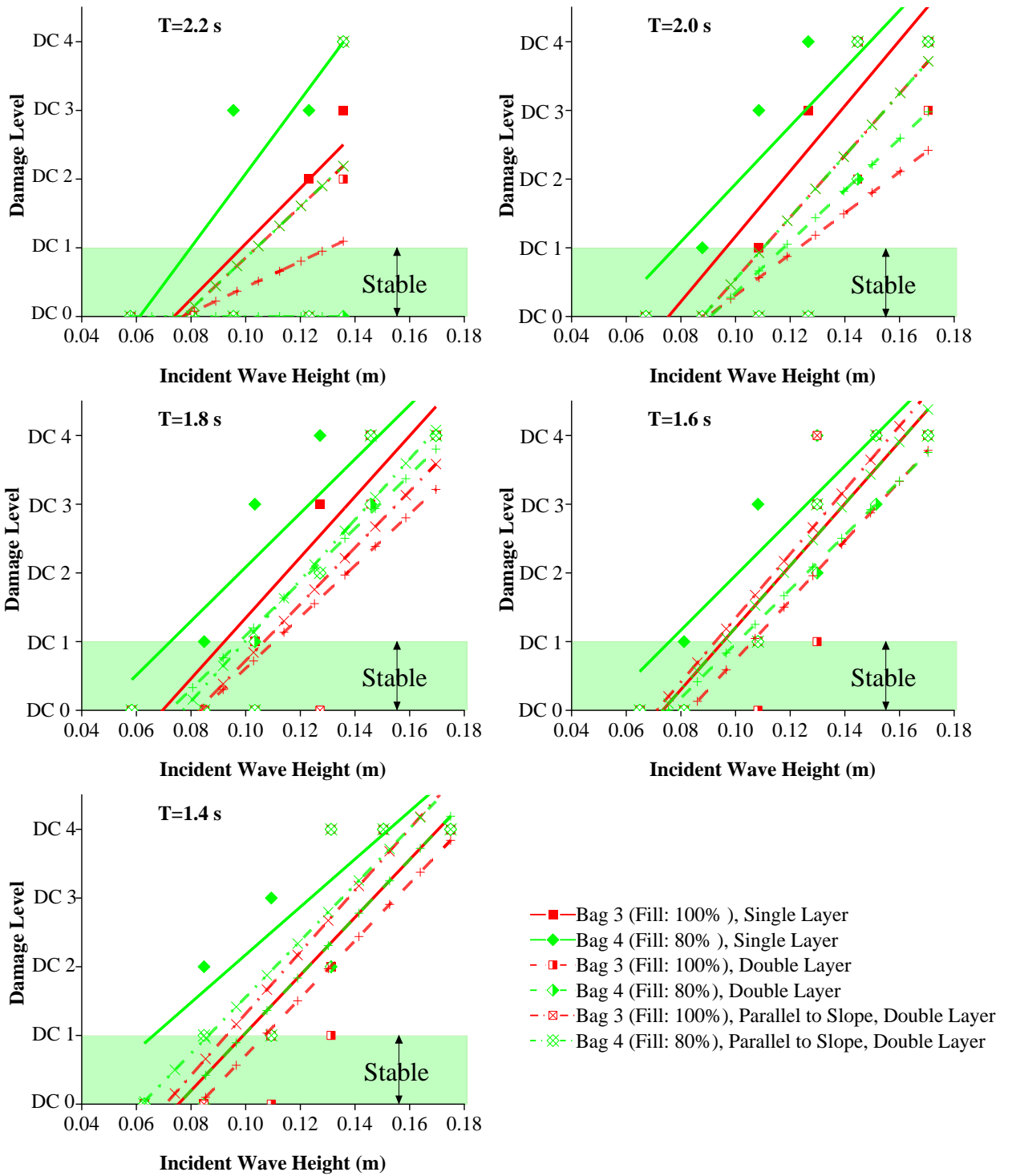


Fig. 4.44 Graphs representing non-damaging incident wave height showed by various configurations involving Bag 3 and Bag 4.

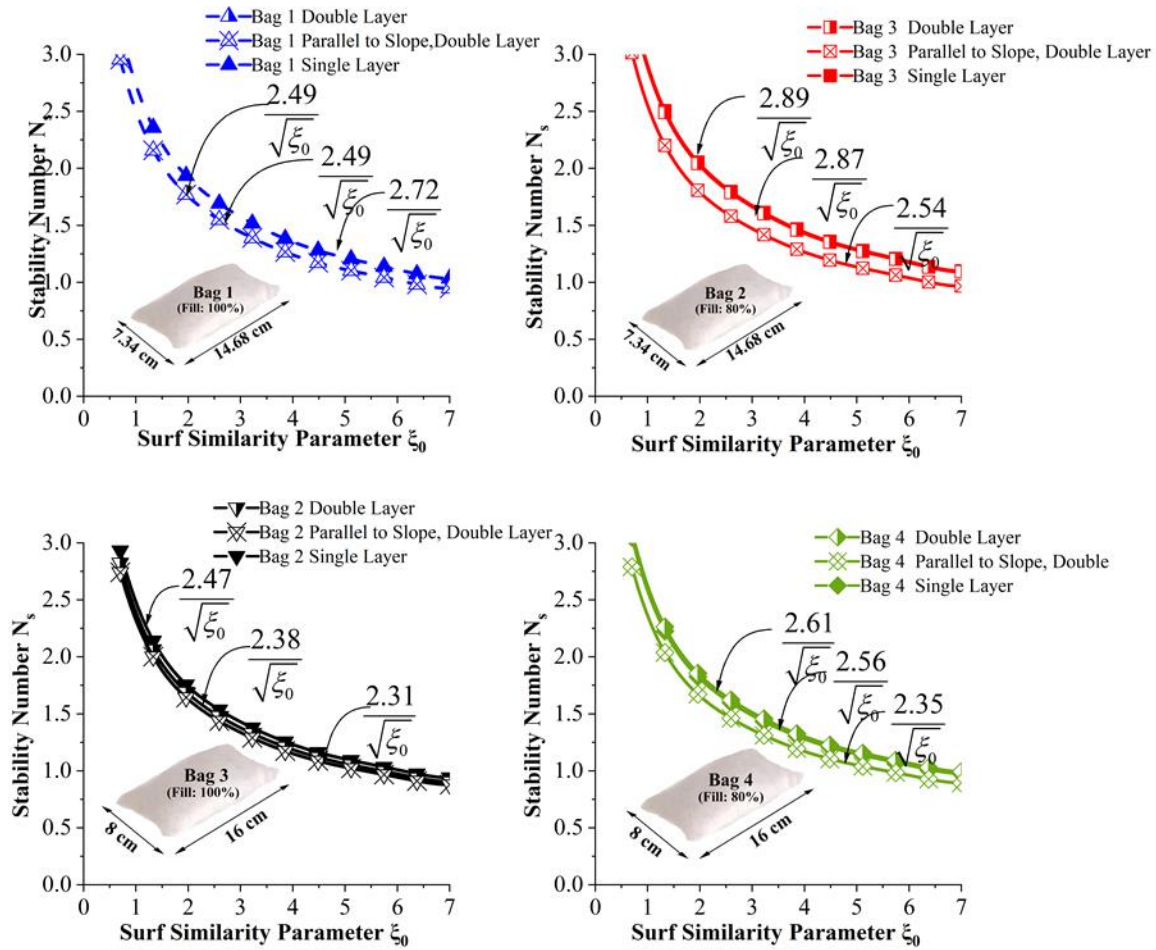


Fig. 4.45 Graphs representing comparative analysis of stability curves of different placement modes

Lower stability compared to all single-layer placements. It is observed that in slope parallel placement, damage progression is faster as the displacement of a unit would result in the sliding down of units from its upper layer. Similar sliding movement is not observed in other types of placements. Additionally, units are readjusted to form a new stable arrangement in single and double layer placements.

An important conclusion deduced is that stability of the breakwaters (armoured with sand filled GSCs) increases with the number of layers (single or double). Hydraulic parameters

like reflection, runup, and rundown can reduce, as more wave dissipation can occur in double-layer structures due to increased porosity and void spaces.

4.2.4.7 Stability Nomograms

This section compiles the results of all the previous sections. The stability nomograms reveal that maximum stability is for bigger bags (Bag 3 in the present case) placed in double layers (see Fig. 4.46).

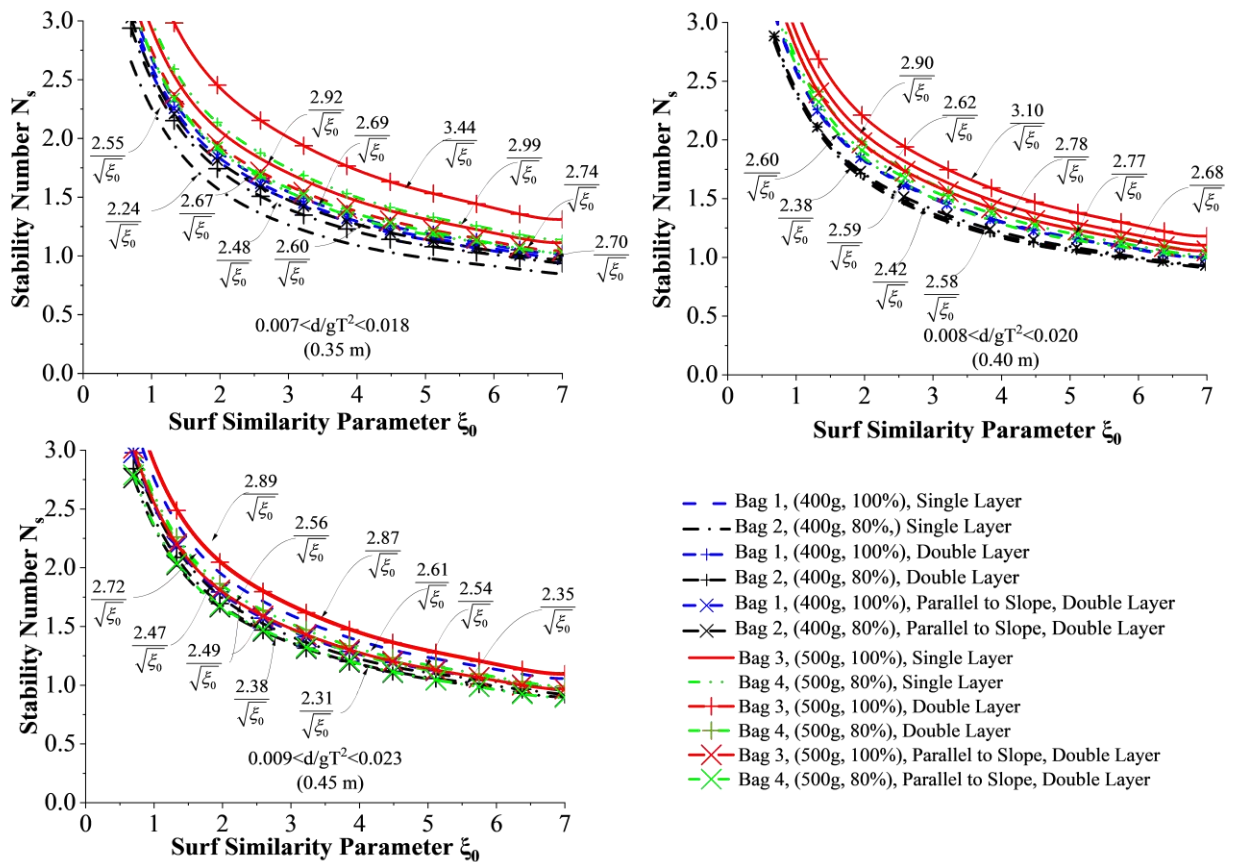


Fig. 4.46 Stability nomograms for GSC breakwaters of different relative water depths.

Bag 3 is found to be up to 17.8% stable when placed in double layers than when placed in a single layer. Similarly, Bag 1 is found to be up to 5.38% stable in double-layer placement. 80% filled bags are less stable in all cases, with slope parallel placement being the most

unstable configuration. These nomograms are the major research outcome as they can be used in field applications for planning and designing GSC breakwaters.

Since GSC breakwaters with double-layer arrangement possess maximum stability, it can be implemented in the field. When the breakwater is supplemented with two armour unit layers, damage progression can be controlled. In the case of single-layer GSC armour arrangements, even displacement of some bags may result in the exposure of the core material. This can be avoided by supplementing an additional outer layer so that even when the outer layer gets affected, the inner layer will be intact. Therefore, breakwaters with double-layer GSC armour units are highly advisable for actual field applications.

Breakwaters with slope-parallel GSC armour units were experimented as it was observed to possess high stability during initial testing. Had they proved stable, such breakwaters could have potentially reduced construction costs, as fewer GSC units were required for the construction. However, detailed experimentation on such models revealed that damage progression is faster after the initiation of GSC displacement. Therefore, breakwaters with slope-parallel GSC units cannot be suggested for field application, as its failure progression cannot be curbed after the initiation of GSC displacement.

4.3 STUDIES ON GEOTEXTILE BREAKWATERS FILLED WITH CEMENT AND SAND

This section details the results of studies conducted on geotextile breakwaters filled with sand and cement. From the previous experiments, Bag 3 is found to be the best-performing model. This best-performing model of Bag 3 is then filled with sand and cement to analyse its efficacy. In this context, the following configurations are tested in the wave flume;

1. Bag 3 filled with 15% cement, stacked in single layer.
2. Bag 3 filled with 20% cement, stacked in single layer.
3. Bag 3 filled with 20% cement, stacked in double layers.

As far as the hydraulic performance and stability are considered, breakwater structures with GSC armour units filled with 20% cement is observed to perform better than those units

filled with 15% cement. Therefore, studies on structures with double layer GSC units filled with 15% cement are not carried out in the present study.

4.3.1 Wave runup studies

Wave runup height is measured to calculate the relative runup height (R_u/H_0), which is beneficial for understating the overtopping and transmission of water over the crest of the structure. Relative runup of all tested breakwater configurations is represented in Fig. 4.47. This shows that single-layer Bag 3 with 15% cement showed the maximum relative runup, with double layer 20% configuration being the least. Bag 3 with 15% single layer breakwater configuration exhibited a maximum of 15.9 and 33.33% higher relative runup with respect to those with single layer of 20% and double layer with 20% cement bags, respectively.

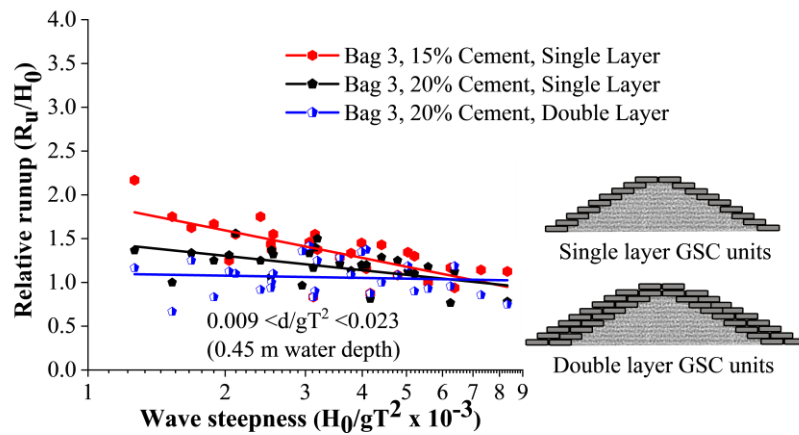


Fig. 4.47 Relative runup of all tested configurations

Relative runup vs wave height to depth ratio (H_0/d) of all the tested breakwater configurations are represented in Fig. 4.48, this shows that single-layer Bag 3 with 15% cement showed the maximum relative runup, with double layer 20% configuration being the least. This plot is helpful in analysing the efficacy of various placement modes. 15% cement filled bags showed a tendency to break within. Those broken bags tend to readjust

in the structure slope resulting in the closure of certain pore spaces. As a result, wave dissipation reduced, leading to increased runup

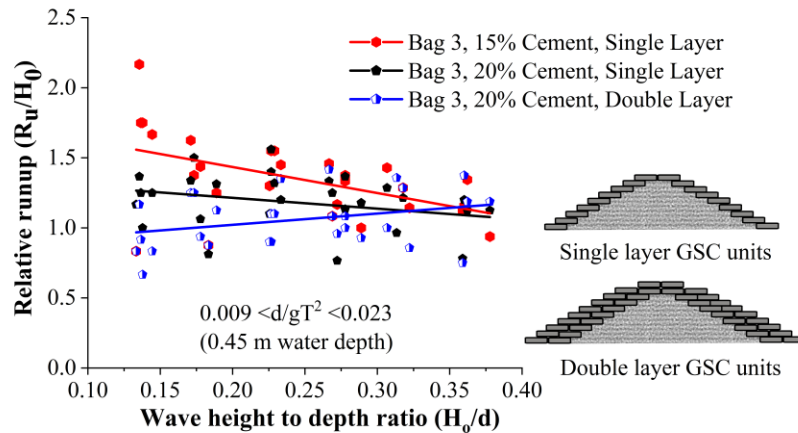


Fig. 4.48 Relative runup vs wave height to depth ratio (H_0/d) of all the tested configurations

When the bags were filled with 20% cement, they acted like solid units, creating more pore spaces. Those solid units provided no scope of readjustments, as a result, the pore spaces were not covered. This promoted increased wave dissipation on the structure slope resulting in the reduced runup. Further, when an additional layer was provided, the porosity of the structure increased, resulting in further wave dissipation on the structure slope. This resulted in the reduced runup rates of double-layer arrangement.

4.3.2 Wave rundown studies

Wave rundown is beneficial for understating the behaviour of water retreating from the structure surface. The relative rundown of all tested configurations is represented in Fig. 4.49. This shows that breakwater of single-layer Bag 3 armour with 15% cement showed the maximum relative rundown, with double layer breakwater structure of 20% cement units being the least. Bag 3, 15% single layer configuration represented 5 and 31.25% higher relative rundown with respect to single layer 20% and double layer 20% arrangements, respectively. The relative rundown versus wave height to depth ratio (H_0/d) tested for all configurations are illustrated in Fig. 4.50. This shows that single-layer Bag 3

with 15% cement showed the maximum relative runup, with double layer 20% configuration being the least. This plot is helpful in analysing the efficacy of various placement modes.

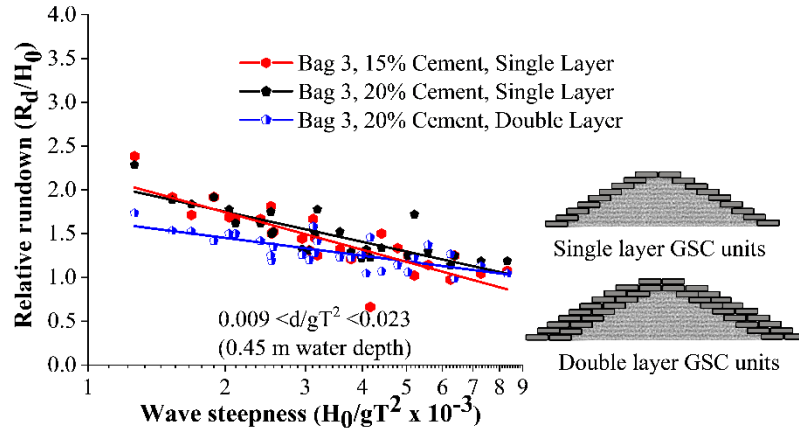


Fig. 4.49 Relative rundown of all tested configurations

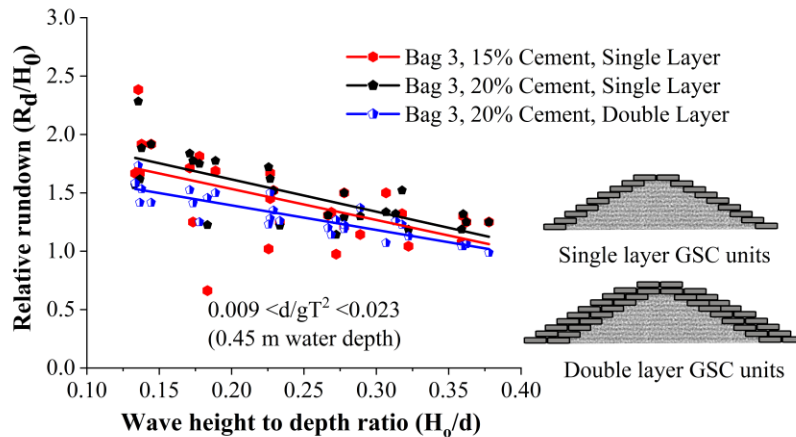


Fig. 4.50 Relative rundown vs wave height to depth ratio (H_0/d)

Single layer placements nearly represent a similar rundown behaviour, a maximum of 5% variation. This can be due to the similarity in porosity provided by both the armour units. When the armour units are arranged in double layers, increased porosity helps in wave dissipation, as a result, wave rundown decreased for double layer structures.

4.3.3 Reflection Analysis

Analysis of wave reflection from the breakwater are presented in this section. The three probes method by Isaacson (1992) is adopted in the estimation of reflection coefficient K_r . The variation of K_r with wave steepness parameter for all the tested cases is represented in Fig. 4.51. It is evident that all the test cases exhibited lower K_r values compared with convention breakwaters, as appeared in (Zanuttigh and van der Meer 2008). Breakwater structure with single-layer configuration with 20% cement fill showed the maximum reflection, up to 76% higher than other models. The fitted curves exhibit poor correlation coefficient, which is just up to 19%. Decreased K_r values are a result of increased porosity and consequent increase in wave dissipation on the structure slope.

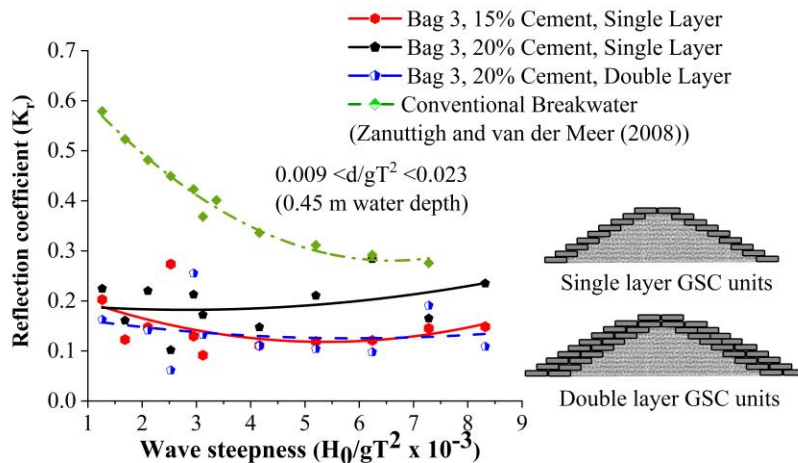


Fig. 4.51 Calculated K_r values for all the tested cases

4.3.4 Stability and Damage Analysis

Stability and damage analysis is carried out similarly as in the above-mentioned experimentations. It is noted that when the geotextile containers are filled with sand and cement, the resulting breakwater structure produces more pore spaces than containers with sand alone (Fig. 4.52). Internal displacement of sand, when subjected to wave action, has been arrested due to the cementation process. Additionally, the hard units tend to be comparatively stable than its sand alone counterparts. In most cases, pull-out was observed

as the major failure mode. The process of pulling out of containers occur due to wave attack on armour units. According to Recio (2008), interface friction is the major factor controlling the pullout of GSC units. The friction properties of the material and contact area between two containers controls the interface friction. In the cement-filled bags case, the bags become bulky after solidification reducing the contact area between two containers, as a result interface friction reduces resulting in increased pullout of GSC armour units.



Fig. 4.52, Image showing sand container filled to 15% cement and arranged to a single layer. Note the bulkiness of the units contributing higher porosity.

Incipient motion curves are obtained for Bag 3 filled to 15% cement, arranged to a single layer in Fig. 4.53. Experimentations are carried out at three different relative water depths $0.007 < d/gT^2 < 0.018$ (0.35 m), $0.008 < d/gT^2 < 0.020$ (0.40 m) and $0.009 < d/gT^2 < 0.023$ (0.45 m). as seen from the graph, stability at lowest water depth (0.35 m) was found to be 25 to 29% higher than at 0.40 and 0.45 m water depths respectively. Higher wave activity, wave energy at increased depth of water can be the possible reason for this. Moreover, wave runup and rundown will be higher at higher depths of water resulting in increased instability, see section 4.2.4.3 for more details of effect of water depth.

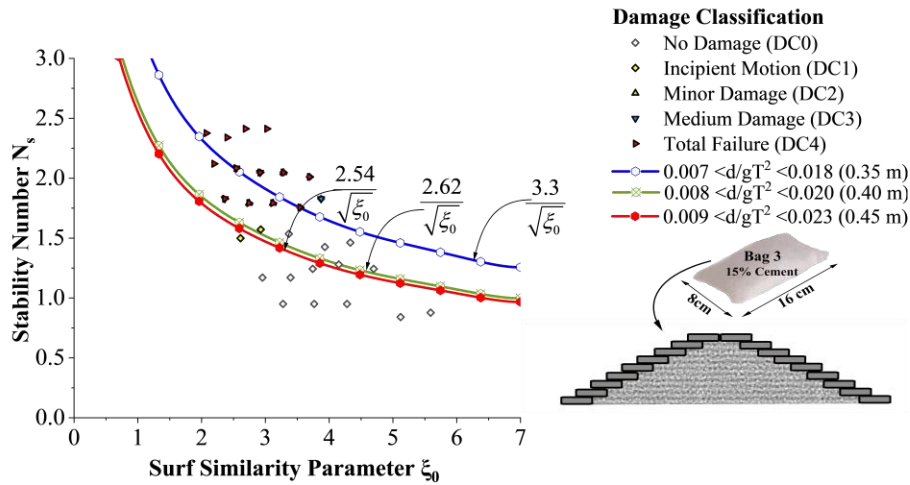


Fig. 4.53 Incipient motion curves for Bag 3 filled to 15% cement, single layer

Incipient motion curves are obtained for Bag 3 filled to 20% cement, arranged to a single layer in Fig. 4.54. Experimentations are carried out at three different relative water depths

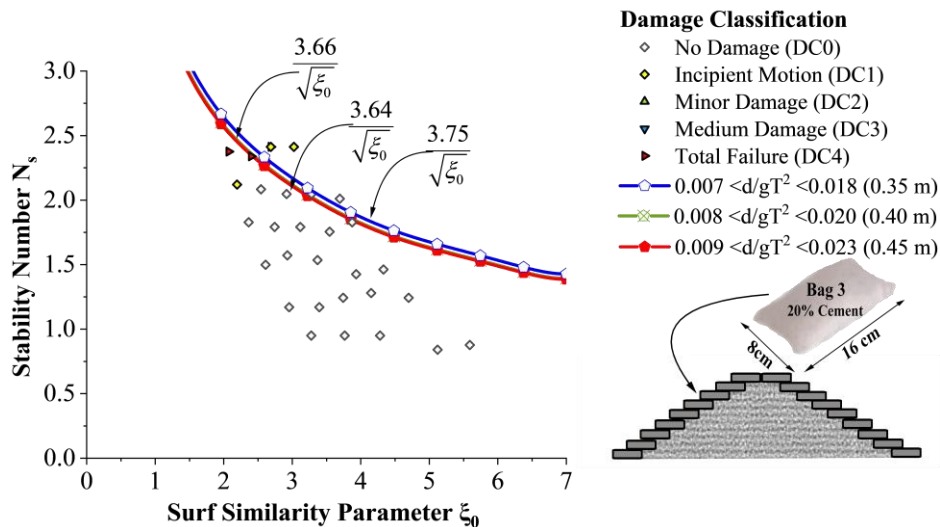


Fig. 4.54 Incipient motion curves for Bag 3 filled to 20% cement, arranged to single layer

0.007 <math><d/gT^2 < 0.018</math> (0.35 m), 0.008 <math><d/gT^2 < 0.020</math> (0.40 m) and 0.009 <math><d/gT^2 < 0.023</math> (0.45 m). as seen from the graph, stability at lowest water depth (0.35 m) was found to be 2.4 to 3.5% higher than at 0.40 and 0.45 m water depths respectively. Wave runup was

lesser at 0.35 m water depth thus deformations occurred during runup will be comparatively lesser (check section 4.2.4.3 for more details about effect of water depth on structural stability). But the deviation of stability is found to be comparatively lesser than 15% cement filled case. Moreover, when the cement content in bags increased from 15% to 20%, the stability of the structure shot up to a maximum of 43.3%. Incipient motion curves are obtained for Bag 3 filled to 20% cement, arranged in double layers is shown in Fig. 4.55. Experimentations are carried out at three different relative water depths $0.007 < d/gT^2 < 0.018$ (0.35 m), $0.008 < d/gT^2 < 0.020$ (0.40 m) and $0.009 < d/gT^2 < 0.023$ (0.45 m). as seen from the graph, stability at lowest water depth (0.35 m) was found to be 4.5 to 8.1% higher than at 0.40 and 0.45 m water depths respectively. Higher wave activity, wave energy at deeper depth can be the possible reason for this (check section 4.2.4.3 for more details about effect of water depth on structural stability). Moreover, when the number of layers increased from one to two, a considerable decrease of stability, up to 23.6%, is exhibited. Major reasons behind these observations will be discussed in the subsequent sections.

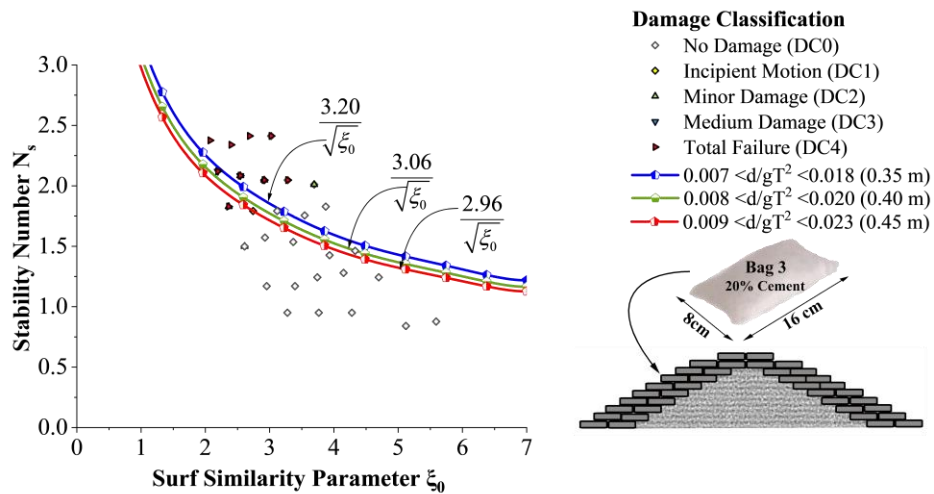


Fig. 4.55 Incipient motion curves for Bag 3 filled to 20% cement, double layer.

4.3.4.1 Effect of the number of layers and cement percentage.

The effect of the number of layers and cement percentage has been tested in this section. Stability curves of all experimented configurations are analysed for a relative water depth $0.007 < d/gT^2 < 0.018$ (0.35 m actual water depth in flume) in Fig. 4.56. 20% cement-filled bags arranged to single layer exhibited increased stability, 13.63 and 17.18% higher than 15% cement single layer and 20% cement double-layer configurations, respectively.

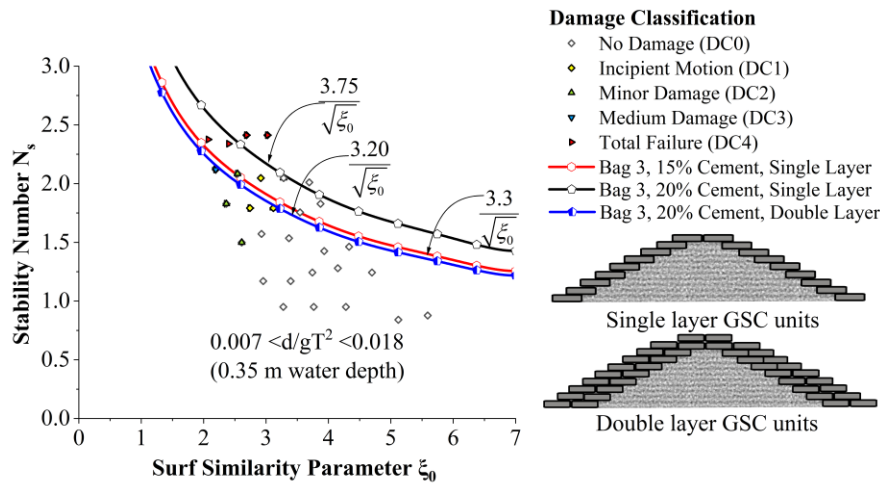


Fig. 4.56 Stability curves of all experimented configurations for a relative water depth $0.007 < d/gT^2 < 0.018$ (0.35 m actual water depth in flume)

The effect of the number of layers and cement percentage has been tested in this section. Stability curves of all experimented configurations are analysed for a relative water depth $0.008 < d/gT^2 < 0.020$ (0.40 m actual water depth in flume) in Fig. 4.57. 20% cement-filled bags arranged to a single layer exhibited the highest stability, which is 39.6 and 19.6% higher compared to 15% cement single layer and 20% cement double-layer configurations, respectively. The effect of the number of layers and cement percentage have been discussed in this section. Stability curves of all experimented configurations are analysed for a relative water depth $0.009 < d/gT^2 < 0.023$ (0.45 m actual water depth in flume) in Fig. 4.58. 20% cement-filled bags arranged to a single layer exhibited the highest stability, which is 43.3 and 22.9% higher compared to 15% cement single layer and 20% cement double-layer configurations, respectively.

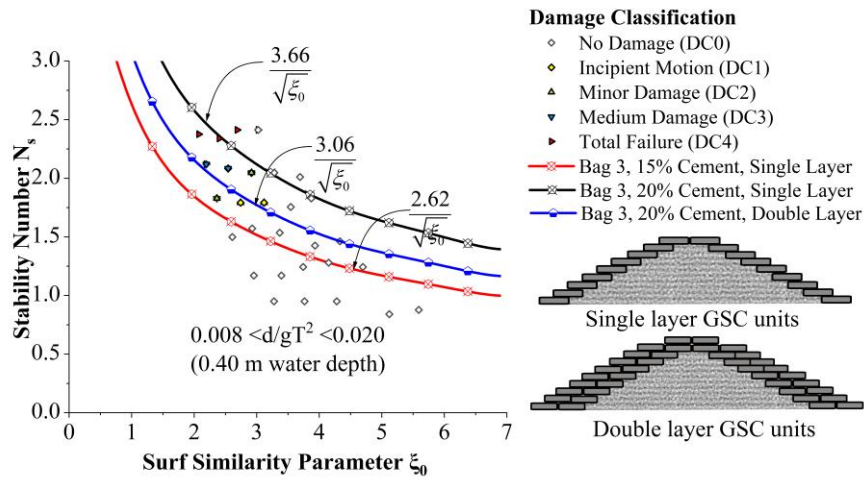


Fig. 4.57 Stability curves of all experimented configurations for a relative water depth of $0.008 < d/gT^2 < 0.020$ (0.40 m actual water depth in flume)

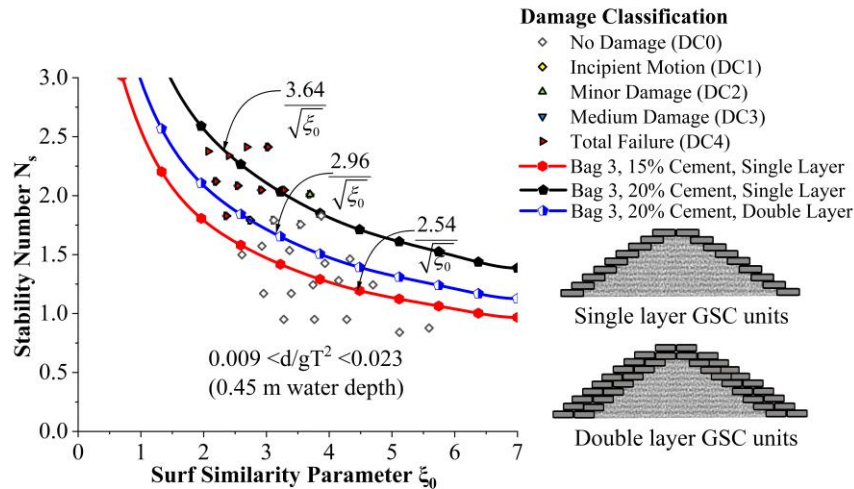


Fig. 4.58 Stability curves of all experimented configurations for a relative water depth $0.009 < d/gT^2 < 0.023$ (0.45 m actual water depth in flume)

From the above analysis, it has been observed that when cement content is increased from 15 to 20%, there is a considerable increase in stability, i.e. 13.6 to 43.3%. Sand bag structure with 20% cement content exhibited higher strength because of an increased percentage of cement in it. This can be the reason why it could withstand higher wave activity. However, the hardened material inside certain 15% cement-filled bags showed a

tendency to break within the container, making it vulnerable to detachment on higher wave activity

Similarly, when 20% cement-filled bags are altered from single layer to double layer, a 17.18 to 22.9% decrease in stability is observed. This observation contradicted the general concept that stability increases when the number of outer armour layers increases. The reduction in stability of the double-layer structure can be mainly attributed to the lack of friction experienced by the outer armour layer. As a result, units from the outer layer tend to get detached at lower wave heights.

4.4 COMPARISON OF CEMENT AND SAND-FILLED CONFIGURATIONS WITH OTHER CONFIGURATIONS

4.4.1 Comparative analysis of wave runup

Fig. 4.59 shows the comparative analysis of the runup behaviour of all the tested configurations in the second experimentation phase. The runup curves tend to vary from 0.5 to 2.7 on a scale of relative runup rate (R_u/H_0), of double-layer configuration of Bag 3 armour (20% cement-filled) showing the least runup rates and parallelly placed configuration showing the highest runup rates. Out of all tested configurations, runup rates are the lowest for cement-filled configurations. This is due to the increased wave dissipation in the structure slope resulting in reduced runup rates because of higher structure porosity. Cement-sand-filled structures experience higher porosity as there is no scope for readjustments so that the pores can be covered, as in the case of GSCs. Closer observation on Fig. 4.60 reveals that as the number of layers increases from one to two, there is a considerable reduction of relative wave runup. Single-layer Bag 3 structure with armour filled with sand alone exhibited a 13.15% to 8% reduction in run-up rates compared with the double-layer arrangement. Similarly, up to 31% reduction is experienced in the runup rates on Bag 3 cement-sand filled double-layer configuration compared to its single layer counterpart. As the layer increases, more pore spaces are created, accelerating wave dissipation over the structure, thus reducing runup.

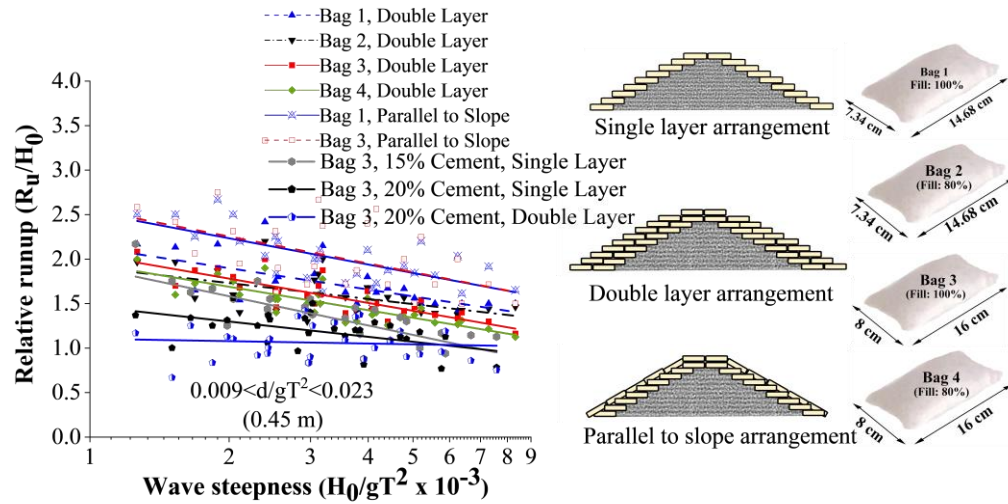


Fig. 4.59 Comparative analysis of runup behaviour of all the tested configurations

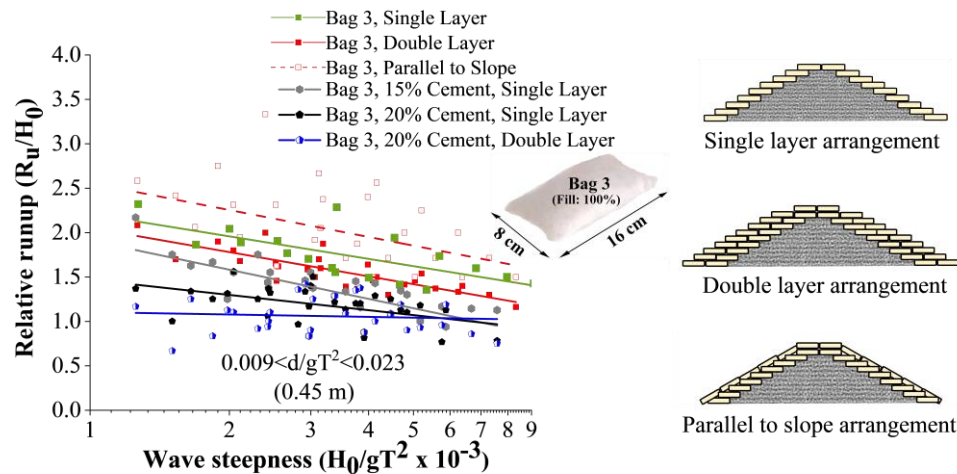


Fig. 4.60 Relative wave runup for various placement modes of Bag 3

As far as placement method is compared, slope-parallel placement is observed to possess higher run-up rates. Slope parallel placement exhibited up to 31.5% and 16.27% increased relative runup than double and single layer structures, respectively. The main reason behind this observation is the continuous covering mechanism in slope-parallel placement, reducing the porosity of the structure. As a result, more wave energy gets reflected due to its inability to dissipate energy on the surface.

4.4.2 Comparative analysis of wave rundown

As far as wave rundown is considered, the maximum value is exhibited by the slope parallel placements, which ranged up to 2.5 times the incident wave height (See Fig. 4.61). Whereas, the least rundown values are exhibited by the structures with 20% cement content (relative rundown ranging from 1.1 to 1.5). The rundown values exhibited by all other models lie between these two cases. The main reason behind high rundown is the continuous covering mechanism in slope-parallel placement, reducing the porosity of the structure. As a result, water glides and remains on the structure slope without getting absorbed or dissipated through the pores. Also, 20 to 30% decrease in rundown is exhibited as the size of armour unit increased. As discussed in the previous sections, increasing porosity of the structure with increasing armour unit size can be the major contributing factor to reduced runup.

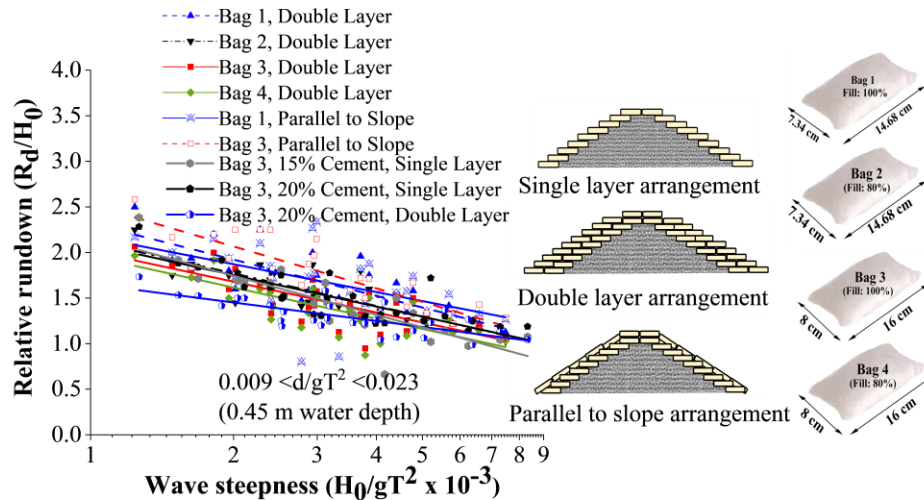


Fig. 4.61 Comparative analysis of rundown behaviour of all the tested configurations

4.4.3 Comparative analysis of reflection

The reflection values appear scattered as illustrated in Fig. 4.62. One can observe that all other tested configurations exhibit lower reflection rates than the conventional breakwater

except GSC single layer configuration. It has to be noted that, sand -cement configurations exhibit very low reflection rates, with a maximum reflection coefficient K_r of 0.2. Increased porosity in that case could be the possible reason for reduction in reflection.

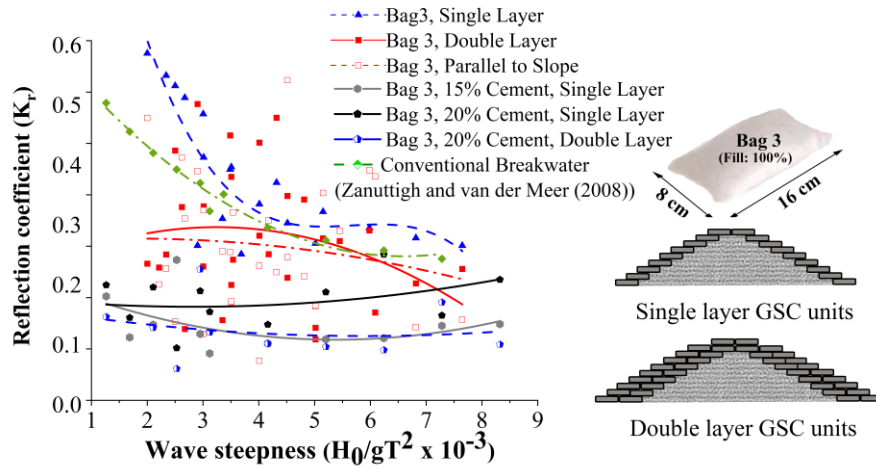


Fig. 4.62 Reflection curves

4.4.4 Comparison of stability

Stability curves for all the tested GSC breakwater configurations help in the analysis of the efficacy of various placement techniques. In the present case of investigation, structure with 'Bag 3' armour is experimented in all types of arrangements, including single and double layer, slope parallel placements and cement-sand filling. Therefore, stability curves of Bag 3 armour with all the tested arrangement for a water depth of 0.45 m have been represented in Fig. 4.63. This depth of water was the most damaging depth among all the experimentation cases, therefore, critical cases of stability tests are only investigated. Bags of sand-cement ratio of 20% with single layer configuration shows the maximum stability, with slope parallel placements and single layer (15% cement) case being the weakest. The stability of single layer bag 3 structure with sand alone was found to be higher than that of the stability of single layer structure with 15% cement. This may be due to the additional instability caused due to the breakage of some solidified 15% cement-filled units.

As observed, when GSC units are filled with cement, single-layered structures were up to 22% more stable than double-layer structures. This is contradictory to the fact that stability increases with the number of layers. The possible reason for this instability may be the lack of friction between the layers, as geotextiles are used. Additionally, these GSC units formed pillow-shaped solids (susceptible to easy displacement) with poor interlocking when the cement-sand mixture solidified within the bags. Out of all tested configurations, slope parallel placement showed the least stability due to decreased porosity and increased runup and destabilising activity on structure slope.

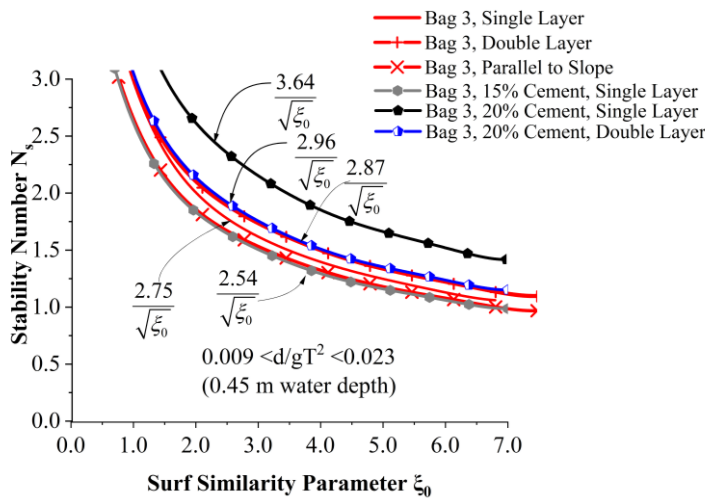


Fig. 4.63 Stability curves for Bag 3 with all the tested arrangements

CHAPTER 5

CONCLUSIONS

5.1 GENERAL CONCLUSIONS OF EXPERIMENTATION ON BREAKWATERS ARMOURED WITH SINGLE LAYER GSC UNITS.

The main aim of the present experimentation was to investigate the feasibility of using GSCs as the armour units of a breakwater, thus countering the unavailability of huge natural rocks, environmental degradation and logistics problems so that a possible replacement for the conventional structures can be proposed. A comprehensive literature review assisted in designing the GSC breakwater model and deciding the dimensions of experimental GSC units. Hydraulic performance and stability of various breakwater models with GSC armour units placed in single and double layers were investigated. As a preliminary study, some models are tested with mortar-filled GSCs to evaluate the difference in the structure behaviour. The structure could be easily constructed on-site with lesser risk of vandalism with extensive validation checks. Physical model studies on GSC single-layer breakwaters reveal that the structure can be an effective alternative to conventional breakwaters, up to a design wave height of 2.9 m under adopted test conditions. Test models of varying sand fill ratios and sizes and their failure modes are visualised through exhaustive investigations. From the extensive experimentations, the following conclusions are drawn;

- Due to its lesser porosity, GSC breakwaters exhibit higher reflection, runup, and rundown trends than conventional rubble mound breakwaters. Still, GSC structures can be an eco-friendly and efficient substitute for conventional breakwaters.
- Changing bag fill percentage from 100 to 80% resulted in a 12.05 to 64.5% reduction in wave runup rates. 80% filled bags exhibited 5.45 to 45.23% lesser rundown rates than 100% filled bags.
- Increasing the size of armour units resulted in up to a 34.8% reduction in runup rates. Similarly, rundown values were also found to be reduced up to 34.5%.

- Reflection coefficient (K_r) shows a wide range from 0.29 to 0.69 and tends to increase with increasing wave period, wavelength, and surf similarity parameter. At the same time, K_r exhibited an inverse relationship between wave steepness and incident wave height.
- 11.53 to 33.33% reduction in K_r is observed when the period of waves varied from 2.2 s to 1.4 s.
- Changing bag fill percentage from 100 to 80% resulted in a 16.3 to 43.7% reduction in reflection coefficients due to increased absorption of 80% filled bags. Whereas increasing bag size resulted in up to 10.07% reduction in K_r .
- For conservative and confident stability results, the performance of the test models has to be investigated for a wave attack of a minimum of 2000 waves.
- 100% filled bags are up to 14% more stable. Increased empty spaces, reduced self-weight and sand migration results in instability of 80% filled bags, which predominantly failed by pullout and sliding.
- Out of the two armour sizes considered, due to higher self-weight, inter-bag pore spaces, contact surface area and overlapping length, Bags with larger dimensions (Bag 3 and 4) exhibited 4.2 to 8% increased stability than smaller units (Bag 1 and 2).
- When the sand fill ratio and armour unit size are considered, the sand fill ratio determines the stability of GSC breakwater than the armour unit size.
- On the contrary to the usual observation, stability of GSC breakwater is found to be increasing up to 4.4% in $0.009 < d/gT^2 < 0.023$ (i.e. 0.45 m water depth).
- Incident wave heights have a direct impact on the stability of the structure. 'Bag 3' remained stable up to 0.099 m in model scale (2.97 m in prototype). 10.14% increased incident wave heights when the wave period is increased from 1.4 to 2.2 s (max range of selected wave period).

- Literature suggests empirical coefficient C_w be a value between 2.5 to 2.7 C_w for GSC breakwater is found to be ranging from 2.24 to 2.75 where values below 2.5 are obtained for 80% filled cases, indicating its lower stability.

Out of the four configurations tested, the breakwater structure armoured with ‘Bag 3’ exhibited maximum stability.

5.2 GENERAL CONCLUSIONS OF EXPERIMENTATION ON BREAKWATERS ARMoured WITH DOUBLE LAYER GSC UNITS.

The study aided in analysing the stability and hydraulic performance of double-layer GSC breakwaters with different placement modes. On a general note, GSC breakwater is found to perform better when supplemented with double layers of armour units. Each factor affecting the structure's stability as well as hydraulic performance has been extensively reviewed, and the following concluding remarks have been deduced.

1. The placement mode of GSC armour units has exhibited a considerable effect on the hydraulic performance of the structure. Armour units placed parallel to slope have shown higher relative runup, rundown and reflection coefficient compared to double-layer placement
2. All the newly tested double-layer models exhibited lower reflection rates (up to 32%) than conventional breakwater structures.
3. Up to a 24.3% increase in runup is observed when the bag fill percentage is varied from 80 to 100. As water depth increased from 0.35 m to 0.45 m, up to 30.5% increase in relative runup is observed.
4. Changing the fill from 100 to 80% resulted in up to 34.23% reduction of rundown, whereas increasing the size of bags has helped only up to 19.5% reduction in rundown.
5. As far as damage levels of sand-alone, double-layer GSC breakwaters are concerned, double-layer placement tends to have fewer ‘Total Failure’ cases

(less than 30%). Single and Slope parallel arrangements exhibited up to 50% total failure cases, with slope parallel placement rapidly reaching total failure (DC4) once displacement of units initiates. Therefore, this type of placement need not be considered.

6. The stability of the structure decreased with increasing water depth as runup, rundown and destructive wave forces are more at higher water depth. Bigger bags tend to be up to 21.5% stable in lower depth.
7. Double layer placement with Bag 3 is found to be stable up to a wave height of 0.132 m on the model scale, which will be 3.96 m in the prototype.
8. As far as the armour unit size is concerned, larger units are found to be 2.6 to 28.83% higher in stability than their smaller counterparts.
9. 4.6 to 12.8% increase in stability is observed when the sand filling of the bags is varied from 80% to 100%.

5.3 GENERAL CONCLUSIONS OF EXPERIMENTATION ON BREAKWATERS ARMoured WITH CEMENT-FILLED GSC UNITS.

The study aided in analysing the stability and hydraulic performance of sand and cement-filled GSC breakwaters. Each factor affecting the structure's stability as well as hydraulic performance has been extensively reviewed, and the following concluding remarks have been deduced.

1. Of all the tested configurations, breakwater armoured with Bag 3 filled with 15% cement exhibited the maximum wave runup and rundown up to 33% and 31%, respectively.
2. GSC units with 15% cement are observed to have a higher tendency to break within the bag.

3. Of all the tested configurations, breakwater structures with single layer GSC units filled with 20% cement exhibited up to 76% higher wave reflection, with all the other tested cases exhibiting lower reflection than conventional breakwaters.
4. When the cement content is increased from 15 to 20%, there is a considerable increase in stability from 13.6 to 43.3%.
5. Single-layer breakwater structure with GSC units containing 20% cement shows maximum stability, while slope parallel placements are the weakest in terms of stability.
6. Similarly, when breakwater structures with GSC units containing 20% cement are altered from a single layer to double layers, a 17.18 to 22.9% decrease in stability is observed.

When the armour units of GSC breakwaters are filled with sand and cement, up to 43% increased stability is observed with a considerable decrease in wave runup and rundown. As a result, cement-sand-filled GSC units can be suggested as a possible alternative to sand-alone-filled units where vandalism has to be countered. Additionally, the durability and wave resistance of the breakwaters increases when solidified sand units are used. But when cement is used, single-layer placement is up to 23% more stable than double-layer placement. The preliminary investigation on stability and hydraulic performance nomograms can be projected as a significant research outcome, as it aids coastal engineers in designing and planning GSC breakwaters.

5.4 SUMMARY OF CONCLUSIONS

Owing to lower porosity, single-layer GSC breakwater type exhibit high reflection, runup, and rundown trends compared to conventional rubble mound breakwaters. But when GSCs are arranged in double layers, porosity increases, resulting in up to a 32% reduction in reflection, runup and rundown than conventional breakwaters. Slope parallel placement, which is a different double layer placement, exhibited poor performance regarding stability and hydraulic responses. As a result, slope parallel placement cannot be suggested for field

applications or further experimentations. As far as the stability is considered, a different approach to damage classification is adopted, which requires a storm duration of 2000 waves to completely define the stability of a model. As increasing, armour unit weight and sand-fill ratio showed an increasing trend in the stability of the structure. From all the model studies, Bag 3 (The biggest bag with 100% sand-fill) was identified as the optimum armour unit for all the tested models, with an ability to withstand up to 3.6 m waves in prototype when placed in double layers. As cement percentage increased from 15 to 20, a considerable increase of up to 43% is observed in the structure stability. In contrast to the general conception, the structure stability was found to decrease up to 22% when double layers are provided. As a result, when filled with mortar, it is advisable to give a single layer of GSC armour units in field practices instead of two.

To conclude, the stability of structure increases with armour unit weight, sand fill ratio and the number of armour unit layers. Bag 1 and Bag 3 (fully filled bags) showed 5.38 and 17.8% higher stability when placed in double layers than in a single layer. 80% filled bags are found to be less stable in all cases, with slope parallel placement being the most unstable configuration. When the GSCs are filled with sand and cement, up to 43% increased stability is observed. For sand-alone bags, up to 24.3% and 34.23% respective increase in runup and rundown is observed when the bag fill percentage is varied from 80 to 100. Moreover, when water depth increased from 0.35 m to 0.45 m, up to 30.5% and 32% increase in relative runup and rundown is observed. Wave runup and rundown are also found to decrease with the number of layers and when filled with cement mortar. The stability and hydraulic performance nomograms can be projected as the major research outcome, as it aids coastal engineers in designing and planning GSC breakwaters.

5.5 FUTURE SCOPE

The present work is limited to physical model studies on GSC breakwaters. Comparison of the research outcomes can be carried out through soft-computing. As it possibly changes the porosity and interlocking of the structure, alteration in GSC shapes could pose a scope of future investigation. The present model is designed as a non-overtopping emerged

structure. Wave overtopping rates over a GSC breakwater can be investigated if the crest height of the structure is lowered. Additionally, variations in parameters such as crest width, breakwater slope etc., can be adopted in further studies.

REFERENCES

Akter, A., Pender, G., Wright, G., and Crapper, M. (2013). "Performance of a geobag revetment. Quasi-physical modelling." *Journal of Hydraulic Engineering*, ASCE, 139(8), 865–876.

Albert, J., and Bhaskaran, P. K. (2020). "Ocean heat content and its role in tropical cyclogenesis for the Bay of Bengal basin." *Climate Dynamics*, Springer, 55(12), 3343–3362.

Ashis, M. (2015). "Application of geotextiles in coastal protection and coastal engineering works : An overview." *International Research Journal of Environment Sciences*, Indore: International Science Community Association, 4(4), 96–103.

Battjes, J. A., and Ary, R. (1976). "Characteristics of flow in run-up of periodic waves." *15th International Conference on Coastal Engineering*, ASCE, Honolulu, Hawaii, 11-17 July, 781–795.

Bezuijen, A., and Pilarczyk, K. W. (2012). "Geosynthetics in hydraulic and coastal engineering: filters, revetments and sand filled structures." *5th European Geosynthetics Congress*, Ghent, Belgium, 16-19 September, 65–80.

Bezuijen, A., Oung, O., Klein Breteler, M., Berendsen, E., &, and Pilarczyk, K. W. (2002). "Model tests on geocontainers, placing accuracy and geotechnical aspects." *Proceedings of 7th international conference on geosynthetics*, Nice, France, September, 1001–1006.

Binumol, S., Rao, S., and Hegde, A. V. (2020). "Multiple Nonlinear Regression Analysis for the Stability of Non-overtopping Perforated Quarter Circle Breakwater." *Journal of Marine Science and Application*, Springer, 19(2), 293–300.

Borrero, J. C., Mead, S. T., and Moores, A. (2010). "Stability considerations and case studies of submerged structures constructed from large, sand filled, geotextile containers." *Coastal Engineering*, Elsevier, 32(1), 1–12.

Coastal Engineering Manual. (2008). *Coastal Engineering Manual*. US Army Corps of Engineers, Washington D C, April, Part IV, 20-222.

Corbella, S., and Stretch, D. D. (2012). “Geotextile sand filled containers as coastal defence: South African experience.” *Geotextiles and Geomembranes*, Elsevier, 35(6), 120–130.

Dassanayake, D. T., and Oumeraci, H. (2012a). “Hydraulic stability of coastal structures made of geotextile sand containers.” *Coastal Engineering Proceedings*, 33(1), 55–69.

Dassanayake, D. T., and Oumeraci, H. (2012b). “Engineering properties of geotextile sand containers and their effect on hydraulic stability and damage development of low-crested / submerged structures.” *International Journal of Ocean and Climate Systems*, Sage Publishing, 127(3), 135–150.

Dassanayake, D. T., and Oumeraci, H. (2013). “Geotextile sand container structures for shore protection -Hydraulic stability formulae and nomograms.” *Second International Workshop on Geosynthetic and Modern Materials In Coastal Protection and Related Applications*, IIT Madras, 4-5 March, 68–81.

Dhinakaran, G., Sundar, V., Sundaravadivelu, R., and Graw, K. U. (2010). “Regular wave measurements on a submerged semicircular breakwater.” *Journal of Offshore Mechanics and Arctic Engineering*, ASME, 132(3), 1–6.

Diwedat, A. I. (2016). “Investigating the effect of wave parameters on wave runup.” *Alexandria Engineering Journal*, Elsevier, 55(1), 627–633.

Faraci, C. (2018). “Experimental investigation on hydro-morphodynamic performances of a geocontainer submerged reef.” *Journal of Waterway, Port, Coastal and Ocean Division*, ASCE, 144(2), 1–10.

Fowler J, Stephens, C., Santiago, M., and Bruin, P. (2002). “Amwaj islands constructed with geotubes, Bahrain.” *Proceedings of CEDA Conference*, Denver, Colorado, USA, 1–

14.

Foyer, G. (2013). "Prediction Formulae for Processes on and in Porous Bonded Revetments – An Experimental and Numerical Study." Ph.D. Thesis, Technical University Carolo-Wilhelmina Braunschweig. 50-140.

Hanson, and Kraus. (1990). "Shoreline response to a single transmissive detached breakwater." *Proceedings. 22nd Coastal Engineering Conference.*, ASCE, Hague, 2-6 July, 1-18

Heerten, G., Jackson, L. A., Restall, S., and Saathoff, F. (2000). "New developments with mega sand containers of non-woven needle-punched geotextiles for the construction of coastal structures." *27th International Conference on Coastal Engineering*, Sydney, Australia, ASCE, 25-28 July, 2342-2355.

Hegde, A. V. (2010). "Coastal erosion and mitigation methods - global state of the art." *Indian Journal of Geo Marine Sciences*, 39(4), 521–530.

Hegde, A. V., Kamath, K., and Magadum, A. S. (2007). "Performance characteristics of horizontal interlaced multilayer moored floating pipe breakwater." *Journal of Waterway, Port, Coastal, and Ocean Engineering*, ASCE, 133(4), 275–285.

Hornsey, W. P., Carley, J. T., Coghlan, I. R., and Cox, R. J. (2011). "Geotextile sand container shoreline protection systems: Design and application." *Geotextiles and Geomembranes*, Elsevier, 29(4), 425–439.

Isaacson, M. (1992). "Measurement of regular wave reflection." *Journal of Waterway Port Coastal and Ocean Engineering*, ASCE, 117(6), 553–569.

Jackson, L. A. (2010). "Design and Construction of low crested reef breakwaters using sand-filled geotextile containers." *Geosynthetics and Modern Materials for Coastal Protection and Related Applications*", Indian Institute of Technology Madras (IITM)., 6-7 August, 1–8.

Jackson, L. A. (2016). "Coastal stabilisation – Advancement in geotextile design & construction methods as an alternative to rock." *Proceedings of 3rd International Conference on Coastal Zone Engineering and Management in The Middle East (Arabian Coast)*, 20-23 November, 321–342.

Jackson, L. A., Corbett, B. B., King, S., and Restall, S. (2008). *Technical note SFGC Characteristics*. Technical note of International Coastal Management, Australia, Extracted from Researchgate, 1-7

Jackson, L. A., Corbett, B., and Restall, S. (2006). "Failure modes & stability modelling for design of sand filled geosynthetic structures." *Proceedings of the 30th International Conference on Coastal Management (ICCE) San Diego, 2-8 September*. 1-22.

Jackson, L. A., Tomlinson, R., Corbett, B., and Strauss, D. (2012). "Long term performance of a submerged coastal control structure: A case study of the Narrowneck multi-functional artificial reef." *Coastal Engineering*, Elsevier, 33(1), 54-67.

Jones, D. L., Davis, J. E., Curtis, W. R., and Pollock, C. E. (2006). "*Geotextile tube structures guidelines for contract specifications*". *U S Army Corps of Engineers*.1-14

Jugal, K. T. (2018). "Construction of Geo-tube embankment at Pentha in Kendrapara district of Odisha- A case study." *Proceedings of Seminar on Geosynthetics for Erosion Control and Coastal Protection*, CBIP, Bhubaneswar, Odisha., 33–40.

Kannan, R., Abhrankash, K, Ramamurthy, M. V.,and Ramana, K.(2018). "Shoreline evolution along Uppada coast in Andhra Pradesh using multi-temporal satellite images." *Proceedings of Seminar on Geosynthetics for Erosion Control and Coastal Protection*,CBIP Bhubaneswar, Odisha., 25–32.

Khajenoori, L., Wright, G., and Crapper, M. (2021). "Laboratory investigation of geobag revetment performance in rivers." *Geosciences (Switzerland)*, MDPI, 11(8), 1–17.

Kim, H. J., Park, T. W., Dinoy, P. R., Kim, H. S., and Kim, H. J. (2018). "Design and

consolidation analysis of geotextile tubes for the Saemangeum project in Korea.” *Geosynthetics International*, ICE Publishing, 25(5), 507–524.

Kiran, A. S., Ravichandran, V., and Sivakholundu, K. M. (2015). “Stability analysis and design of offshore submerged breakwater constructed using sand filled geosynthetic tubes.” *Procedia Engineering*, Elsevier, 166 (1), 310–319.

Kobayashi, N., and Jacobs, B. K. (1985). “Stability of armour units on composite slopes.” *Journal of Waterway Port Coastal and Ocean Engineering*, ASCE, 111(5), 880–894.

Koffler, A., Choura, M., Bendriss, A., and Zengerink, E. (2008). “Geosynthetics in protection against erosion for river and coastal banks and marine and hydraulic construction.” *Journal of Coastal Conservation*, Springer, 12(1), 11–17.

Kriel, H. J. (2012). “Hydraulic stability of multi-layered sand-filled geotextile tube breakwaters under wave attack.” Ph.D. Thesis, Stellenbosch University. 19-149

Krishnan, A., Bhaskaran, P. K., and Kumar, P. (2021). “CMIP5 model performance of significant wave heights over the Indian Ocean using COWCLIP datasets.” *Theoretical and Applied Climatology*, Springer, 145(1–2), 377–392.

Kudale, M. D., Mahalingaiah, A. V, and Tayade, B. R. (2014). “Use of sand-filled geotextile tubes for sustainable coastal protection- case studies in Indian scenario.” *Indian Journal of Geo-Marine Sciences*, National Institute of Science Communication and Information Resources (NISCAIR), 43(7), 1241–1246.

Lawson, C. R. (2008). “Geotextile containment for hydraulic and environmental engineering.” *Geosynthetics International*, ICE Publishing, 15(6), 384–427.

Losada, M. A., and Gimenez-curto, L. A. (1981). “Flow characteristics on rough, permeable slopes under wave action.” *Coastal Engineering*, Elsevier, 4, 187–206.

Mani, J. S., and Jayakumar, S. (1995). “Wave Transmission by Suspended Pipe

Breakwater.” *Journal of Waterway, Port, Coastal, and Ocean Engineering*, ASCE, 121(6), 335–338.

Mead, S. T., Blenkinsopp, C., Andrew Moores, A., and Borrero, J. (2010). “Design and construction of the Boscombe multi-purpose reef.” *Proceedings of the 32nd International Conference on Coastal Engineering*, Shanghai, China., 58–67.

Meer, J. W. van der. (1988). “Rock slopes and gravel beaches under wave attack.” Ph.D. Thesis, Delft University, The Netherlands, 10-150.

Meer, J. W. van der, and Pilarczyk, K. W. (1985). “Stability of rubble mound slopes under random wave attack.” *Proceedings of 19th International Conference on Coastal Engineering*, ASCE, Houston, Texas, U.S. 3-7 September, 2620–2634.

Meer, J. W. van der, and Stam, M. (1992). “Wave runup on smooth and rock slopes of coastal structures.” *Journal of Waterway Port Coastal and Ocean Engineering*, ASCE, 118(5), 534–550.

Nasar, T., Balaji, R., and Sundar, V. (2004). “Hydrodynamic characteristics and stability of rubble mound breakwater with geobags as the core.” *3rd Indian National Conference on Harbour & Ocean Engineering*, Goa, India, 7-9 December, 492–497.

Neves, L. P. (2011). “Experimental stability analysis of geotextile encapsulated-sand systems under wave-loading.” Ph.D. Thesis, University of Porto, Portugal, 38-330

Nishold, S. P., Sundaravadivelu, R., and Saha, N. (2014). “Analysis and design of geotube saline embankment.” *International Conference on Computational and Experimental Marine Hydrodynamics*, 3-4 December, 292–300.

Nishold, S. P., Sundaravadivelu, R., and Saha, N. (2018). “Geotextile tube and gabion armoured seawall for coastal protection an alternative.” *PIANC-World Congress Panama City, Panama*. 7-11 May, 1-12.

Nishold, S. P., Sundaravadivelu, R., and Saha, N. (2019). "Physical model study on geotube with gabion boxes for the application of coastal protection." *Arabian Journal of Geosciences*, Springer, 164(12), 1–11.

Oh, Y. I., and Shin, E. C. (2006). "Using submerged geotextile tubes in the protection of the E. Korean shore." *Coastal Engineering*, Elsevier, 53(11), 879–895.

Oumeraci, H., Hinz, M., Bleck, M., and Kortenhaus, A. (2003). "Sand-filled geotextile containers for shore protection." *Proceedings of Coastal Structures 2003, Portland, Oregon, USA*, 1–15.

Oumeraci, H., and Kortenhaus, A. (2011). "Core made of geotextile sand containers for rubble mound breakwaters and seawalls: Effect on armour stability and hydraulic performance." *Ocean Engineering*, Elsevier, 38(1), 159–170.

Oumeraci, H., and Recio, J. (2018). "Geotextile sand containers for shore protection". *Handbook of Coastal and Ocean Engineering*. World Scientific Publishers, 776-822

Oumeraci, H., Stall, T., Pfortner, S., and Ludwigs, G. (2010). "Hydraulic performance, wave loading and response of ELASTOCOAST revetments and their foundations." *11th National Coastal Engineering Days - Civil Engineering*, Les Sables d'Olonne, France, 22-25 June, 709–740.

Parthasarathy, K. S. S., Saravanan, S., Deka, P. C., and Devanatham, A. (2020). "Assessment of potentially vulnerable zones using geospatial approach along the coast of Cuddalore district, East coast of India." *ISH Journal of Hydraulic Engineering*, Taylor and Francis, 28 (Supplimentary-1), 422-432.

Pilarczyk, K. W. (1987). "*Dutch guidelines on dike protection*". International conference on coastal and port engineering in developing countries. Beijing, China, September, Technical report extracted from Researchgate, 282-302.

Pilarczyk, K. W. (1997). "Geotextile systems in coastal engineering — An Overview." *25th*

International Conference on Coastal Engineering, ASCE, Orlando, Florida, United States, 2-6 September, 2114–2127.

Pilarczyk, K. W. (2000). "Geosynthetics and geosystems in hydraulic and coastal engineering". Taylor and Francis.100-230.

Pilarczyk, K. W. (2003). "Design of low-crested (submerged) structures – an overview." *6th International Conference on Coastal and Port Engineering in Developing Countries*, Colombo, Sri Lanka , 15-19 September, 1–19.

Pilarczyk, K. W., Breteler, M., and Bezuijen, A. (1995). "Wave forces and structural response of placed block revetments on inclined structures." *Wave forces on inclined and vertical wall structures.*, ASCE, 1–38.

Plaut, R. H., and Klusman, C. R. (1999). "Two-dimensional analysis of stacked geosynthetic tubes on deformable foundations." *Thin-Walled Structures*, Elsevier, 34(3), 179–194.

Radhakrishnan, R. (2013). "Innovative Application of Geosynthetics in Civil Engineering Construction." *Second International Workshop on Geosynthetic and Modern Materials in Coastal Protection and Related Applications*, IIT Madras, 4-5 March, 227–233.

Rajagopal, K., Vijaya, R., Raghunath, K., and Rautela, R. (2013). "Some trails on the use of geosynthetics for environmentally sustainable coastal stabilisation solutions." *Proceedings of the 2nd International Workshop on Geosynthetics and Modern Materials in Coastal Protection and. Related Applications.IIT Madras*, 4-5 March, 25–36.

Rao, S., Shirlal, K. G., Varghese, R. V., and Govindaraja, K. R. (2009). "Physical model studies on wave transmission of a submerged inclined plate breakwater." *Ocean Engineering*, Elsevier, 36(15–16), 1199–1207.

Rao, S., Subrahmanya, K., Rao, B. K., and Chandramohan, V. R. (2008). "Stability aspects of nonreshaped berm breakwaters with reduced armor weight." *Journal of Waterway, Port,*

Coastal and Ocean Engineering, ASCE, 134, 81–87.

Rasmeemasuang, T., Chuenjai, W., and Rattanapitikon, W. (2014). “Wave run-up on sandbag slopes.” *Maejo International Journal of Science and Technology*, Maejo University, 8(01), 48–57.

Recio, J. (2008). “Hydraulic stability of geotextile sand containers for coastal structures - Effect of deformations and stability Formulae.” Ph.D Thesis, Faculty of Architecture, Civil Engineering and Environmental Sciences of the Technical University Carolo-Wilhelmina, Braunschweig, 20-167.

Recio, J., and Oumeraci, H. (2007). “Effect of deformations on the hydraulic stability of coastal structures made of geotextile sand containers.” *Geotextiles and Geomembranes*, Elsevier, 25, 278–292.

Recio, J., and Oumeraci, H. (2008). “Hydraulic permeability of structures made of geotextile sand containers: Laboratory tests and conceptual model.” *Geotextiles and Geomembranes*, Elsevier, 26(6), 473–487.

Recio, J., and Oumeraci, H. (2009). “Process based stability formulae for coastal structures made of geotextile sand containers.” *Coastal Engineering*, Elsevier, 56(5–6), 632–658.

Rowe, R. K., Abdelaal, F. B., and Zahirul Islam, M. (2014). “Aging of high-density polyethylene geomembranes of three different thicknesses.” *Journal of Geotechnical and Geoenvironmental Engineering*, ASCE, 140(5), 1–11.

Rowe, R. K., Islam, M. Z., Brachman, R. W. I., Arnepalli, D. N., and Ewais, A. R. (2010). “Antioxidant depletion from a high density polyethylene geomembrane under simulated landfill conditions.” *Journal of Geotechnical and Geoenvironmental Engineering*, ASCE, 136(7), 930–939.

Rowe, R. K., and Shoaib, M. (2017). “Effect of brine on long-term performance of four HDPE geomembranes.” *Geosynthetics International*, Ice Publishing, 24(5), 508–523.

Saathoff, F., Oumeraci, H., and Restall, S. (2007). “Australian and German experiences on the use of geotextile containers.” *Geotextiles and Geomembranes*, Elsevier, 25, 251–263.

Sathyanarayana, A. H., Suvarna, P. S., Umesh, P., and Shirlal, K. G. (2021). “Performance characteristics of a conical pile head breakwater: An experimental study.” *Ocean Engineering*, Elsevier, 235(1), 109395.

Schimmels, S., Vousdoukas, M., Wziatek, D., Becker, K., Gier, F., and Oumeraci, H. (2012). “Wave runup observations on revetments with different porosities.” *Coastal Engineering Proceedings*, 33(1), 73-87.

Shankar, N. J., and Jayaratne, M. P. R. (2003). “Wave run-up and overtopping on smooth and rough slopes of coastal structures.” *Ocean Engineering*, Elsevier, 30(1), 221–238.

Shin, E. C., and Oh, Y. I. (2003). “Analysis of geotextile tube behaviour by large- scale field model tests.” *Geosynthetics International*, Ice Publishing, 10(4), 134–141.

Shin, E. C., and Oh, Y. I. (2007). “Coastal erosion prevention by geotextile tube technology.” *Geotextiles and Geomembranes*, Elsevier, 25, 264–277.

Shirlal, K. G., and Mallidi, R. R. (2015). “Physical model studies on stability of geotextile sand containers.” *8th International Conference on Asian and Pacific Coasts (APAC 2015) Procedia Engineering*, Elsevier, Chennai, India, 7-10 September, 567–574.

Shirlal, K. G., Rao, S., Ganesh, V., and Manu. (2006). “Stability of breakwater defenced by a seaward submerged reef.” *Ocean Engineering*, Elsevier, 33(5–6), 829–846.

Shirlal, K. G., Rao, S., and Manu. (2007). “Ocean wave transmission by submerged reef— A physical model study.” *Ocean Engineering*, Elsevier, 34(14–15), 2093–2099.

Shore Protection Manual (1984). *U.S. Army Corps Engineers, Waterway Experimentation Station*, Washinton D C, Vol I and Vol II, Chapter 1, 2, 6.

Silvester, B. R. (1986). “Use of grout-filled sausages in coastal structures.” *Journal of*

Waterway Port Coastal and Ocean Engineering, ASCE, 112(1), 95–114.

Sindhu, S., Shirlal, K. G., and Manu. (2015). “Prediction of wave transmission characteristics at submerged reef breakwater.” *8th International Conference on Asian and Pacific Coasts(APAC 2015) Procedia Engineering*, Elsevier, Chennai, India, 7-10 September, 116(1), 262–268.

Soysa, V. A. N., Dassanayake, D. T., and Oumeraci, H. (2012). “Hydraulic Stability of Submerged GSC structures.” *Engineer-Journal of the Institution of Engineers, Sri Lanka*, 45 (4), 31–40.

Sreelakshmi, S., and Bhaskaran, P. K. (2020). “Wind-generated wave climate variability in the Indian Ocean using ERA-5 dataset.” *Ocean Engineering*, Elsevier, 209(10),74-86.

Stegg, P. V, Vastenburg, E., and Gijt, D. J. (2011). “Large-scale physical model tests on sand-filled geotextile tubes and containers under wave attack.” *Proceedings of the 6th International Conference, Coastal Structures*, ASCE, Yokohama, Japan, September,1083–1094.

Sundar, V. (2013). “Coastal protection measures along few stretches of Indian coast.” *Second International Workshop on Geosynthetic and Modern Materials In Coastal Protection and Related Applications*, IIT Madras, 4-5 March, 147–158.

Sundar, V., Maiti, D. K., Sannasiraj, S. A., and Venkatraman, M. (2009). “Geosynthetic application for coastal protection at Shankarpur, West Bengal, India.” *Asian and Pacific Coasts(APAC)*, World Scientific Publishers, Singapore, 13-16 October, 58–64.

Sundaravadelu, R. (2013). “Design and construction of geotube saline embankment at Pentha, Odisha.” *Second International Workshop on Geosynthetic and Modern Materials In Coastal Protection and Related Applications*, IIT Madras, 4-5 March, 143–147.

Suvarna, P. S., Sathyanarayana, A. H., Umesh, P., and Shirlal, K. G. (2021). “Hydraulic performance of perforated enlarged pile head breakwaters through laboratory

investigation.” *Ocean Engineering*, Elsevier, 241(1), 110089.

Tayade, B. R., Mahalingaiah, A. V., Gokhale, N. V., and Kudale, M. D. (2015). “Importance of location and alignment of geotextile tubes for the coastal protection measures.” *Aquatic Procedia (ICWRCOE 2015)*, Elsevier, 4, 190–197.

Yamini, O. A., Kavianpour, M. R., and Mousavi, S. H. (2018). “Wave run-up and rundown on ACB Mats under granular and geotextile filters condition.” *Marine Georesources & Geotechnology*, Taylor and Francis, 36(8), 895–906.

Zanuttigh, B., and Meer, J. W. van der. (2008). “Wave reflection from coastal structures in design conditions.” *Coastal Engineering*, Elsevier, 55(10), 771–779.

Zornberg, J. G. (2013). “Recent examples of innovation in projects using geosynthetics.” *Proceedings of the 1st Iberic Conference on Geosynthetics, Geosintec Iberia 1*, 05-06 November, Sevilla, Spain, 37–50.

PUBLICATIONS

1. “Geosynthetic Containment Systems for Coastal Protection - An Indian Timeline”, Tom Elias, Kiran G. Shirlal, Proceedings of 5th International Conference in Ocean Engineering (ICOE 2019), Conducted by Indian Institute of Technology Madras and University of Mauritius. Mauritius, August 2019, Published in Springer, Lecture Notes in Civil Engineering. DOI: [10.1007/978-981-15-8506-7_38](https://doi.org/10.1007/978-981-15-8506-7_38).

2. “Physical model studies on damage and stability analysis of breakwaters armoured with geotextile sand containers”, Tom Elias, Kiran G. Shirlal, Kajal E. V. 2021, 49(3) pages 604-618, Geotextile and Geomembranes, Elsevier Publication.
<https://doi.org/10.1016/j.geotexmem.2020.12.001>

3. “Effect of armour unit layers and placement mode in the determination of stability of geotextile breakwaters”, Tom Elias, Tiruveedula Geetha, Kiran G. Shirlal, 2022, 50(3), pages 444-454, Geotextiles and Geomembranes, Elsevier Publication
<https://doi.org/10.1016/j.geotexmem.2022.01.003>

4. “Experimental investigation on the hydraulic performance of breakwater structures with geotextile armour units”, Tom Elias, Kiran G. Shirlal, 2022, 148(3), pages 04022006, 1-13 Journal of Waterway, Port, Coastal and Ocean Engineering, American Society of Civil Engineers, (ASCE).
[https://doi.org/10.1061/\(ASCE\)WW.1943-5460.0000708](https://doi.org/10.1061/(ASCE)WW.1943-5460.0000708)

5. “Preliminary investigation on stability and hydraulic performance of geotextile sand container breakwaters filled with sand and cement”, Tom Elias, Kiran G. Shirlal, Scientific Reports, Nature Publications, 12(1), 1-16, September 2022.
DOI: [10.1038/s41598-022-19673-9](https://doi.org/10.1038/s41598-022-19673-9)

RESUME

NAME : **Tom Elias**

Date of Birth : 02-06-1993

Mobile No: : +91 890 724 6776

Email id : tomelias00@gmail.com

Permanent Address : Poovathummoottil House
Chingavanam P.O, Kottayam
Kerala, India, 686531.

Qualifications : B.Tech (Civil Engineering)
Cochin University of Science and Technology

: M.Tech (Coastal and Harbour Engineering)
Kerala University of Fisheries and Ocean Studies

Publications : International Journals -4
International Conferences -2

